

Amylin and pramlintide modulate γ -secretase activity and APP processing in lipid rafts

by

Youssef Mousa

A dissertation submitted to the Graduate Faculty of
Auburn University
in partial fulfillment of the
requirements for the Degree of
Doctor of Philosophy

Auburn, Alabama
August 3, 2019

Keyword: Amylin; Pramlintide; Lipid rafts; Gangliosides; Alzheimer's; TgSwDI

Copyright 2019 by Youssef Mousa

Approved by

Amal Kaddoumi, Chair, Professor, Department of Drug Discovery and Development
Robert D. Arnold, Professor, Department of Drug Discovery and Development
Murali Dhanasekaran, Professor, Department of Drug Discovery and Development
Wendy Qiu, MD/Associate Professor, Boston University School of Medicine

Abstract

The misfolded amyloid- β ($A\beta$) peptide is generated in higher amounts in Alzheimer's disease (AD), making this peptide a clinical hallmark for AD. A major site to produce $A\beta$ is the lipid rafts, which are integral part of the cell membrane and enriched with cholesterol and sphingolipids. These rafts contain proteins and enzymes that are involved in the production of $A\beta$, in addition to other proteins such as synaptic markers and transport proteins. To isolate these rafts, in the first project, I developed and optimized a density-based separation method utilizing discontinuous sucrose gradient with ultracentrifugation. Different factors could control the efficiency of rafts fractionation, such as type of detergent, ultracentrifugation time and speed, rotor type, and cells or tissue type, thus, these factors were initially optimized to isolate lipid rafts containing proteins of interest in one fraction. Consequent to the optimization, membrane rafts were successfully isolated and localized in one fraction, which contained proteins related to my second project objective including proteins related to $A\beta$ production, synaptic markers and gangliosides.

Several studies have reported the protective effect of amylin pramlintide against AD. On the other hand, other studies demonstrated amylin rather worsen AD pathology. In either case, the mechanisms by which amylin improved or deteriorated AD pathology are not well investigated. In addition, studies evaluated the effect of pramlintide against AD are limited. Thus, the purpose of this work was to investigate the effect of amylin and pramlintide on $A\beta$ -related pathology in TgSwDI mice as a model for AD, and to investigate the predisposing mechanism for the observed effect. Therefore, in the second project, we explored the effect of amylin and pramlintide on $A\beta$ -

related pathology in TgSwDI mice. After chronic intraperitoneal treatment for 30 days with amylin or pramlintide, brains were collected and evaluated. Findings from immunostaining and ELISA demonstrated increased accumulation of A β in mice brains treated with amylin or pramlintide when compared to vehicle treated mice. To explain the observed effect, findings from total brain homogenate didn't provide a clear justification for A β increase, thus lipid rafts were used for further studies. Results from lipid rafts analyses demonstrated that both peptides increased A β burden by increasing the level of amyloid precursor protein (APP) and γ -secretase, an A β producing enzyme, in lipid rafts. One major pathway that control the localization of APP and γ -secretase activity in lipid rafts, and increased A β production and aggregation is the increased level of gangliosides, such as GM1 and GM2 gangliosides. Pramlintide increased GM1 and GM2 levels in lipid rafts and total brain homogenate, respectively. As expected, increased A β burden in mice brains was associated with synaptic loss, apoptosis, microglial activation, and increased A β deposition on brain microvessels. In conclusion, findings from this work demonstrated amylin and pramlintide increased A β levels and related pathology in TgSwDI mice brains, implying that the increased amylin level or the therapeutic use of pramlintide might increase the risk of AD.

Acknowledgments

First, thanks to the LORD “Allah” forever and for everything.

I would show my sincere gratitude to my supervisor Dr. Amal Kaddoumi for giving me the opportunity to join her laboratory and to be a part of her research team. Also, I want to thank her endless patience, motivation, guidance and strong solid knowledge.

I am also thankful for my committee members and university readers, Dr. Robert D. "Rusty" Arnold, Dr. Murali Dhanasekaran, Dr. Wendy Qui, and Dr. Douglas Martin, for their continuous guidance and enlightening suggestions as well as building the confidence in myself.

I am thankful to my lab mates Dr. Khaled EL Elfakhri, Dr. Yazan Batarseh, Dr. Quoc-Viet Duong, Dr. Andrew Branon, Ihab, Kamal, Sweilem, Lucy, Euitaek. I spent a joyful time with you guys.

My mother, my father, my wife, without you I would not be what I'm now. Thank you for your support and prayers. Also, I am thankful to my American mother, Donna Alexander Cary for taking care of me during my study.

Table of Contents

Abstract	ii
Acknowledgments.....	iv
Table of Contents.....	v
List of Tables	x
List of Figures.....	xi
List of Abbreviations	xiii
CHAPTERS	1
1. REVIEW OF LITERATURE	1
1.1. The case of Augusta D	1
1.2. Alzheimer’s disease types	1
1.2.1. Early-onset AD (EOAD) and genetic mutations	2
1.2.2. Late-onset AD (LOAD)	2
1.3. Alzheimer’s disease diagnosis	2
1.4. Clinical presentation of Alzheimer’s disease	3
1.5. Neuropathology of AD.....	3
1.5.1. A β peptide and synaptic dysfunction.....	5
1.6. Risk factors of Alzheimer’s disease.....	6
1.6.1. APOE	7
1.6.2. APP and Presenilin Mutations	7

1.6.3.	Down syndrome	8
1.6.4.	Cardiovascular Health.....	8
1.6.5.	Diabetes mellitus.....	9
1.6.6.	Traumatic brain injury	10
1.6.7.	Plasma lipid levels	10
1.6.8.	Smoking	11
1.7.	APP processing by secretases	12
1.7.1.	Secretases	13
1.8.	Role of IAPP in Alzheimer’s disease.....	13
1.8.1.	Synthesis of IAPP	13
1.8.2.	IAPP receptors	14
1.8.3.	Physiological role of IAPP and its analogue pramlintide	15
1.8.4.	IAPP aggregation	15
1.8.5.	IAPP aggregates pathology in AD development	16
1.8.6.	The protective effect of soluble IAPP and pramlintide	18
1.9.	Lipid rafts	19
1.9.1.	Composition of lipid rafts	19
1.9.2.	Isolation of membrane lipid rafts	20
1.9.3.	Protein composition of lipid rafts	21
1.9.4.	Lipid rafts and Alzheimer's disease connection.....	21
1.10.	Gangliosides	22
1.10.1.	Synthesis and metabolism of gangliosides glycolipids.....	22
1.10.2.	Functions of gangliosides.....	24

1.10.3.	GM1 ganglioside and Alzheimer's disease.....	25
1.10.4.	Pre-requisite of GM1 ganglioside clustering to induce GAB β generation	28
1.10.5.	Lipid rafts and ganglioside-protein interactions.....	29
1.11.	The TgSwDI mouse model	29
1.11.	Hypothesis and aims.....	30
2.	ISOLATION AND CHARACTERIZATION OF LIPID RAFTS FROM TgSwDI MOUSE MODEL BRAIN.....	31
2.1.	Abstract	31
2.2.	Introduction	32
2.3.	Methodology.....	34
2.3.1.	Materials and chemicals.....	34
2.3.2.	Optimization of fractionation.....	34
2.3.3.	Characterization of lipid rafts by SDS-PAGE	36
2.4.	Results.....	37
2.4.1.	The fractionation of lipid rafts was not optimized in the first three trials.	37
2.4.2.	Lipid rafts are localized in fraction 2 in the final optimization	37
2.4.3.	The amyloidogenic pathway proteins are localized in membrane rafts.....	37
2.4.4.	Different proteins other than the amyloidogenic pathway proteins were observed in lipid rafts.	38
2.5.	Discussion	39
2.6.	Figures and legends.....	41
3.	AMYLIN AND PRAMLINTIDE MODULATE γ -SECRETASE ACTIVITY AND APP PROCESSING IN LIPID RAFTS	47

3.1.	Abstract	47
3.2.	Introduction	48
3.3.	Methodology	50
3.3.1.	Materials and Chemicals.....	50
3.3.2.	Preparation of amylin and pramlintide	51
3.3.3.	Mice and treatment protocols.....	51
3.3.4.	Brains collection and handling.....	52
3.3.5.	Homogenization of mice brains	52
3.3.6.	A β extraction from mice brain homogenates.....	53
3.3.7.	A β quantification by ELISA	53
3.3.8.	Immunoblotting by SDS-PAGE	54
3.3.9.	Cryosectioning of mice brains	58
3.3.10.	Immunohistochemistry.....	58
3.3.11.	GM2 ganglioside analysis by ELISA.....	59
3.3.12.	Assay of lysosomal enzyme activities.....	60
3.3.13.	Isolation of lipid rafts	60
3.3.14.	Statistical analysis	60
3.4.	Results	61
3.4.1.	Treatment with amylin or pramlintide increases A β burden measured by ELISA.	61
3.4.2.	Treatment with amylin or pramlintide increases A β deposition as measured by IHC analysis	61
3.4.3.	Amylin and pramlintide have no clear effect on APP processing when measured in brain homogenate.....	62

3.4.4.	Amylin and pramlintide modulate APP processing in lipid rafts	63
3.4.5.	Amylin or pramlintide modulate GM1, GM2 and B4GALNT1 in total homogenate and/or lipid rafts	63
3.4.6.	Amylin and pramlintide decrease post-synaptic marker PSD-95 and induce the formation of cleaved caspase-3.....	65
3.4.7.	Amylin and pramlintide increase microglial activation without altering astrocytes and IDE	65
3.4.8.	LRP1 localization in lipid rafts is decreased by both peptides	66
3.4.9.	Amylin receptor level does not change after treatments.....	66
3.5.	Discussion	67
3.6.	Figures and legends	72
4.	SUMMARY AND CONCLUSION	92
4.1.	Future directions.....	93
5.	REFERENCES	94

List of Tables

Table 2.3. 1. Table of chemicals used for lipid rafts isolation.....	34
Table 3.3. 1. Table of chemicals utilized in this project.	50
Table 3.3. 2. The list of primary antibodies used to probe the membranes in Western blotting..	55
Table 3.3. 3. The preparation of polyacrylamide gels for SDS-PAGE.....	57
Table 3.4. 1. Lysosomal enzyme specific activity in mice brain tissues.	64

List of Figures

Figure 1.7. 1. APP processing pathways.....	12
Figure 1.8. 1. Primary amino acid sequence for human amylin, pramlintide, mouse and rat amylin.	16
Figure 1.10. 1. The biosynthesis of gangliosides.....	23
Figure 1.10. 2. The interaction of A β with GM1.....	26
Figure 2.6. 1. The optimization of lipid rafts fractionation	41
Figure 2.6. 2. The separation of lipid rafts using discontinuous sucrose gradient and ultracentrifugation.....	42
Figure 2.6. 3. Characterization of APP and BACE1 in lipid rafts.....	43
Figure 2.6. 4. Characterization of γ -secretase complex subunits in lipid rafts	44
Figure 2.6. 5. Characterization of P-gp, LRP1, and RAMP3 in lipid rafts.....	45
Figure 2.6. 6. Characterization of GCS, B4GALNT1, and GM1 in lipid rafts.....	46
Figure 3.6. 1. Effect of amylin and pramlintide treatments on A β burden in TgSwDI mice brains measured by ELISA.....	72
Figure 3.6. 2. Effect of amylin and pramlintide treatments on total A β burden in TgSwDI mice brains measured by IHC.....	74

Figure 3.6. 3. Effect of amylin and pramlintide treatments on total A β burden in TgSwDI mice brains measured by IHC.....	75
Figure 3.6. 4. Effect of amylin and pramlintide on APP and BACE1 in total brain homogenate.	77
Figure 3.6. 5. Effect of amylin and pramlintide on sAPP production in total brain homogenate.	78
Figure 3.6. 6. Effect of amylin and pramlintide on γ -secretase in total brain homogenate	79
Figure 3.6. 7. Effect of amylin and pramlintide on APP and BACE1 in lipid rafts	80
Figure 3.6. 8. Effect of amylin and pramlintide on γ -secretase complex subunits in lipid rafts ..	81
Figure 3.6. 9. Effect of amylin and pramlintide effect on ganglioside production measured from total brain homogenate.....	82
Figure 3.6. 10. Effect of amylin and pramlintide on ganglioside production measured from lipid rafts	83
Figure 3.6. 11. The effect of amylin and pramlintide on GM2 gangliosides production in total brain homogenate and lipid rafts.....	84
Figure 3.6. 12. Treatments with amylin and pramlintide impair the post-synaptic marker PSD-95.	85
Figure 3.6. 13. Treatment with amylin and pramlintide did not alter synaptic markers in lipid rafts	86
Figure 3.6. 14. The effect of amylin and pramlintide on caspase-3 and MMP9	87
Figure 3.6. 15. The effect of amylin and pramlintide on neuroinflammation and IDE	88
Figure 3.6. 16. The effect of treatment on astrocytes activity determined by IHC	89
Figure 3.6. 17. The effect of treatments on P-gp and LRP1 in lipid rafts.....	90
Figure 3.6. 18. The effect of treatments on amylin receptor.....	91

List of Abbreviations

ABC	ATP-binding cassette
AD	Alzheimer's disease
ADAM10	A Disintegrin and metalloproteinase domain-containing protein 10
AICD	APP intracellular domain
APLP	APP like protein
APOE	Apolipoprotein E
APP	Amyloid precursor protein
A β	Amyloid beta
B3GALT4	Beta-1,3-Galactosyltransferase 4
B4GALNT1	Beta-1,4-N-Acetyl-Galactosaminyltransferase 1
BACE1	Beta-site amyloid beta precursor protein-cleaving enzyme
BBB	Blood-brain barrier
BCA	Bicinchoninic acid
BSA	Bovine serum albumin
CAA	Cerebral amyloid angiopathy
CNS	Central nervous system
Cox-2	Cyclooxygenase-2
CSF	Cerebrospinal fluid
CTE	Chronic Traumatic Encephalopathy

CTF	C-terminal fragment
CTR	Calcitonin receptor
CVD	Cardiovascular disease
DRM	detergent resistant microdomains
DS	Down syndrome
EDTA	Ethylenediaminetetraacetic acid
ELISA	Enzyme linked immunosorbent assay
EOAD	Early onset Alzheimer's disease
GABA	Gamma-Aminobutyric acid
GAPDH	Glyceraldehyde 3-phosphate dehydrogenase
GCS	Glucosylceramide synthase
GPCR	G-protein coupled receptor
GWAS	Genome wide association study
Hex	Hexaminidase
HRP	Horseradish peroxidase
IAPP	Islet amyloid polypeptide
Iba1	Ionized calcium binding adaptor molecule 1
IDE	Insulin degrading enzyme
IgG	Immunoglobulin G
I κ B- α	Nuclear factor of kappa light polypeptide gene enhancer in B-cells inhibitor, alpha
IL-1 β	Interleukin-1 β
I.P.	Intraperitoneal
JAM	Junctional adhesion molecule

LOAD	Late onset Alzheimer's disease
LRP1	Low density lipoprotein receptor-related protein 1
LTD	Long-term depression
LTP	Long-term potentiation
MCI	Mild cognitive impairment
MMP9	Matrix metalloproteinase
nAChr	Nicotinic acetylcholine receptor
NFT	Neurofibrillary tangles
NMDAR	N-methyl-D-aspartate receptor
NP-40	4-Nonylphenyl-polyethylene glycol
O.C.T	Optimal cutting temperature
PBS	Phosphate buffer saline
PEN2	Presenilin enhancer 2
PET	Positron emission tomography
P-gp	P-glycoprotein
PMSF	Phenylmethylsulfonyl fluoride
PSD-95	Post-synaptic density-95
PSEN	Presenilin
PVDF	Polyvinylidene difluoride
RAMP	Receptor activity modifying protein
RNA	Ribonucleic acid
sAPP	Soluble amyloid precursor protein
SDS-PAGE	Sodium dodecyl sulfate – Polyacrylamide Gel Electrophoresis

SNAP-25	Synaptosome Associated Protein-25
SORL1	Sortilin-related receptor 1
SP	Senile plaques
T2DM	Type 2 diabetes mellites
TBI	Traumatic brain injury
TBST	Tris-buffered saline and tween-20
TEMED	Tetramethylethylenediamine
Thio-S	Thioflavin-S
TNE	Tris-NaCl-EDTA
VAMP	Vesicle-associated membrane protein
ZO-1	Zona occludens-1
α -Man	α -Mannosidase
β -gal	β -galactosidase

CHAPTERS

1. REVIEW OF LITERATURE

1.1. The case of Augusta D

Augusta D was the first patient to credit the dementia diagnosis by Dr. Alois Alzheimer (1). Her condition was known later as Alzheimer's disease (AD). Alzheimer described the case in a conference as women aged 51 years having 'peculiar disease of the cerebral cortex' with escalating language and memory deterioration, delusion, and hallucination (1, 2). These features are the basic for AD symptoms these days.

1.2. Alzheimer's disease types

The amyloid hypothesis of AD is built on the accumulation of amyloid β ($A\beta$) protein which causes synapse deterioration and neuronal cell destruction (3). The prevalence of AD due to autosomal dominant mutations is less than 1% according to Alzheimer's Association (4). Most commonly, these mutations are encoded in the genes of $A\beta$ producing proteins (5-7), which cause familial AD in subjects younger than 65 years of age (8, 9). In contrast, most of the etiological features that trigger the development of late onset AD are not well characterized (10).

1.2.1. Early-onset AD (EOAD) and genetic mutations

A β is generated from amyloid precursor protein (APP) after its processing by the β -site APP cleaving enzyme 1 (BACE1) followed by γ -secretase, a complex protein of different subunits including presenilin 1 and 2 (PSEN1/2), APH1, PEN2, and nicastrin. It was observed that mutations in APP, PSEN1, or PSEN2 will lead to the development of EOAD in most cases (5-7). These mutations initiate overproduction of A β which eventually will form oligomers and senile plaques (SP) which are neurotoxic (11, 12). Human subjects younger than 45 years of age have the highest possibility for developing EOAD due to mutations in these three genes, which is strongly associated with family history (8).

1.2.2. Late-onset AD (LOAD)

LOAD is considered a typical AD due to the different pathological and etiological factors that are involved in the development of the disease (13-16). Patients with LOAD express different biomarkers including the levels of tau and A β in the cerebrospinal fluid (CSF) and the incidence of carrying apolipoprotein ϵ 4 (APOE ϵ 4) allele (17). The allelic frequency of APOE ϵ 4 is 20-25% among general people; however, patients with LOAD have 50-65% chance to be APOE ϵ 4 carriers (8), highlighting APOE ϵ 4 as the most common genetic factor for sporadic AD (18). Moreover, homozygote APOE ϵ 4 decrease the age of initiating AD by 10 years compared to noncarriers (19). On the other hand, ϵ 2 allele provides some protection against AD (20).

1.3. Alzheimer's disease diagnosis

The current methods help in diagnosing AD and other forms of dementia separately (21) and they are based on using the positron emission topography (PET) scan that utilizes different radiolabel tracers which detect A β plaques in living human brains (22). The PET scan has 96% sensitivity

and 100% specificity in AD diagnosis (23). Another diagnostic method include measuring the level of A β ₄₂ and p-tau in the CSF (24) which has 85-95% accuracy (22). Multiple research groups are trying to find less invasive diagnostic procedures such as blood test (25) or microRNA profiling (26).

1.4. Clinical presentation of Alzheimer's disease

In AD, the overall cognitive impairment is designated by impairment of memory, language, praxis, visuospatial and executive functions; however, memory might be retained in AD cases with focal cortical symptoms (8). In addition, the posterior cortical atrophy (apraxic or visual presentations) seems to be associated with younger subjects at onset with mean around 60 years than does typical AD (amnestic presentation or LOAD) (27-29). Non-memory phenotypes in early-onset AD is seen roughly in one fourth of cases in whom language phenotypes and visual or apraxic are most frequent (30, 31).

1.5. Neuropathology of AD

AD causes significant structural and functional disruption of healthy brain. There is a progressive loss of pyramidal cells in the cortex which mediate higher cognitive functions (32). Moreover, early synaptic dysfunction and impairment of neuronal circuit communication are also observed in AD (3). Neurodegeneration starts in the entorhinal cortex and hippocampus (33), triggering early memory impairment and learning shortage in AD (34). Subsequently, the neurodegeneration spread throughout the temporal cortex and parietal areas, then to the frontal cortex and eventually to the remaining of neocortex (34). Furthermore, AD causes damage to the limbic system (35) including the hippocampus and the fibers that connect the hippocampus to the cerebral cortex, thalamus, amygdala, and cingulate gyrus (34), which result in behavioral changes and cognitive

impairment (35). Beside cognitive impairment, AD patients can't perform daily life activities and they experience emotional, personality, and psychiatric disturbances (34).

In AD, the neuropathological findings are characterized by extracellular deposition of SP and intracellular neurofibrillary tangles (NFT) of hyper-phosphorylated tau protein (36). Deposition of SP starts in the basal region of the temporal, frontal, and occipital lobes and spread to affect the primary sensory areas (36). In contrast, NFT first affects the transentorhinal regions and progress to the limbic system and eventually to the neocortex (37). One study described 3 patterns of distribution for NFT in AD: the typical pattern as mentioned above, hippocampal spread with less atrophy (more NFT in the cortex compared to hippocampus), and finally the predominant limbic pattern (38). In contrast, SP density is consistent between the three patterns (36). The preserved hippocampal pattern is correlated with early onset AD which is more aggressive with higher prevalence of atypical pre-sensation (36). Although the formation of NFT occurs earlier and its pattern is different, the onset of AD would also be determined by A β deposits (39). Generally, typical EOAD cases have increased NFT (40, 41) and SP (42) and higher neuronal death as compared to atypical EOAD (43) or LOAD cases (31). Therefore, it seems that LOAD requires a less pathological load compared to EOAD to exhibit AD symptoms (41).

The soluble oligomeric A β in LOAD and EOAD are more toxic to neuronal cells than fibrillary A β (36). Few studies have shown good correlation between neurotransmitter activity and the level of oligomers (44). Moreover, these studies showed a different oligomeric pattern between LOAD and EOAD: LOAD has less pentamers in the insoluble fraction compared to EOAD (44) which could be another explanation for the difference in the pathogenesis of LOAD and EOAD. In elderly, the association of amyloid load and dementia is not strong compared to younger patients, because in old patients, vascular diseases have a significant contribution in dementia (45).

1.5.1. A β peptide and synaptic dysfunction

The synaptic dysfunction induced by A β is still an important factor in AD (46-48) and there is unstoppable effort to understand how it contributes to AD development and progression. The monomeric A β which is produced from APP forms fibrils, protofibrils, and annular structure (49), and oligomers (50, 51). A β oligomers can organize into dimers, trimers, tetramers, and high orders arrays which form annular structures (52). The fact that oligomeric A β , compared to A β plaques, disrupts synaptic function and induce memory loss came from the report by Lambert et al (1998) who showed that soluble A β oligomers, interfered with synaptic function, triggered loss of dendritic spines and disrupted NMDAR dependent long-term potentiation (LTP) (53). Since then, different research group confirmed that A β oligomers facilitate NMDA dependent long-term depression (LTD) and disrupt NMDA dependent LTP (54-57). It is apparent that A β at higher concentrations interferes with pre-and postsynaptic transmission (58). Initially, it was hypothesized that A β directly affects post synaptic processes after the finding that A β localized in spines of dissociated hippocampal neurons (59) suggesting the synaptic dysfunction could be a result of agonist effect on NMDARs (60). Moreover, the localization of A β in post synaptic ends in AD cases further confirmed this hypothesis (61). A β was also detected inside the neuronal cells in healthy subjects (62), implying that intraneuronal accumulation of A β peptides preceded NFT or SP formation (63, 64).

Multiple reports demonstrated that A β_{42} is the major intraneuronal A β peptide (64). Intraneuronal A β was also found at the presynaptic endings of glutamatergic neurons in AD cases (65, 66) and it was observed that brief exposure of neurons to a low concentration of A β increased basic transmission and LTP, whereas higher concentration or longer exposure inhibited NMDAR dependent LTP and diminished the excitatory postsynaptic potential (67). These observations were

supported by the findings that soluble A β oligomers gradually increased the amount of glutamate at the synaptic cleft and providing an agonist effect on NMDARs (65, 67, 68). This hypothesis was confirmed by the findings that synaptic deficits was induced after acute exposure of neurons to low concentrations of A β , whereas postsynaptic alteration was induced after prolonged exposure to higher concentrations of A β (69). In addition, A β oligomers accumulate in the presynaptic terminals of glutamatergic neurons (70).

The ultrastructural assessment study by Gibson (71) was the first study that reported a possible decline in AD. Gibson reported the absence of decline in the superior frontal cortex in few AD cases compared to healthy subjects. One year after Gibson report, a study that was specifically designed to assess AD-related synaptic changes showed a loss of synapsin I, a synaptic protein, only in the hippocampus (72). Subsequent studies reported changes in specific synaptic proteins in the hippocampus (73, 74), temporal (75), frontal (76) and parietal lobes (77). These changes include both presynaptic (SNAP 25, synapsin I, synaptobrevin, synaptophysin, syntaxin, rab3a, VAMP2, and synaptotagmin) and postsynaptic (PSD-95 and drebrin) markers.

Synaptic damage begins very early in AD, and patients with MCI have shown loss of pre-synaptic proteins such as: SNAP-25, VAMP2, Synapsin 1, and synaptophysin and post-synaptic markers such as PSD-95 and Shank1 (78). Moreover, ultrastructural reports elucidated the progressive alteration of synapses at earlier stages of AD and in APP transgenic models (79, 80). In addition, the synaptic loss is much greater than cortical neuronal loss, suggesting that synaptic loss comes before the death of neuronal cells (81) with the remaining synapses compensating for the loss (82).

1.6. Risk factors of Alzheimer's disease

The risk factors of AD provide important aspect to AD predisposition prior to onset and provide designation of subjects who may be at higher risk. Aging is the most significant risk factor, also

other genetic, non-genetic, and modifiable risk factors are considered determinants of AD. The genome wide association studies (GWAS) have shown multiple new genes that increased AD disposition (83).

1.6.1. APOE

APOE is a 34 kDa protein produced from astrocytes, and it is encoded on chromosome 19q13 and it has three alleles which provides $\epsilon 2$, $\epsilon 3$ and $\epsilon 4$ isoforms (18). One major function of APOE in the CNS is to transport cholesterol to neurons (84). APOE $\epsilon 3$ is present in approximately 60% of the population and it does not carry a risk of AD (85, 86). In contrast, the second most common allele is $\epsilon 4$ followed by the $\epsilon 2$ allele. The GWAS have identified the $\epsilon 4$ allele of APOE gene as the greatest risk for AD (87, 88); in addition, APOE $\epsilon 4$ homozygosity or APOE $\epsilon 4$ /APOE $\epsilon 3$ heterozygosity has a significant risk of AD disposition from 8-12 to 3 fold, respectively (89). APOE $\epsilon 4$ is identified in 40% of AD cases (90) and subjects with APOE $\epsilon 4$ have deprived cognitive functions in childhood and develop AD earlier than those with APOE $\epsilon 3$ (91). The Multi Institutional Research of Alzheimer Genetic Epidemiology (MIRAGE) study revealed that subjects with head injury had a significant increased risk to develop AD (92) and patients who carried APOE $\epsilon 4$ allele and had suffered a head injury had a ten-fold increased risk to develop AD, unlike APOE $\epsilon 4$ non-carriers who have two-fold increased risk (93). Interestingly, $\epsilon 2$ isoform protects from developing AD and has a decreased risk than $\epsilon 3$ allele (86) which could be explained by the high frequency of $\epsilon 2$ allele among centenarians (94).

1.6.2. APP and Presenilin Mutations

As mentioned above mutations in the genes (PSEN1/2 and APP) are associated with the overproduction of A β . The 695 amino acid protein is the most common transcript variant of APP

in the CNS (95). More than 30 coding mutations in the APP have been recognized to cause autosomal dominant EOAD due to the overproduction of A β , increased susceptibility of A β to form aggregates, and shifts in the synthesis of pathologic A β_{42} (96). In contrast, one mutation in APP was found to protect from AD development (96). Mutations in presenilin 1, the active subunit in γ -secretase, are the most common genetic factor that triggers the development of EOAD (97). These mutations in presenilin alter its activity toward favoring more A β_{42} production (97).

1.6.3. Down syndrome

Down Syndrome (DS) is characterized by trisomy 21 and it is the most frequent chromosomal abnormality of 1 per 733 live births (95). This trisomy will result in three copies of APP protein, and that causes overproduction of A β and the development of EOAD in many of these subjects. Seventy percent of DS cases will develop AD with a lifespan 55-60 years of age (98).

1.6.4. Cardiovascular Health

Studies have reported substandard cognitive performance in patients suffering a cardiovascular disease (CVD) compared to healthy subjects (99). However, studying the role of CVD in AD is complexed by several issues, particularly severe CVD and dementia may favor a diagnosis of multi-infarct dementia and prohibit the clinical diagnosis of AD (100). Interestingly, in a population-based study, it was reported that the cohort groups with AD had lower risk of coronary artery disease and ischemic stroke (101). Different studies have shown discrepancy and inconsistency about the effect of hypertension due to the differences in study design such as variation in the age and time between measuring blood pressure and assessment of cognitive function (102-104). In contrast, observational studies showed consistent correlation between increased blood pressure in mid-life and later-life cognitive impairment, dementia, and AD (105).

The potential of hypertension to induce substandard performance could be explained by the increased injury of brain capillaries and increased protein infiltration (106), which in turn will trigger neuronal injury and A β accumulation (107). Interestingly, with increasing age, the elevated blood pressure becomes protective from developing AD. These observations were based on the fact that after AD development, the blood pressure decreased because of stiffening blood vessels, weight loss, and changes in blood flow (108).

1.6.5. Diabetes mellitus

Patients with type 2 diabetes mellitus (T2DM) have double the risk to develop AD (109, 110). The association of T2DM with sporadic AD is not well understood. The fact that T2D is associated with infarcts, but not with LOAD (111) suggests that infarcts decrease the threshold for amyloid to cause cognitive decline which could explain the link between T2D and LOAD (108). The Religious Orders Study has shown that patients with DM (> 55 years of age) have 65% greater risk to develop AD after mean age of 5.5 years period (112). Those patients had cognitive impairment particularly in perceptual speed (112). The molecular mechanism behind poor cognitive function with DM relies on the competition between insulin and A β for insulin degrading enzyme (IDE), thereby increases A β accumulation (89). Also, peripheral insulin infusion increased the level of A β ₄₂ in the CSF, A β deposition and tau hyperphosphorylation in LOAD (113, 114). Moreover, A β aggregation is increased by the increased age-related advanced glycation end-products that can occur in DM (89). Peripheral hyperinsulinemia was shown to decrease insulin uptake into the brain because of saturation, an effect which would result in downregulating the expression of IDE and decreasing A β clearance (108). These observation encouraged the use of insulin sensitizer, rosiglitazone, and intranasal insulin against sporadic AD (115). However, other

clinical studies have shown that the anti-inflammatory effect of antidiabetic is responsible for restoring the cognitive performance in patients who were diagnosed with AD and DM (89).

1.6.6. Traumatic brain injury

Traumatic brain injury (TBI) becomes significant healthcare problem (116, 117). Patients with TBI suffer chronic psychological and neurological morbidities (118). The ‘punch drunk syndrome’ is the first syndrome due to TBI that grab attention to neurodegeneration, and it is known as chronic traumatic encephalopathy (CTE) which affects sport professionals and veterans (119, 120). CTE shares common features with AD and TBI has been recognized to reduce AD onset time (121). Recent studies showed that AD and TBI share chronic inflammation features within the brain parenchyma (122). Following TBI the level of A β increases because of multiple factors. Firstly, the expression of APP increases post-TBI (123), secondly, upregulation of BACE1 and γ -secretase enzymes (124, 125). These factors offer explanation to how TBI increases the risk of AD development (126).

The degree of amyloid insult post-TBI is affected by neprilysin (89). Neprilysin is a membrane zinc metalloprotease that cleaves A β within the brain (89). In one study by Johnson and colleagues, it was shown that amyloid burden in post-TBI patients was the highest among those with more than 41 GT repeats in the promotor region of neprilysin gene, resulting in impaired A β clearance (127). However, neprilysin expression is increased post-TBI which would increase the amyloid clearance, although there is an increase in the expression of intra-axonal APP and PSEN1 (128).

1.6.7. Plasma lipid levels

Same as blood pressure, studies that link dyslipidemia to late life AD are inconsistent (129, 130); however, studies have shown a harmful effect of lipid profile measured in mid-life and risk of AD

development (108). These findings were supported by multiple genetic studies which revealed the susceptible genes in AD including APOE, ATP-binding cassette subfamily A member 7 (ABCA7), apolipoprotein J (APOJ), and sortilin-related receptor (SORL1). Functional studies have demonstrated the role of lipid rafts cholesterol in modulating APP processing by BACE1 and γ -secretase which lead to altered A β production (108). In contrast, epidemiological studies showed discrepancy in the association between dyslipidemia and the risk of AD, molecular studies showed little exchange between plasma and brain cholesterol, and randomized controlled trials showed no beneficial effect of statin therapy against AD (108).

1.6.8. Smoking

A meta-analysis explored the association between smoking and AD while accounting for tobacco-industry affiliation found no association in cross-sectional studies (131). However, studies with industrial affiliation showed protective effect of smoking against AD. Cohort studies, lacking tobacco-industry affiliation, found increased risk of AD due to smoking (108) especially in APOE4 non-carriers (132). Even though the relative risk for AD is small (RR = 1.2-1.6), 14% of AD cases are attributed to smoking due to its high prevalence (133). Smoking may affect inflammation, leading to activation of phagocytes and oxidative damage, or increase the free radicals, resulting in oxidative stress (134). In addition, smoking could increase AD risk by triggering CVD (108). On the other hand, tobacco may have protective effect, suggesting that nicotine induces increase in nicotinic acetylcholine receptors (nAChR) which opposing the loss of nAChR observed in AD (108).

1.7. APP processing by secretases

APP is a type I integral membrane proteins and it is ubiquitously expressed (135-137). The cleavage of APP occurs at many different cellular sites including plasma membrane, mitochondrial membrane, and trans-Golgi network (138). The parent protein, the 695-770 amino acid APP, is cleaved in most cell types by α -secretase (non-amyloidogenic pathway) to release sAPP- α and leaving the C-terminal fragment APP-CTF α or C83 peptide (139-141). The C83 peptide is then cleaved by γ -secretase to release APP intracellular domain (AICD) and 16 amino acid peptide, termed P3 (142). However, the amyloidogenic version of APP processing includes cleavage by BACE1 leaving the C-terminal fragment as APP-CTF β or C99 within the membrane and releases sAPP- β into the extracellular space followed by γ -secretase processing of C99 fragment, releasing the 40-43 amino acid A β and AICD (140, 141) (Figure 1.7.1). A β_{42} has higher aggregation behavior and more neurotoxic than A β_{40} . Despite that fact that APP is highly conserved evolutionarily, the peptide sequence of A β is not; in addition, non-human derived A β does not have aggregation behavior (142).

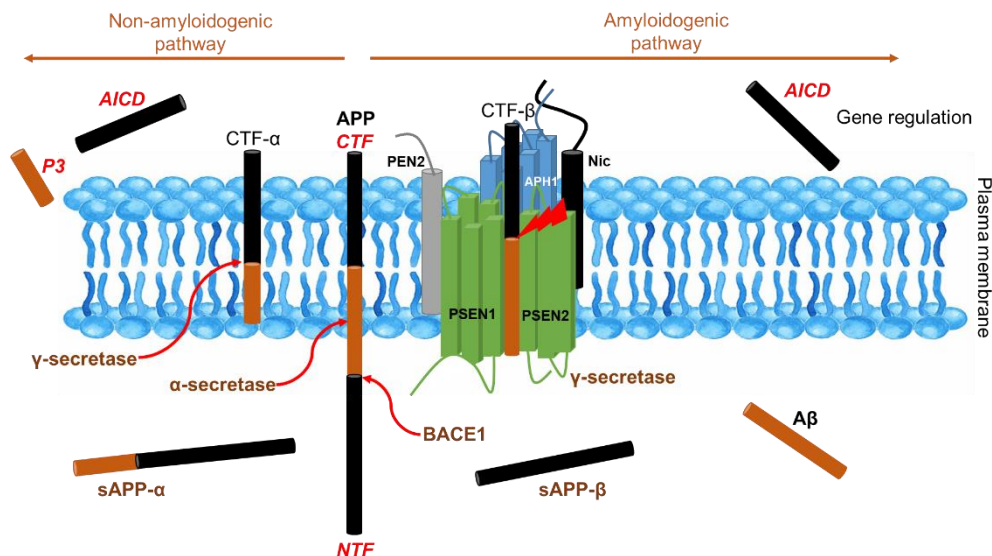


Figure 1.7. 1. APP processing pathways. Modified from reference (143).

1.7.1. Secretases

The cleavage function of α -secretase is not limited to APP, but it includes the processing of other peptides, for instance, TNF- α , TGF- α , and L-selectin (144). The processing of APP by α -secretase depends on A disintegrin and metalloproteinase domain-containing protein 10 (ADAM10) and MDC9 (145, 146). ADAM10 is expressed in different cellular organelles such as Golgi apparatus as well as the cell membrane, suggesting the processing of APP by α -secretase in these compartments (147, 148).

BACE1 is type I integral membrane aspartyl proteinase that functions at low pH (149). It has higher affinity for APP with Swedish type missense mutation (K595M596 to N595L596) which causes EOAD (familial AD) (150). BACE1 is usually expressed in Golgi apparatus and endosomes (151). These findings supported the notion that BACE1 cleaves APP, after its trafficking from cell membrane, in endosome to generate A β (152). However, opposite results were obtained from APP harboring the Swedish mutation where they demonstrated generation of A β independent of endocytosis (152-154).

γ -secretase is aspartyl protease and its complex is composed from different subunits including presenilin 1, presenilin 2, nicastrin, presenilin enhancer 2 (PEN2), and anterior pharynx defective 1 (APH1). PSEN1 and PSEN2 contain eight transmembrane domains (155) and they are localized in the membrane of endoplasmic reticulum, cis-Golgi apparatus (156, 157), and cell membrane (158, 159).

1.8. Role of IAPP in Alzheimer's disease

1.8.1. Synthesis of IAPP

The highly conserved human amylin or Islet Amyloid Polypeptide (IAPP) is a 37-amino acid (aa) that is coded by a single-copy gene on chromosome 12 (160, 161). Amylin is first synthesized as 89-aa pre-proIAPP containing a 22-aa signal peptide (162, 163). The 67-amino acid proIAPP is produced after the removal of signal peptide (164). ProIAPP is processed to IAPP via consequent cleavage of the C-terminus by prohormone convertase (PC) 1/3 in the Golgi apparatus followed by PC2 mediated cleavage of the N-terminus in the secretory vesicles (165). Then, the dibasic amino acids are removed by carboxypeptidase E at the C-terminus (166). In addition, post-transcriptional modifications such as amidation of C-terminus tyrosine, O-glycosylation of threonines, and disulfide bridge formation occur before the release from the islet β -cells (167, 168). IAPP is co-stored with insulin in a ratio of 1-2:50 and they are secreted together (169, 170). IAPP has a half-life of 13 min when measured in rat and it is eliminated primarily by the kidney (171); in addition, IAPP is cleared by the action of IDE (172).

1.8.2. IAPP receptors

IAPP receptor is a seven transmembrane domain G-protein coupled receptor (GPCR) that is composed from a heterodimer complex of the calcitonin receptor (CTR) and a receptor activity modifying protein (RAMP) (173, 174). RAMP is a non-receptor protein that has three isoforms RAMP1-3 (164). IAPP has low affinity to CTR, but by forming the heterodimer complex CTR-RAMP, the receptor activity increased significantly (175, 176). IAPP has shown high selectivity to CTR complexed with RAMP2 or RAMP3 (164). IAPP has a broad distribution in the brain which explains its physiological effect in the CNS (177).

1.8.3. Physiological role of IAPP and its analogue pramlintide

IAPP has multiple physiological roles including controlling glucose level by decreasing the post-prandial glucagon release (169, 178), without affecting the release of glucagon as a response to hypoglycemia (179). Furthermore, IAPP inhibits the gastric emptying, which delays the intestinal absorption of glucose (180), an effect of its clinically available analogue pramlintide as well (181). The most important function of IAPP is to serve as a satiating hormone (182) by binding to different brain regions including the area postrema, hypothalamus, and the nucleus of solitary tract (183), thus IAPP controls food consumption (184, 185). In addition, IAPP lowers body weight and increases energy expenditure as shown in rats (186). Mechanistic studies have shown that IAPP increases the brown adipose tissue activity (187) and pretreatment with IAPP receptor antagonist AC187 eliminated the effect of IAPP on brown adipose tissue (187).

Because of the self-aggregation behavior of IAPP, which lead to toxic effect, pramlintide was developed to replace amylin in the treatment of DM (188). The amino acids sequence of pramlintide is similar to rodent IAPP amino acid sequence (Figure 1.9.1.); however, it does not form aggregates like hIAPP and it keeps the same physiological activity of hIAPP (189). Pramlintide was used in several studies against obesity and T2DM. It increases the level of leptin sensitivity, resulting in decrease meal volume (190), and it control blood glucose and insulin demand (191).

1.8.4. IAPP aggregation

The misfolded IAPP, was first isolated from pancreatic extracts from T2DM patients in the form of elongated fibrils with many stranded β sheets (192). Although IAPP is highly conserved, the middle amino acid sequence (aa22-29aa) is different between species. In mice and rats, the middle sequence of IAPP has three proline residues which prevent the formation of β -sheet conformation

that is required for IAPP aggregation; however, the amyloidogenic region in human IAPP (hIAPP), does not have proline residues (193, 194). The amyloidogenic region (aa22-29aa) of hIAPP is important for in vitro and in vivo aggregation (Figure 1.8.1) (195-197). On the other hand, IAPP aggregation can result from overexpression or impaired processing of proIAPP (198-200).

Human IAPP

Lys-Cys-Asn-Thr-Ala-Thr-Cys-Ala-Thr-Gln-Arg-Leu-Ala-Asn-Phe-Leu-Val-His-Ser-Ser-Asn-Asn-Phe-Gly-**Ala**-Ile-Leu-**Ser-Ser**-Thr-Asn-Val-Gly-Ser-Asn-Thr-Tyr-NH₂

Pramlintide

Lys-Cys-Asn-Thr-Ala-Thr-Cys-Ala-Thr-Gln-Arg-Leu-Ala-Asn-Phe-Leu-Val-His-Ser-Ser-Asn-Asn-Phe-Gly-**Pro**-Ile-Leu-**Pro-Pro**-Thr-Asn-Val-Gly-Ser-Asn-Thr-Tyr-NH₂

Rat/Mouse amylin

Lys-Cys-Asn-Thr-Ala-Thr-Cys-Ala-Thr-Gln-Arg-Leu-Ala-Asn-Phe-Leu-Val-**Arg**-Ser-Ser-Asn-Asn-Phe-Gly-**Pro-Val**-Leu-**Pro-Pro**-Thr-Asn-Val-Gly-Ser-Asn-Thr-Tyr-NH₂

Figure 1.8. 1. Primary amino acid sequence for human amylin, pramlintide, mouse and rat amylin. Adapted from reference (193).

1.8.5. IAPP aggregates pathology in AD development

IAPP fibrils and oligomers were identified in patient with T2DM and cognitive decline (201), as well as in rodent models expressing hIAPP, which led to neurological defects (202). Importantly, IAPP was observed to co-precipitate with A β to form diffuse and dense SP (201, 203). The de novo IAPP produced in the brain is undetectable (201, 202), indicating that cerebral amylin is obtained from peripheral source. This notion was confirmed by demonstrating that IAPP deposits were detected in the pericapillary spaces and blood vessels walls in the brain (201). Moreover,

IAPP oligomers access the brain from blood by inducing inflammatory response that destroys BBB integrity (204, 205). There are different pathways through which IAPP aggregates could accelerate the progression of AD which are discussed below:

1.8.5.1. Interaction with A β

The co-precipitation of IAPP and A β in SP indicates that they exert toxic effect synergistically (201, 203). There are two regions of hIAPP (aa 8 to 20 and aa 21 to 37) that have increased binding affinity for A β . Accordingly, A β has two regions that have high binding affinity to hIAPP (aa 11 to 21 and aa 23 to 37) (206). Furthermore, hIAPP and A β can form β -sheet-rich U-bend fibrillar structure (207, 208).

1.8.5.2. Exerting independent toxic effect

Amyloid aggregates from different proteins have global toxic responses (209-211). IAPP shares similar cytotoxic effect with A β (212-214), suggesting that IAPP aggregates have neurotoxic effect and can provoke AD pathology. The independent toxic effect of IAPP can occur through different pathways including interaction with lipid components of cell membrane and inducing disruption of cell membrane (215-217). The interaction of IAPP with cell membrane introduces a channel-like pore on the cell membrane which destabilizes the intracellular homeostasis and induces cell death (218, 219). Moreover, IAPP oligomers have induced astrocytes and neuronal cell death by altering Ca²⁺ homeostasis (213, 220). Other cytotoxic pathways have been reported such as activating pro-inflammatory IL-1 β (221, 222), which induces pancreatic β -cells death (223). IL-1 β has been observed to increase BACE1 expression (224), stimulate A β production, and disrupt synaptic function (225). One recent study used a rat model overexpressing hIAPP and the findings showed accumulation of activated microglia in IAPP deposition sites which was accompanied by cognitive impairment (202). Furthermore, an early study demonstrated that IAPP aggregates

induces oxidative stress genes such as I κ B- α and cox-2 in rat cortical neurons, which led to cell death (226).

1.8.6. The protective effect of soluble IAPP and pramlintide

It has been observed that in AD rodent models, IAPP aggregates and its co-precipitation with A β were not detected in the brain, even in the presence of T2DM (227). In addition, patients in advanced age with MCI or AD have lower level of soluble IAPP in plasma than age matched healthy subjects (177, 228). However, during T2DM progression, soluble IAPP exists in low concentration due to its aggregation and the death of islet β -cells. Using soluble IAPP (or pramlintide) against AD is based on the notion that A β competes with amylin on amylin receptor to induce its toxic effect; therefore, increasing the level of soluble IAPP would decrease the binding of A β to amylin receptor and provide neuroprotection (177, 228). Zhu et al have showed that chronic treatment with human amylin reduced the level of inflammatory markers Iba1 and CD68, phosphorylated-tau, and A β in AD mouse models. These effects were abolished by amylin receptor antagonist (229). Furthermore, amylin treatment recovered the expression of different genes in the cortexes of 5XFAD mouse model toward similar expression as in the wild-type mice (230). The two genes influenced by amylin treatment were CD68 (proinflammatory protein) and ATP5b (a mitochondrial protein), and human data demonstrated that the expression of CD68 and ATP5b were significantly correlated with NFT and cognition (230). In another study, treatment with amylin or pramlintide showed improvement in cognitive function, increased the clearance of A β ₄₂ into the CSF, and increased the clearance of A β from brain to blood (231). Furthermore, pramlintide reduces A β -induced oxygen species in the brain (232), ameliorate inflammation in a rodent model of AD (228), and decreased the deficiency in LTP induced by IAPP and A β (233).

1.9. Lipid rafts

The lipid structure of cell membrane is known as lipid rafts. The concept of lipid rafts was first introduced to explain the generation of glycolipid-rich apical membrane of epithelia cells (234). Later, these rafts were identified as a principle of membrane sub-compartmentalization in different membrane functions including endocytosis, post-Golgi trafficking, and signaling (235). The notion of lipid rafts was introduced at the 2006 Keystone Symposium of Lipid Rafts and Cell Function: “Lipid rafts are small (10–200 nm), heterogeneous, highly dynamic, sterol- and sphingolipid-enriched domains that compartmentalize cellular processes. Small rafts can sometimes be stabilized to form larger platforms through protein-protein and protein-lipid interactions” (236). These rafts are enriched with cholesterol and glycosphingolipids with highly saturated fatty acids compared to the surrounding membrane areas (237). These saturated fatty acids introduce compactness with sphingolipids, which eventually results in phase separation (237). The insolubility of lipid rafts in nonionic detergent is attributed to the this kind of compactness and phase separation (238).

1.9.1. Composition of lipid rafts

Lipid rafts composition have been analyzed by several preparations techniques which collectively showed that lipid rafts are enriched with cholesterol and glycosphingolipids (237). For example, the isolated rafts from MDCK cells by 1% Triton X-100 contained 14 mol% sphingomyelin and 32 mol% cholesterol compared to 1 mol% sphingomyelin and 12 mol% cholesterol in whole cells (239). In addition, membrane rafts from DMCK cells were enriched with 5-fold in gangliosides and sulfatides compared to the intact cell. In rafts isolated from RBL-2H3 cells, 50% of the fatty acids in the plasma membrane are saturated or contain a single double bond; however, the percentage increases to 60% in fatty acid from rafts prepared by 0.1% Triton X-100 extraction

(240). Thus, saturated fatty acids are moderately enriched in lipid rafts compared to plasma membrane. Lipid rafts prepared by detergent-free protocol from KB cells have 2-fold increase in cholesterol and 30% increase in sphingomyelin compared to bulk plasma membrane (241), and they are supplemented with ethanolamine plasmalogens (241).

Plasma membrane has two leaflets, the exofacial (which contains lipid rafts) and cytofacial (which contains ethanolamine-containing glycerophospholipids) leaflets, stating that rafts are bilayer structure (241). Membrane rafts prepared from KB cells had lower glycerophospholipids compared to nondetergent rafts. In addition, membrane rafts had lower level of phosphatidylethanolamine at the cytofacial leaflet as well as low level in ethanolamine plasmalogens compared to nondetergent rafts (241). On the other hand, 60% of the rafts' phospholipids contained monounsaturated and saturated fatty acids; however, 40% of plasma membrane and nondetergent lipid rafts contain monounsaturated and saturated fatty acids (241).

1.9.2. Isolation of membrane lipid rafts

Lipid rafts are known as DRM (detergent-resistant membrane) because of insolubility in cold 1% Triton X-100 (239). The detergent molecule forms holes after their partitioning in plasma membrane, followed by micellar fragments formation (242). Temperature is a crucial factor in determining lipid behavior; therefore, reduction in the temperature alone could potentially alter lipid organization (243). The formation of holes results in mixing the two leaflets and alteration of their lipid composition. Even without mixing, the two leaflets have different composition and different sensitivity to Triton X-100 (243). DRMs are fractionated by ultracentrifugation using discontinuous sucrose gradient where rafts float at the top fraction (usually 5% sucrose) (239). These top fractions are enriched with cholesterol, glycosylphosphatidylinositol (GPI)-linked proteins, and lipid raft marker (flotillin-1) (237). Other detergent such as NP-40, Lubrol, CHAPS,

octyl-glucoside, Brij 98, and low concentrations (< 1%) of Triton X-100 are utilized to isolate lipid rafts (244, 245). Although there is overlap in the isolated proteins between these different detergents, significant differences were observed (244, 245). Therefore, the products of lipid rafts depend mainly on the method of isolation. On the other hand, detergent-free preparations, such as sodium bicarbonate, have been used. The high pH of sodium bicarbonate buffer aids in the isolation of peripheral membrane proteins after sonication and ultracentrifugation in discontinuous sucrose gradient (246).

1.9.3. Protein composition of lipid rafts

Different proteins were identified in DRMs including flotillins, caveolins, GPCR, growth factor receptors, kinases, APP, BACE1, γ -secretase, PSD-95, SNAP-25 and many other proteins (246-253). Different mechanisms are involved in anchoring these proteins to lipid rafts. For instance, the transmembrane of some proteins partitions in cholesterol-enriched membrane domains (254), whereas other proteins are localized in DRMs because of lipid modification like the Src family kinases and GPI-anchored proteins. (255, 256).

1.9.4. Lipid rafts and Alzheimer's disease connection

1.9.4.1. Association of secretases with lipid rafts

Lipid rafts are considered the stage for APP processing. BACE1 was shown to be an inhabitant of lipid rafts (257), and anchoring BACE1 to lipid rafts demonstrated enhanced APP cleavage (258-260) and increased generation of A β (261). This effect was mediated by the level of cholesterol in the cell membrane, because the intermediate reduction of cholesterol enhanced the β -cleavage of APP outside the raft domains by bringing BACE1 and APP together (262). Unlike BACE1, cholesterol depletion studies did not show the link of α -secretase with lipid rafts (261).

γ -secretase is localized in membrane rafts as well (263). Such localization is highly responsive to reduction in cholesterol level, which implies a stringent criterion for localization in rafts (264, 265). Several biochemical studies have indicated that γ -secretase is localized with APP CTFs in membrane rafts of adult brain (266, 267) and neuroblastoma cells (268). Also, it was shown by Matsumura et al that γ -secretase cleaves β -CTF in stepwise sequential manner in lipid rafts (269).

1.9.4.2. Lipid rafts and $A\beta$

In a study by Kokubo et al, results from electron microscope revealed that 10% of lipid rafts with senile plaques showed colocalization of $A\beta_{42}$ with flotillin-1, without colocalization outside the plaques. These results suggest that lipid rafts are the initial site for $A\beta$ deposition (270).

1.10. Gangliosides

1.10.1. Synthesis and metabolism of gangliosides glycolipids

Glycolipids contain lipid moiety that linked to carbohydrate residue(s) through a glycosidic linkage (271). Glycolipids encompass lipid moiety as either a ceramide or a sphingoid are known as glycosphingolipids (271). These glycosphingolipids can be classified into different series based on the basic carbohydrate structure, namely, lacto-, lactoganglio-, neolacto-, ganglio-, isoganglio-, globo-, isoglobo-, gala-, neogala-, arthro-, schisto-, muco-, mollu-, and spirometo-series. Gangliosides are categorized as glycosphingolipids containing sialic acid (N-glycolylneuraminic acid or N-acetylneuraminic acid) residue (s). These glycosphingolipids have 0, 1, 2, and 3 sialic acid residue(s) bind to the galactose residue and they are categorized as asialo-, a-, b-, and c-series gangliosides, respectively (271).

The glycosylceramide synthase (GCS) catalyzes the initial step of ganglioside biosynthesis by glycosylating ceramide (272). The synthesis of endogenous glycosphingolipids starts in the

endoplasmic reticulum followed by adding different carbohydrate moieties in the Golgi apparatus (273). The synthesis of gangliosides from glycosphingolipids is depicted in Figure 1.10.1.

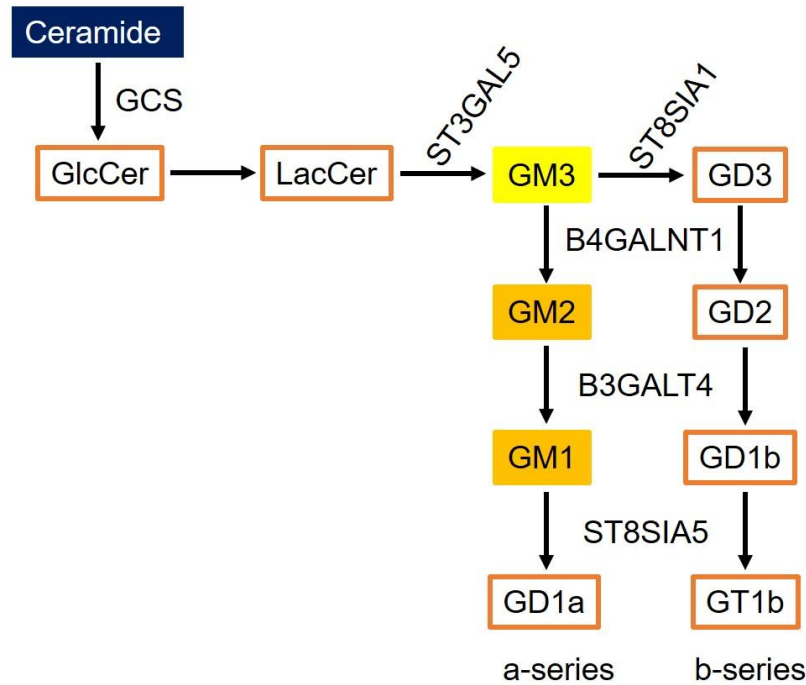


Figure 1.10. 1. The biosynthesis of gangliosides.

GCS, glycosylceramide synthase; GlcCer, glycosylceramide; LacCer, Lactosylceramide; ST3GAL5, ST3 Beta-Galactoside Alpha-2,3-Sialyltransferase 5 (or GM3 synthase); ST8SIA1, ST8 Alpha-N-Acetyl-Neuraminide Alpha-2,8-Sialyltransferase 1 (or GD3 synthase); B4GALNT1, Beta-1,4-N-Acetyl-Galactosaminyltransferase 1 (or GM2/GD2 synthase); B3GALT4, Beta-1,3-Galactosyltransferase 4 (or GM1/GD1b synthase); ST8SIA5, ST8 Alpha-N-Acetyl-Neuraminide Alpha-2,8-Sialyltransferase 5. Adapted from (274).

Gangliosides are enriched in lipid rafts (275) and their expression undergoes dramatic change during brain development (276, 277). For instance, in embryonic brains of rodents and humans, GD3 and GM3 are predominant. With developing, the production of GM3 and GD3 is down-

regulated with parallel up-regulation of GM1, GD1a, GD1b, GT1b. These changes are controlled by transcription factors (271), and possible epigenetic modification (278), which regulate the expression of glycosyltransferases (271, 276).

1.10.2. Functions of gangliosides

Gangliosides are ubiquitous molecules found in different body tissues, especially in the CNS (279). Gangliosides have different biological functions such as signaling, cell-cell adhesion and recognition within lipid rafts (280), or caveolae (281). Furthermore, gangliosides play a role in intracellular calcium homeostasis (282). The essential biological functions of these gangliosides were revealed by analysis of mice deficient in gangliosides synthases. For instance, the absence of GM3 synthase and GM2 synthase induced deafness and decreased nerve conduction velocity/altered motor function in mice, respectively (283-285). Mice overexpressing GM3 with no “brain-type” gangliosides, generated by knocking down of B4GALNT1 and ST8SIA1, had compromised memory and learning with aging, sensory abnormalities and weight loss (286, 287). When both B4GALNT1 and ST8SIA1 were knocked out, it led to cortical Purkinji neurons degeneration, cell death, axonal deterioration and severe lethality due to the absence of all gangliosides types, apart from GM3 (288, 289).

GM1 has been implicated in maintaining neuronal viability, conduction velocity and excitability through regulation of Na⁺ channels, and in combination with GD1a, neuronal Ca²⁺ homeostasis and improving synaptic plasticity in the CA3 hippocampal region (290). Also, GM1 regulates intracellular trafficking of the GluR2 subunit of AMPA type glutamate receptor where GluR2 subunit binds specifically to GM1 (291). These observations suggested that gangliosides have a biological modulatory function in the storage and transmission of information involved in memory.

1.10.3. GM1 ganglioside and Alzheimer's disease

In AD-brain tissues, there is a reduction in the level of gangliosides and changes in their regional distribution (272). The total gangliosides level is reduced in several brain regions in EOAD and LOAD patients (292, 293). When analyzed in brain cortexes from AD patients, low level of most common brain gangliosides was observed, but with increased GM2 and GM3 levels (294); however, the cortical lipid rafts of AD patients contained more GM1 and GM2 (295). In post mortem AD brains, GD1a and GM1 were bound to A β plaques forming GA β complexes, which inferred the role of GD1a and GM1 in AD pathology (296). The interaction of A β with gangliosides is an important step in understanding the pathological significance of gangliosides in A β assembly. In the formation of misfolded-type amyloidogenesis, the amyloidogenic protein forms an α -helix structure before the formation of β -sheet structure (297, 298). Kato and his colleagues showed that two α -helical structures are formed in A β through the interaction with lyso-GM1 micelles and this interaction was dependent on the carbohydrate part of GM1 but not on the carbohydrate part (299, 300). Different suggestions were made to explain the interaction between A β and GM1 (GA β). One possible scenario is that once GA β is formed on neuronal membrane, then another soluble A β binds to GA β and gets same conformation as GA β , which also considered a seed for another soluble A β binding (301). It was postulated that soluble A β originally interacts with GM1 on the cell membrane and then transforms to β -sheet structure as the bulk of A β on the cell membrane increases (302, 303). Alternatively, another group showed that the initial formation of α -helical structure of A β , after the interaction with GM1 containing membranes, induced dimerization to β -strand structure which potentially lead to higher-ordered structural aggregates (Figure 1.10.2.) (304, 305). GA β was detected at meaningful levels in an hAPP transgenic mouse model at 3months of age, at such age amyloid deposition has not been developed yet (306). This

finding supports the discovery of $\text{GA}\beta$ in the human brains with early but not advanced AD (307). Thus, GM1 may have role(s) in initiating the pathogenesis of AD, such as the nucleation and/or seeding of $\text{A}\beta$ oligomers and/or fibrils.

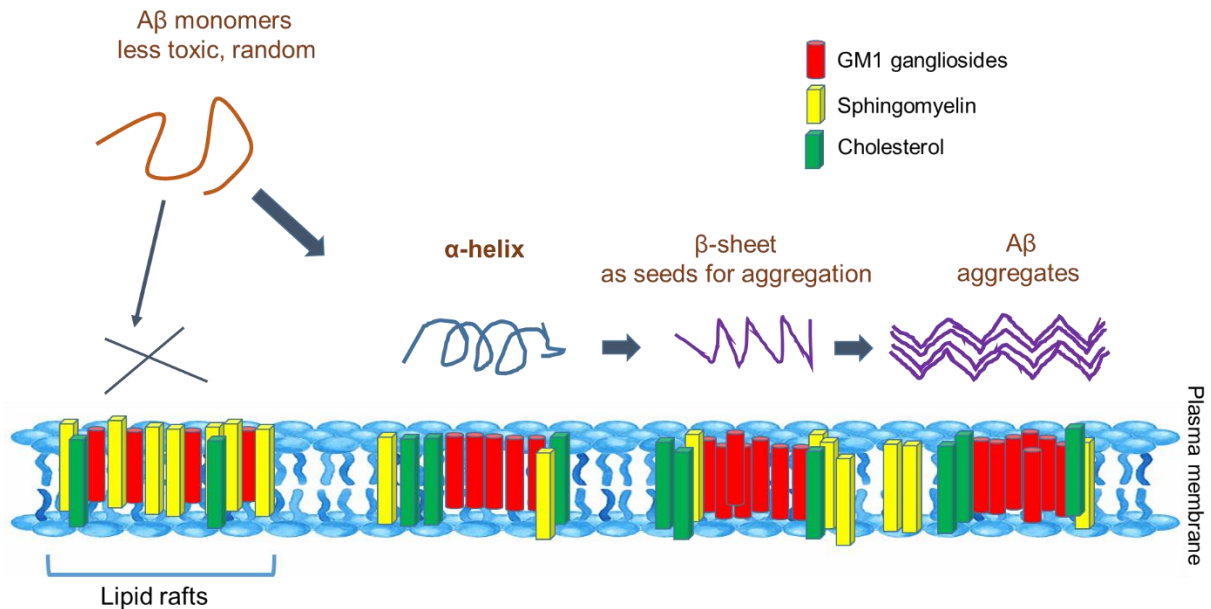


Figure 1.10. 2. The interaction of $\text{A}\beta$ with GM1. The depicted presentation was modified from (308)

One study compared the aggregation of human and rat $\text{A}\beta$ on raft model membranes, on neuronal cells, and in buffer (309). The authors of this study found that in buffer, rat $\text{A}\beta$ formed amyloid fibrils similar to human $\text{A}\beta$. In contrast, unlike rat $\text{A}\beta$, human $\text{A}\beta$ formed more toxic amyloid fibrils on neuronal cell membranes and raft-like membranes.

APP processing is also influenced by GM1 and other gangliosides. Gangliosides extract increased γ -secretase activity and increased the ratio of generated $\text{A}\beta_{42}$ to $\text{A}\beta_{40}$ (310). In addition, GCS inhibition led to significant reduction of $\text{A}\beta$ production, whereas the addition of exogenous brain ganglioside increased the production of $\text{A}\beta$, suggesting that the reduction in total gangliosides synthesis is beneficial in AD (311). Gangliosides regulate APP transport in the secretory pathway

which alters APP processing (311). PSEN and APP were demonstrated to regulate GCS gene expression, where the diminished γ -secretase activity increased the GCS gene expression and increased gangliosides level; therefore, the de novo synthesis of gangliosides is modulated by APP processing and deregulated in AD (312). Treatment of neuroblastoma cells with GM1 showed an increase in A β production and reduction in sAPP- α level (313). In contrast, another study showed that peripheral injection of GM1 in AD mouse model led to reduction in the cerebral A β burden, suggesting A β degeneration in the periphery (314). In addition, the accumulation of GM3, GM1, and GD1a via GD3S deficiency led to almost complete elimination of A β -related pathology with the absence of cognitive decline (315). The addition of GM3 resulted in decreasing the level of A β , whereas GD3 synthase product, GD3, treatment increased A β release. The activity of GD3 synthase is regulated by APP processing and it is inhibited by the direct interaction of GM3 with A β , which led to reduced substrate availability and altered conversion of GM3 to GD3 (272). Furthermore, the expression of GD3 synthase is downregulated by AICD, suggesting regulatory feedback, in which AICD and A β increase GM3/GD3 ratio resulting in potential reduction of the amyloidogenic APP processing (316). These results imply the association between gangliosides homeostasis and AD.

One study had forced the expression of GM1, GM2, and GD2 by transfection the SK-MEL-28-N1 cells with B4GALNT1 cDNA, and it showed accumulation of the β CTF and α CTF, extended BACE1 half-life, and increased BACE1 level in membrane rafts (274).

Diabetes mellitus (DM) is also associated with GM1 pathology. Amylin (IAPP) is a hormone that is produced from the pancreas and involved in AD pathology (317, 318). It has been shown that the amylin interacts with GM1 and significantly decreases its lateral diffusion on the plasma membrane of living neuroblastoma cells (319). In a nonhuman primate study, the authors showed

that DM accelerates A β pathology and increased GA β accumulation in the brain of DM-affected monkeys (320).

In a mouse model of GM1 gangliosidosis, an increase in the local microglial activation and expression and extravasation of inflammatory cells in the cerebral environment were observed (321).

1.10.4. Pre-requisite of GM1 ganglioside clustering to induce GA β generation

De novo brain cholesterol induces the congregation of GM1 on the cell membrane which is necessary for A β binding (322). Furthermore, using cultured cells, it has been shown that sphingomyelin induced GM1 clustering, leading to GA β generation (323). In addition, lipids extracted from synaptosomes isolated from aged mice brain have induced GM1 clustering (324). Cholesterol is the strongest triggering force that induces GM1 clustering. One study analyzed synaptic plasma membranes isolated from cerebral cortex from human brains of aged individuals, and the authors of this study found that APOE ϵ 2 significantly reduced the level of cholesterol in these synaptic membranes (325). In addition, the level of GM1 in lipid rafts of synaptosomes is increased by getting older and this accumulation was much higher in APOE ϵ 4 than the APOE ϵ 3 knocked-in mice (326).

It is largely known that risk factors for AD, such as endosomal-lysosomal alteration, precede A β deposition and cause impairment in the neuronal membranes' lipid composition (301). Yuyama et al have demonstrated in in-vitro study that endocytic disorder of cultured neuronal cells induced GM1 buildup (327), which potentially led to GA β -dependent amyloid deposition at presynaptic neuritic terminals (328, 329). The enhancement of GA β generation by endosomal-lysosomal disorder was established and confirmed in a mouse model of human lysosomal dysfunction disorders (330). Thus, multiple risk factors of AD could induce alteration in the composition and/or

distribution of neuronal membrane lipid, resulting in GM1 clusters formation and GA β generation. Furthermore, the structural composition of gangliosides could be responsible for the GA β formation as reported by Oikawa et al who found that the imbalance in the length of fatty acid side chain and length of gangliosides could be responsible for GA β -dependent A β assembly in isolated synaptic plasma membranes from human brains (331).

1.10.5. Lipid rafts and ganglioside-protein interactions

Gangliosides are preferentially localized in lipid rafts (332). Under common conditions of lipid rafts isolation with 1% Triton X-100 in cold aqueous buffer, gangliosides enter the soluble phase and redistribute to other membranes (333, 334). However, under different isolation methods with detergent other than Triton X-100, gangliosides do not redistribute (291).

1.11. The TgSwDI mouse model

Mutations of the APP gene that are close to the sites of processing by both secretases lead to the overproduction of A β_{42} (140, 335, 336), but when APP is mutated in A β region, aa 21-23, it leads to familial CAA. The first identified mutation in the A β region was the Dutch E22Q mutation which causes the production of diffuse A β deposition and severe CAA, resulting in hemorrhagic incidents at mid-life (337, 338). The second known mutation in A β region is the Iowa D23N mutation which was found in patients with late onset dementia with severe CAA and NFT (8). Different studies have demonstrated that Dutch E22Q and Iowa D23N mutant A β peptides display higher fibrillogenic and pathogenic properties in an in vitro model of CAA (339-341).

The TgSwDI mouse model is expressing the isoform 670 of APP gene harboring the three mutations Swedish (K670N/M671L), Dutch (E693Q), and Iowa (D694N). At three months of age, the hemizygotes have increased accumulation of insoluble A β_{40} and A β_{42} in the brain microvessels,

and increased deposits of A β diffuse plaques in the cortex and hippocampus. In addition, this mouse model develops deposits of fibrillar A β in the cerebral microvessels at six months of age (342). The TgSwDI model develops marked increase in astrocytes and microglia activation at the age 6-24 months with lesser magnitude in the cortex compared to the subiculum and thalamus (343).

1.11. Hypothesis and aims

Number of studies have elaborated the pathological character of amylin in AD by showing that amylin can induce the inflammatory cascade and apoptosis (201-203, 205, 214). However, the pathological characteristics of amylin are not well understood. Therefore, we hypothesize that amylin and pramlintide alter brain level of A β by modulating APP processing in lipid rafts. Therefore, the aim of this study is,

Aim 1: To optimize the isolation of membrane rafts and characterize the isolated lipid rafts for protein implicated in A β production.

Aim 2: To study the effect of amylin and pramlintide on the APP processing in lipid rafts.

2. ISOLATION AND CHARACTERIZATION OF LIPID RAFTS FROM TgSwDI MOUSE MODEL BRAIN

2.1. Abstract

Lipid rafts are part of the cell membrane, and they are highly enriched with cholesterol and sphingolipids. These rafts are heterogenous, dynamic and control different cellular processes such as signaling and proteins/lipids interactions. Different proteins are localized lipid rafts including proteins that are involved in the production of A β , such as APP, BACE1, and γ -secretase, and different synaptic markers proteins such as PSD-95 and SNAP-25. The fractionation of membrane rafts is highly dependent on the fractionation conditions, including temperature, detergent type and concentration, ultracentrifugation speed and time, type of rotor and the nature of protein localized in lipid rafts. This type of fractionation is based on density separation by using discontinuous sucrose gradient. In this study, the isolation method of membrane rafts from brain homogenates of TgSwDI mice (an AD model) has been optimized by using Brij98 as detergent and centrifugal speed of $260,000 \times g$ for 3 h at 4°C. The results showed that membrane rafts are concentrated in fraction 2 of the sucrose gradient as determined by immunoblotting of lipid rafts marker, flotillin-1. Different proteins were observed in fraction 2, such as APP, BACE1, γ -secretase proteins, P-gp, LRP1, B4GALNT1, and GM1; however, several other proteins were not observed under the optimized separation conditions such as RAMP3 and GCS.

2.2. Introduction

The cell membrane is organized into discrete functional units known as lipid rafts. The concept of lipid rafts was first introduced to explain the generation of glycolipid-rich apical membrane of epithelial cells (234). Later, these rafts were identified as a principle of membrane sub-compartmentalization that possess different functions including endocytosis, post-Golgi trafficking, and cell signaling (235). The notion of lipid rafts was introduced at the 2006 Keystone Symposium of Lipid Rafts and Cell Function: “Lipid rafts are small (10–200 nm), heterogeneous, highly dynamic, sterol- and sphingolipid-enriched domains that compartmentalize cellular processes. Small rafts can sometimes be stabilized to form larger platforms through protein-protein and protein-lipid interactions” (236).

Different proteins were identified in membrane rafts including flotillins, caveolins, GPCR, growth factor receptors, kinases, APP, BACE1, γ -secretase, PSD-95, SNAP-25 and many other proteins (246-253). These rafts are enriched with cholesterol and glycosphingolipids with highly saturated fatty acids compared to the surrounding membrane areas (237). These saturated fatty acids introduce compactness with sphingolipids which eventually results in phase separation (237). The insolubility of lipid rafts in nonionic detergent is attributed to this kind of compactness and phase separation (238).

Lipid rafts are known as DRM (detergent-resistant membrane) because of absence of solubility in cold 1% Triton X-100 (239). DRMs are fractionated by ultracentrifugation using discontinuous sucrose gradient where rafts float at the top fraction (usually 5% sucrose) (239). These top fractions

are enriched with cholesterol, glycosylphosphatidylinositol (GPI)-linked proteins, and lipid raft marker (flotillin-1) (237). Other detergent such as NP-40, Lubrol, CHAPS, octyl-glucoside, Brij 98, and low concentrations (< 1%) of Triton X-100 are utilized to isolate lipid rafts. Although there is overlap in the isolated proteins between these different detergents, significant differences were observed (244, 245). Therefore, the products of lipid rafts depend mainly on the method of isolation

2.3. Methodology

2.3.1. Materials and chemicals

The list of chemicals and material that have been used in this project are shown in Table 2.3.1.

Table 2.3. 1. Table of chemicals used for lipid rafts isolation.

Material	Company
Brij 98	ACROS Organics
PMSF	Sigma-Aldrich
D-sucrose	Fisher Bioreagents
EDTA	G Biosciences
NaCl	Sigma-Aldrich
Tris-HCl	Bio-Rad
Protease arrest	G Biosciences
Na ₃ VO ₄	Sigma-Aldrich

2.3.2. Optimization of fractionation

The complete protocol for the isolation and handling of mice brains is described in detail in the methodology section of CHAPTER 3.

A total of three protocols were tested to isolate lipid rafts. In the first two protocols, the Optima XPN-100 ultracentrifuge (Beckman Coulter) with fixed angle Type 90 Ti rotor was used. In the first isolation protocol, a previously published procedure was followed with modification (344). One hundred micro-liters from each brain homogenate in DPBS was incubated on ice for 30 min with 1 ml of 1% Triton X-100, 10 mM Tris-HCl pH 7.5, 50 mM NaCl, 2 mM EDTA, 1 mM PMSF, and 1 mM Na₃VO₄ with homogenization. The suspension was centrifuged at 5000 × *g* for 5 min at 4°C. One milliliter from each supernatant was mixed with equal volume of 90% (wt/vol) sucrose in TNE buffer (10 mM Tris-HCl pH 7.5, 50 mM NaCl, 2 mM EDTA) and placed at the bottom of the ultracentrifuge tube. Then, 7 ml discontinuous sucrose gradient consisting of 4 ml 35% (wt/vol) sucrose in TNE buffer and 3 ml 5% (wt/vol) sucrose in TNE buffer were overlaid on the top. The sucrose gradient was centrifuged at 270,000 × *g* for 20 h at 4°C. The fractions (900 μl each) from each sample were collected starting from top to bottom of the tube and then stored in -80°C. In the second optimization, the ultracentrifugation time was decreased to 18 h, whereas the other conditions had not changed.

In the third and final optimized protocol, lipid rafts fractionation was performed as reported previously with modification (263). Eighty micro-liters from each brain homogenate in DPBS was incubated on ice for 30 min with 600 μl of 1% Brij®98, 25 mM Tris-HCl pH 7.5, 150 mM NaCl, 5 mM EDTA, 1 mM PMSF, and protease arrest. The suspension was centrifuged at 1000 × *g* for 5 min at 4°C. Five hundred micro-litter from each supernatant was mixed with equal volume of 80% (wt/vol) sucrose in TNE buffer (25 mM Tris-HCl pH 7.5, 150 mM NaCl, 5 mM EDTA) and placed at the bottom of an ultracentrifuge tube. Then, 4 ml discontinuous sucrose gradient consisting of 3 ml 35% (wt/vol) sucrose in TNE buffer and 1 ml 5% (wt/vol) sucrose in TNE buffer were overlaid on the top. The sucrose gradient was centrifuged at 260,000 × *g* for 3 h at 4°C

using Beckman Coulter Optima XPN-100 ultracentrifuge in SW55 Ti rotor (Beckman Coulter). The fractions (500 μ l each) from each sample were collected starting from the top to the bottom of the tube and then stored in -80°C.

2.3.3. Characterization of lipid rafts by SDS-PAGE

Certain volume from each fraction was mixed with 4X laemmli sample buffer and boiled at 95°C for denaturation. Protein separation, probing, blotting, imaging, and analysis were performed as described in CHAPTER 3. Anti-flotillin-1 antibody (1:1000, Invitrogen) was used to probe the membranes as primary antibody which identifies the lipid rafts marker flotillin-1, whereas different antibodies were used to detect different proteins in lipid rafts fraction (Table 3.3.2).

2.4. Results

2.4.1. The fractionation of lipid rafts was not optimized in the first three trials.

The first and second optimizations for lipid raft fractionation were not able to localize the flotillin-1 in a defined fraction. The distribution of flotillin in the sucrose gradient, after the ultracentrifugation and immunoblotting by SDS-PAGE, spread from fraction 10 at the bottom to fraction 4. Fraction 4 in the first two conditions is the interface between 5% and 35% sucrose gradient (Figure 2.6.1.)

2.4.2. Lipid rafts are localized in fraction 2 in the final optimization

The DRMs were prepared and fractions enriched in lipid rafts were identified by immunoblotting of lipid raft marker with antibody against flotillin-1. Findings from optimization and characterization of lipid rafts isolation from brain homogenates demonstrated the highest flotillin-1 localization in fraction 2 (the interface between 5 and 35% sucrose in the gradient) (Figure 2.6.2.), suggesting lipid rafts are enriched in fraction 2, which was used for subsequent analysis for the effect of treatments on protein levels in lipid rafts.

2.4.3. The amyloidogenic pathway proteins are localized in membrane rafts.

APP, BACE1, and γ -secretase complex were detected in lipid rafts fraction (fraction 2) and in the non-raft fractions (fraction 8, 9, and 10) (Figure 2.6.3 & 2.6.4)

2.4.4. Different proteins other than the amyloidogenic pathway proteins were observed in lipid rafts.

Different molecules including P-gp, LRP1, B4GALNT1 and GM1 ganglioside were detected in lipid rafts fraction (Figure 2.6.5. & 2.6.6). Other proteins were measured directly from fraction 2 without measuring them from fraction 1 to 10, these proteins include PSD-95, and SNAP-25 (CHAPTER 3). On the other hand, few proteins were not observed in fraction 2 under the abovementioned separation conditions including RAMP3, B3GALT4 and GCS (Figure 2.6.5 & 2.6.6).

2.5. Discussion

Lipid rafts have high concentration of cholesterol and glycosphingolipids with highly saturated fatty acids, which provide compactness and phase separation (237). Such compactness is responsible for the insolubility of membrane rafts in nonionic detergent such as Triton X-100 and Brij98 (238). In order to fractionate membrane rafts, ultracentrifugation and discontinuous sucrose gradient are utilized and usually the rafts float at the top fractions (5% sucrose) (239). In contrast, many studies showed that lipid raft marker could be distributed in multiple fractions, which will be reflected on the distribution of anchored proteins (263). Although there is overlap in the isolated proteins between these different detergents, significant differences were observed (244, 245). Therefore, the products of lipid rafts depend mainly on the method of isolation.

Limiting the spread of flotillin 1 among the fractions into one defined fraction would make the characterization of these rafts much easier (269, 345). In this study, fraction 2 contained the lipid rafts marker flotillin-1; therefore, the characterization of different proteins in lipid rafts, isolated from total brain homogenate, was determined from fraction 2. However, the absence of few proteins from lipid raft fraction may be due to lipid rafts isolation conditions (244, 266). Multiple fractionation conditions should be considered while dealing with the isolation of lipid rafts including working with cells or tissues, separation speed, time, type of rotor, buffer concentrations, and the nature of detergents such as Triton X-100 or Brij98 (345-348) . The successful isolation

of lipid rafts that contains the amyloidogenic pathway proteins and enzymes would help in studying the effect of treatments on this pathway in membrane rafts.

In a study by Kawarabayashi et al, they isolated the membrane rafts from the brain of Tg2576 AD mouse model. The research group used a different separation method, they homogenized the brain in 50 mM of 2-(N-morpholino) ethanesulfonic acid (MES), 150 mM NaCl, pH 6.5, 1% Triton X-100 and protease arrest. The pellet, after removing the cell debris and nuclei, was reextracted two times with the same buffer. The total volume of Triton extract was mixed with 80% (w/v) sucrose and overlaid with 38% (w/v) and 5% (w/v) sucrose and centrifuged at $100,000 \times g$ in SW41 rotor at 4°C for 19 h. The lipid raft marker was observed in fraction 4 (the top fraction of the 38% sucrose); in addition, different proteins were observed in the same fraction including: APP, BACE1, GM1, PSEN1, PSEN2, APOE, A β and neprilysin. These proteins were observed also in the soluble fractions as well, except GM1 (345). In contrast, the separation method that we used was able to provide the proteins of interest to our research project with much shorter ultracentrifugation time.

In conclusion, the fractionation procedure that we utilized in our study was successful in isolating the membrane rafts and associated proteins in one fraction, making this procedure suitable for characterizing the effect of treatments on the amyloidogenic pathway in membrane rafts.

2.6. Figures and legends

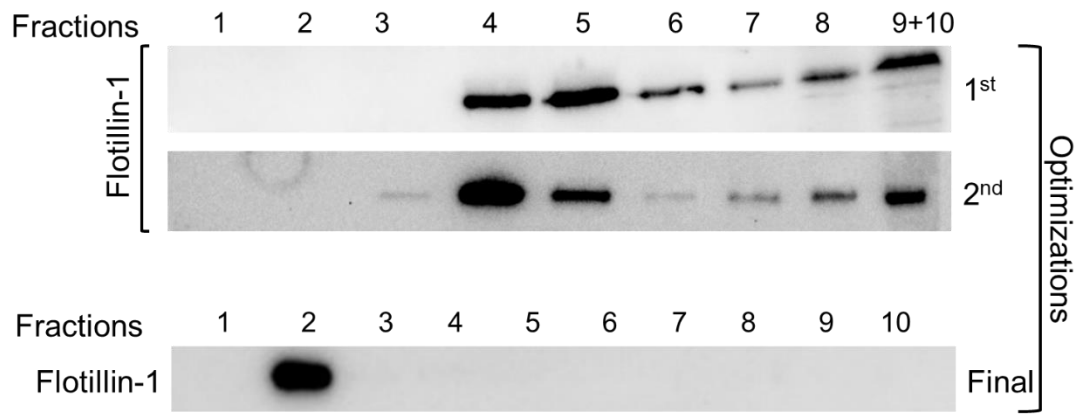


Figure 2.6. 1. The optimization of lipid rafts fractionation. The first and second optimizations for lipid rafts separation were not able to localize the rafts in one or two fractions, especially at the top of sucrose gradient using western blotting. However, the final fractionation method was able to localize the rafts in fraction 2 as visualized by the detection of raft marker, flotillin-1. Lipid rafts isolated from vehicle (PBS) treated mice were used to blot flotillin-1.

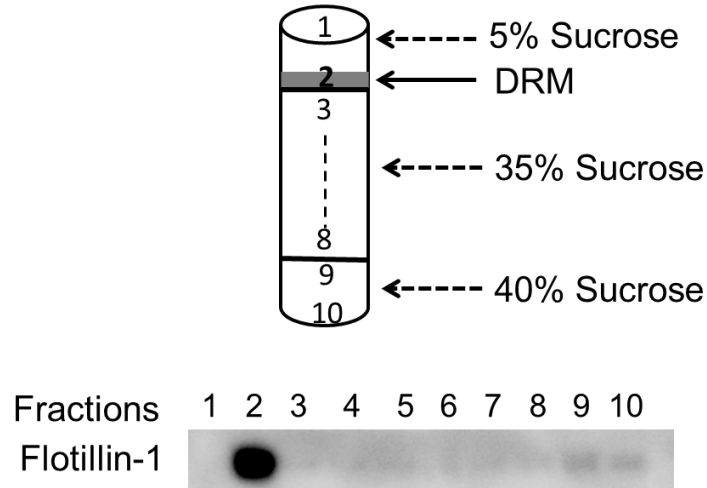


Figure 2.6. 2. The separation of lipid rafts using discontinuous sucrose gradient and ultracentrifugation. Lipid rafts were found in fraction 2 and the non-raft fraction were in fractions 8-10. Lipid rafts isolated from vehicle (PBS) treated mice were used to blot flotillin-1.

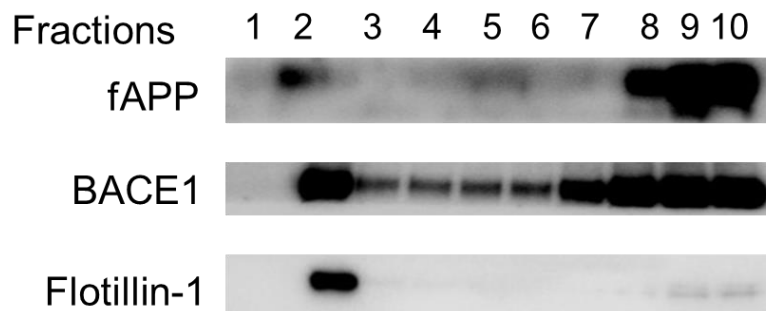


Figure 2.6. 3. Characterization of APP and BACE1 in lipid rafts. APP and BACE1 were observed in fraction 2 and soluble fractions, which confirms the localization of these proteins in lipid rafts. Lipid rafts isolated from vehicle (PBS) treated mice were used to blot these proteins.

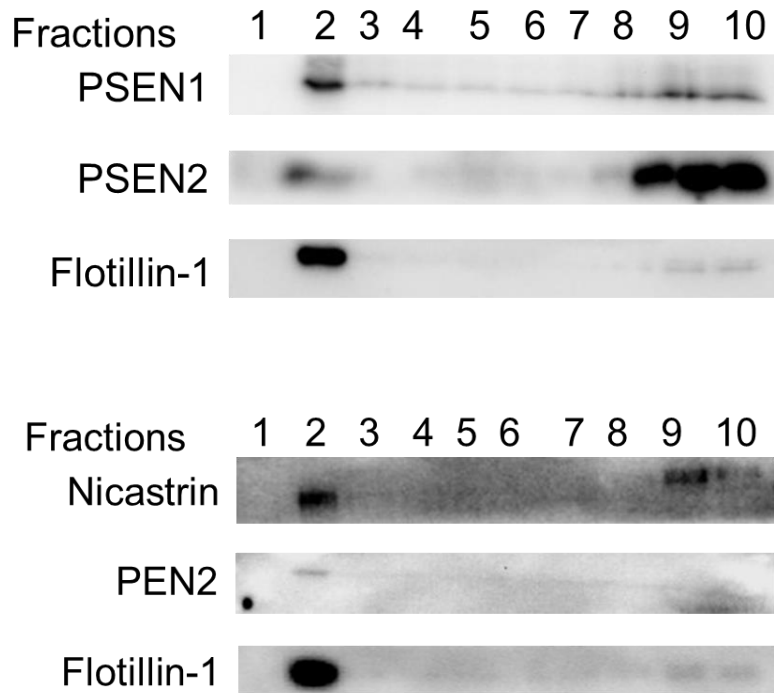


Figure 2.6. 4. Characterization of γ -secretase complex subunits in lipid rafts. PSEN1, PSEN2, PEN2, and nicastrin were observed in fraction 2, which confirms the localization of these proteins in lipid rafts. Lipid rafts isolated from vehicle (PBS) treated mice were used to blot these proteins.

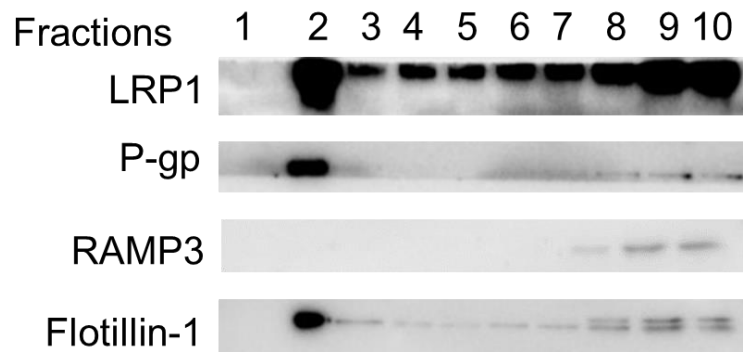


Figure 2.6. 5. Characterization of P-gp, LRP1, and RAMP3 in lipid rafts. Unlike RAMP3, P-gp and LRP1 were observed in lipid rafts, whereas RAMP3 was observed only in the soluble fractions. Lipid rafts isolated from vehicle (PBS) treated mice were used to blot these proteins.

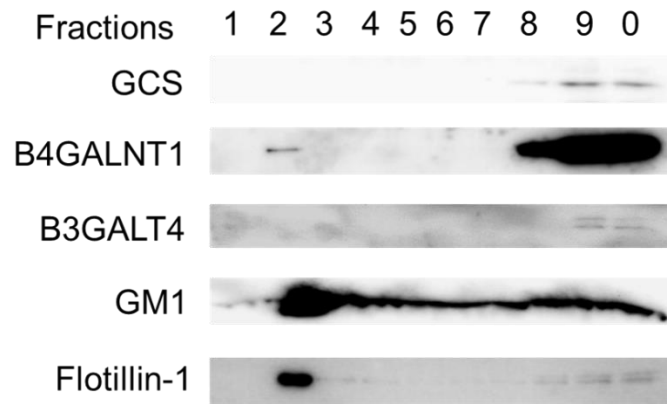


Figure 2.6. 6. Characterization of GCS, B3GALT4, B4GALNT1, and GM1 in lipid rafts.

These proteins were observed in lipid rafts fractions except GCS. Lipid rafts isolated from vehicle (PBS) treated mice were used to blot these proteins.

3. AMYLIN AND PRAMLINTIDE MODULATE γ -SECRETASE ACTIVITY AND APP PROCESSING IN LIPID RAFTS

3.1. Abstract

One of the major hallmarks of Alzheimer's disease is the accumulation of misfolded amyloid- β ($A\beta$) peptide. Several studies have linked AD with type 2 diabetes due to the similarities between $A\beta$ and human islet amyloid polypeptide (known as amylin). This study explores the effect of amylin and pramlintide, an amylin analogue, on AD pathogenesis and the predisposing molecular mechanism(s) behind the observed effects in the TgSwDI mouse model of AD. Our study findings showed that thirty days of intraperitoneal injection with either amylin or pramlintide increased $A\beta$ burden in mice brains. Amylin or pramlintide altered the amyloidogenic pathway and increased $A\beta$ production by modulating the localization of amyloid precursor protein and γ -secretase activity in membrane rafts. The increased levels of B4GALNT1 enzyme and GM1 ganglioside were triggered by amylin or pramlintide, and GM2 ganglioside was increased by pramlintide. The increased synthesis of GM1 and GM2 is an important factor in regulating amyloidogenic pathway proteins in lipid rafts and increase $A\beta$ aggregation. Furthermore, the increased brain $A\beta$ burden by amylin and pramlintide was associated with synaptic loss, apoptosis, and microglia activation. In conclusion, findings from this work showed amylin or pramlintide increase $A\beta$ levels and related pathology in the TgSwDI mice brains, implying that the increased amylin level or the therapeutic use of pramlintide might increase the risk of AD.

3.2. Introduction

Alzheimer's disease causes significant structural and functional disruption of healthy brain. There is a progressive loss of pyramidal cells in the cortex which mediate higher cognitive functions (32). Moreover, early synaptic dysfunction and impairment of neuronal circuit communication are also observed in AD (3). In AD, the neuropathological findings are characterized by extracellular deposition of senile plaques of amyloid beta ($A\beta$) and intracellular neurofibrillary tangles (NFT) of hyper-phosphorylated tau protein (36).

The cleavage of APP occurs at many different cellular sites including plasma membrane, mitochondrial membrane, and trans-Golgi network (138). The parent protein, the 695-770 amino acid APP is cleaved in most cell types by α -secretase (non-amyloidogenic pathway) to release sAPP- α and leaving the C-terminal fragment APP-CTF α or C83 peptide (139-141). The C83 peptide is then cleaved by γ -secretase to release APP intracellular domain (AICD) and 16 amino acid peptide, termed P3 (142). However, the amyloidogenic version of APP processing includes cleavage by BACE1 leaving the C-terminal fragment as APP-CTF β or C99 peptide within the membrane and releases sAPP- β into the extracellular space followed by γ -secretase processing of C99 fragment, releasing the 40-43 amino acid $A\beta$ and AICD (140, 141)

Lipid rafts are considered the site for APP processing. BACE1 was shown to be an inhabitant of lipid rafts (257), and anchoring BACE1 to lipid rafts demonstrated enhanced APP cleavage (258-260) and increased generation of $A\beta$ (261). In addition, several biochemical studies have indicated that γ -secretase is localized with APP CTFs in membrane rafts of adult brain (266, 267) and

neuroblastoma cells (268). Lipid rafts composition have been analyzed by several preparations techniques which showed that membrane rafts are enriched with cholesterol and glycosphingolipids (gangliosides) (237).

Brain cortexes from AD patients demonstrated increased level of GM2 and GM3 (294). On the other hand, the cortical lipid rafts of AD patients contained more GM1 and GM2 (295). APP processing is influenced by GM1 and other gangliosides, for example, gangliosides extract added to purified γ -secretase increased the enzyme activity and increased the ratio of generated $A\beta_{42}$ to $A\beta_{40}$ in CHO cells overexpressing PEN1 (310). In addition, GCS inhibition led to a significant reduction in $A\beta$ production, whereas the addition of exogenous brain gangliosides increased the production of $A\beta$, suggesting that the reduction in total gangliosides synthesis could be beneficial for AD (311). In another study, treatment of neuroblastoma cells with GM1 increased $A\beta$ production and reduced in sAPP- α level (313). Furthermore, the over expression of GM1, GM2, and GD2 by transfecting SK-MEL-28-N1 cells with B4GALNT1 cDNA, demonstrated accumulation of β CTF and α CTF with prominent increase in β -cleavage, extended BACE1 half-life, and increased BACE1 level in membrane rafts (274).

Patients with type 2 diabetes mellitus (T2DM) have double the risk to develop AD (109, 110). The association of T2DM with sporadic AD is not well understood. IAPP fibrils and oligomers have been identified in the brains of patients with T2DM and cognitive decline (201) as well as in rodent models expressing hIAPP, which led to neurological defects (202). Importantly, IAPP has been observed to co-precipitate with $A\beta$ to form diffuse and dense SP (201, 203). The co-precipitation of IAPP and $A\beta$ in SP implies that they exert the toxic effect synergistically (201, 203). The independent toxic effect of IAPP can occur through different pathway including interaction with lipid components of cell membrane and by inducing disruption of cell membrane (215-217).

3.3. Methodology

3.3.1. Materials and Chemicals

The commercial sources of the reagents used in this study are listed in Table 3.3.1.

Table 3.3. 1. Table of chemicals utilized in this project*.

Chemicals	Company
Human Amylin	Anaspec, Cat # AS-60254-1
Pramlintide	Biotang Inc, Cat # BT-HOR-300
D-glucose	Sigma-Aldrich
NP-40 lysis buffer	Alfa-Aesar
BSA	Millipore
PBS	Fisher Bioreagents
Ficol 400	Sigma-Aldrich
Protease arrest	G Biosciences
EDTA	G Biosciences
10x Tris/Glycine/SDS	Bio-Rad
Thioflavin-S	Sigma-Aldrich
Donkey serum	Sigma-Aldrich

Chemicals	Company
O.C.T	VWR
Resolving gel buffer	Bio-Rad
Stacking gel buffer	Bio-Rad
30% polyacrylamide	Bio-Rad
Prism Ultra protein ladder	Abcam
Nonfat dry milk	Santa Cruz Biotechnology
PVDF	Millipore
TEMED	Bio-Rad
Ammonium persulfate	Bio-Rad
SuperSignal West Femto substrate	Thermo Fisher Scientific
4X Laemmli sample buffer	Bio-Rad

*All other chemicals were purchased from VWR.

3.3.2. Preparation of amylin and pramlintide

Amylin and pramlintide were purchased as 1 mg in each vial and then dissolved in 1 ml sterile water and aliquoted according to manufacturers and stored at -20°C . Fifteen minutes before the time of intraperitoneal (i.p.) administration, the aliquots were mixed with 200 μl of PBS.

3.3.3. Mice and treatment protocols

All animal procedures used in this study were approved by the Institutional Animal Care and Use Committee of the University of Louisiana at Monroe and according to the National Institutes of Health guidelines, as in Principles of Laboratory Animal Care (NIH publication No. 86-23, revised

1996). The TgSwDI homozygous transgenic mice were originally purchased from Jackson Laboratory (Bar Harbor, ME) and were maintained on C57BL/6 background at the University of Louisiana at Monroe at the animal facility. The mice (25-28 g; 4 months age) were divided into three groups and had free access to water and food and maintained on a 12 h:12 h light:dark cycle. The mice received intraperitoneal (i.p.) injection of amylin (200 $\mu\text{g}/\text{kg}/\text{d}$; $n = 8$ mice), pramlintide (200 $\mu\text{g}/\text{kg}/\text{d}$; $n = 8$ mice), or equal volume of PBS as vehicle (control group; $n = 8$ mice) for 30 days. The weight (25-28) of each mouse was observed and checked every week. The level of blood glucose was measured before starting and at the end of the treatment period. Blood glucose levels were very close before and after the treatment, and glucose levels at the end of treatment period were 150.7 ± 1 , 151.3 ± 0.9 , 151.5 ± 1.5 mg/dl for the control, amylin, and pramlintide treated mice, respectively. At the end of treatment period mice were sacrificed with ketamine anesthesia and decapitated for brains collection.

3.3.4. Brains collection and handling

After the decapitation, the mouse head skin was cut, and the skull was opened without introducing disruption to the brains. Then the brain was removed gently from inside the skull without introducing disruption. After their isolation, brains were divided into two halves and stored in -80°C .

3.3.5. Homogenization of mice brains

Brain weights were measured and mixed with two volumes of DPBS (137 mM NaCl, 8.1 mM Na_2HPO_4 , 2.7 mM KCl, 0.9 mM CaCl_2 , 5 mM D-glucose, 0.5 mM MgCl_2 , 1.46 mM KH_2PO_4 , 1mM Na-pyruvate) with protease arrest and stroked multiple times until the brain tissues were easily passed through 1 ml tip. Brains were stored in -80°C for biochemical analysis.

3.3.6. A β extraction from mice brain homogenates

The extraction and fractionation of A β were performed as reported before with modifications (349). Brain homogenates in DPBS from each mouse was lysed (1:1.5) in NP-40 lysis buffer with protease arrest on ice for 45 min, then the supernatant was collected after centrifugation at 20,800 $\times g$ for 15 min at 4°C. The supernatant was used to measure the soluble A β_{40} and A β_{42} from total brain homogenates. To measure the oligomeric and insoluble loads of A β_{40} and A β_{42} in the brain tissues, a 2-step serial extraction procedure was used. The pellet after the extraction of soluble A β was mixed with 150 μ L of 2% SDS in PBS containing protease arrest with homogenization followed by sonication for 10 min and centrifugation at 20,800 $\times g$ for 60 min at 22°C. The supernatants, which contains oligomeric A β were collected and stored in -80°C. To isolate insoluble A β , the pellet from the second fractionation was re-suspended in 300 μ L of 70% formic acid in PBS containing protease arrest followed by homogenization and sonication for 10 min and finally centrifugation at 20,800 $\times g$ for 60 min at 4°C and supernatants were collected and stored in -80°C.

3.3.7. A β quantification by ELISA

The samples dilution was optimized before measuring A β by ELISA. The soluble fraction was diluted 1:2, SDS fraction was diluted 1:20 and formic acid fraction was neutralized 1:20 with 1M Tris-HCl/0.5M Na₂HPO₄ and then diluted 1:40. The soluble, oligomeric and insoluble A β_{40} and A β_{42} were measured by commercial ELISA kits for A β_{40} and A β_{42} (Thermo Fisher Scientific). The level of A β_{40} and A β_{42} was normalized to the total protein content in each fraction measured by the Pierce™ BCA Protein Assay Kit (Thermo Scientific). The level of A β_{40} and A β_{42} were expressed as picomol per milligram protein (pmol/mg protein).

3.3.8. Immunoblotting by SDS-PAGE

For western blotting, brain homogenates from each group in DPBS were lysed (1:1.5) in NP-40 lysis buffer with protease arrest on ice for 45 min, then the supernatant was collected after centrifugation at $20,800 \times g$ for 15 min at 4°C . The total protein content was measured and $20 \mu\text{g}$ from each lysate was used for protein separation in each single lane. The lysate volume containing $20 \mu\text{g}$ total protein was mixed and denatured with 4X Laemmli sample buffer and boiled at 95°C for 5 min for protein denaturation. For the immunoblotting of lipid rafts, certain volume from fraction 2 containing lipid rafts from each sample was mixed with 4X Laemmli sample buffer and denatured with heating as mentioned above. Pre-stained protein ladder and samples were loaded and separated on 12% Tris-Glycine-SDS polyacrylamide gels in SDS-PAGE gel chamber in electrophoresis buffer (5 mM Tris, 192 mM glycine, 0.1% SDS, pH 8.3) for 35 min at 240 V. For the electrophoresis of GM1 ganglioside, a 15% Tris-Glycine-SDS polyacrylamide gels were used. After proteins electrophoresis, the stack for blotting was assembled with two absorbent papers wetted with transfer buffer (25 mM Tris, 192 mM Glycine, 20% (v/v) methanol (pH 8.3) and a wet polyvinylidene difluoride (PVDF) membrane pre-soaked in methanol for 10 min for activation. Proteins were blotted on the PVDF membrane at 340 mA for 1 h followed by blocking in 2% nonfat dry milk in TBST (Tris-buffered saline, 20 mM Tris-HCl, 137 mM NaCl, 0.1% Tween-20, pH 7.6) for 1 hr at room temperature with shaking. Then, the membranes were probed with primary antibodies in 3% nonfat dry milk in TBST over night at 4°C . The primary antibodies that were used for SDS-PAGE are listed in Table 3.3.2. After overnight incubation, the membranes were washed 3 times each for 5 min with TBST buffer and probed for 1 h in 2% nonfat dry milk in TBST with secondary antibodies: goat anti-rabbit IgG (H+L)-HRP (1:1000, Invitrogen), goat anti-mouse IgG (H+L)-HRP (1:1000; Invitrogen) or goat IgG HRP-conjugated (1:1000; R&D

systems) followed by washing as mentioned above, then the image was captured for each membrane. For GM1 detection, the membrane was incubated, after blocking, with Cholera Toxin Subunit B (Recombinant)-HRP (1:5000; Invitrogen) for 1 h at room temperature with shaking followed by washing as mentioned above, then the image was captured.

Table 3.3. 2. The list of primary antibodies used to probe the membranes in Western blotting.

Primary antibody	Dilution	Clone	Company
Anti-human sAPP- β	1:1000	-	Immuno-Biological Laboratories Co
Anti-human sAPP- α	1:1000	2B3	Immuno-Biological Laboratories Co
Anti-APP*	1:10,000	22C11	Millipore
BACE1*	1:1000	-	Abcam
LRP1*	1:1000	-	Abcam
GCS*	1:1000	-	Abcam
B4GALNT1*	1:1000	-	Abcam
B3GALT4	1:1000	-	Invitrogen
Iba1	1:1000	-	Abcam
Presenilin 1*	1:1000	D39D1	Cell Signaling
Presenilin 2*	1:1000	D30G3	Cell Signaling
Nicastrin *	1:1000	D38F9	Cell Signaling
PEN2*	1:1000	D6G8	Cell Signaling
Caspase-3	1:1000	-	Cell Signaling

Primary antibody	Dilution	Clone	Company
Synapsine-1	1:1000	-	Cell Signaling
SNAP-25*	1:1000	-	Invitrogen
GAPDH	1:1000	-	Invitrogen
MMP9	1:1000	-	Invitrogen
IDE	1:200	-	Santa Cruz Biotechnology
RAMP3	1:200	-	Santa Cruz Biotechnology
β -tubulin	1:200	-	Santa Cruz Biotechnology
β -actin	1:1000	-	Santa Cruz Biotechnology
ABCB1 (P-gp)*	1:200	-	Biolegend
PSD-95*	1:2000	-	GenTex
Cholera Toxin Subunit B-HRP*	1:10,000	-	Invitrogen

* These antibodies were used also to probe membranes after lipid rafts blotting.

3.3.8.1. Preparation of Tris-Glycine-SDS gels

First, the resolving gel was prepared according to the recipe provided in Table 3.3.3, loaded into the cassette, overlaid with 100% ethanol and incubated at room temperature for 45 min to solidify. Then, the stacking gel was prepared according to Table 3.3.3. and overlaid over the resolving gel after removing the ethanol.

Table 3.3. 3. The preparation of polyacrylamide gels for SDS-PAGE

	12% resolving gel	15% resolving gel	Stacking gel
Chemicals	Volume per gel (ml)	Volume per gel (ml)	Volume per gel
30% Polyacrylamide	2	2.5	0.17
1.5 M Tris (pH 8.8)	1.3	1.3	0.13
10% SDS	0.05	0.05	0.01
10% Ammonium persulfate	0.05	0.05	0.01
TEMED	0.002	0.002	0.001
H ₂ O	1.6	1.1	0.68

3.3.8.2. Immunoblotting of RAMP3 protein

In order to blot the three isoforms (monomers, homodimer, and heterodimer) of RAMP3 proteins, a stain-free kit (Bio-Rad) was used. The gel was prepared following the manufacturer protocol, and protein denaturation and electrophoresis was performed as mentioned above. After electrophoresis, the gel was activated by UV light in ChemiDoc imaging system (Bio-Rad) and the image was captured. After blotting, the gel was imaged to confirm complete proteins blotting on the PVDF membrane. In addition, an image for the PVDF membrane was captured to get an image for total proteins. The blocking, probing with primary and secondary antibody was performed as mentioned above.

3.3.8.3. Image capturing and analysis

Proteins' blots were developed using a chemiluminescence detection kit (SuperSignal West Femto substrate) and bands were visualized by the ChemiDoc imaging system. The captured images were analyzed by Image Lab software v 6.0 (Bio-Rad) which measures the volume of each band with subtraction of background. The level of proteins in each membrane was normalized to the level of house-keeping proteins (GAPDH, β -tubuline, vinculin, or β -actin) or flotillin-1 for proteins blotted from lipid rafts. To quantify the level of RAMP3 isoforms, a multichannel imaging function in Image Lab was used and RAMP3 level was normalized to the total protein content in the corresponding lane.

3.3.9. Cryosectioning of mice brains

One day before sectioning, each frozen half brain was embedded in optimal cutting temperature (O.C.T) liquid and kept on dry ice, then stored in -80°C to the next day. Thirty minutes before the time of sectioning, the brains in the frozen O.C.T were placed in the cryostat at -20°C for optimal temperature adjustment. Brain sections of $16\ \mu\text{m}$ thickness were prepared using Leica CM3050S Research Cryostat. Each two sections were placed on the same glass slide and stored in -80° until the time for immunohistochemistry.

3.3.10. Immunohistochemistry

Previously published protocols were used for the immunohistochemical (IHC) analysis of $\text{A}\beta$, $\text{A}\beta$ plaques, astrocytes, and brain microvessels (350). All brains' sections from each group were methanol-fixed and blocked for 30 min with 10% normal donkey serum in PBS then washed 5 times with PBS. For the detection of $\text{A}\beta$ -plaques load in mice hippocampi and cortexes we followed a previously published protocol with slight modification (350). Briefly, the sections were

immuostained with rabbit polyclonal collagen IV antibody (1:200, Millipore) for detection of brain microvessels followed by 5 times washing with PBS and then stained by donkey polyclonal Alexa Flour 647 antibody to rabbit IgG (1:200, abcam). After that, sections were incubated in filtered 0.02% thioflavin-S (Thio-S) solution, prepared in 70% ethanol, for 30 min. Sections were then washed in 70% ethanol for 15 min and covered with cover-clips and sealed with nail polish for imaging. For total A β load detection, the brain slices were double immunostained for microvessels and Alexa Fluor-488 conjugated anti-A β antibody (6E10) (1:200, Biolegend). Double immunostaining of astrocytes and A β was performed using rabbit GFAP antibody (1:200, Santa Cruz), and for detection donkey polyclonal Alexa Flour 647 antibody to rabbit IgG (1:200, abcam) was used to detect astrocytes, for A β detection, Alexa Fluor-488 conjugated anti-A β antibody (6E10) was used. All antibodies were prepared in 10% normal donkey serum in PBS. Images were captured using Nikon Eclipse Ti-2 inverted fluorescence microscope (Nikon) at a total magnification of 4 \times and 20 \times for A β load, microvessels and A β plaque detection, and 40 \times for astrocytes detection. Quantification of all images was performed using NIS Element AR analysis v5 (Nikon), after adjusting for threshold.

3.3.11. GM2 ganglioside analysis by ELISA

Brain homogenate in DPBS was diluted 1:5 with PBS and centrifuged at 956 \times g for 20 min at 4°C. The supernatant was used to measure GM2 following the manufacturer protocol (MyBioSource, Cat # MBS017456). GM2 was also measured from lipid rafts. The levels of GM2 measured from brain homogenate and rafts were normalized to the total protein content in the total brain homogenate.

3.3.12. Assay of lysosomal enzyme activities

The lysed brain homogenate in NP-40 lysis buffer was diluted 1:1 in citrate phosphate buffer and the lysosomal enzyme activities for beta-galactosidase (β -gal); hexosaminidase A (HexA), total hexosaminidase (A,B and S isozymes; Hex T), and alpha-mannosidase (α -Man) were expressed as nmol 4-methylumbelliferone/mg protein per h at 37°C as described previously (351). Average values were calculated from n = 4 mice from each treatment group. α -Man cleaves lysosomal substrates outside the gangliosides' pathway, and it was used as assay control.

3.3.13. Isolation of lipid rafts

Lipid rafts were isolated from brain homogenates in DPBS as mentioned in details in the final optimization of membrane rafts isolation in CHAPTER 2

3.3.14. Statistical analysis

All values were expressed as mean \pm SEM. Statistical analysis was done with Prism v5.0 software (Graphpad). The statistical significance for all result was assessed by One-way ANOVA with posthoc analysis using Dunnett's test, where the three groups amylin, pramlintide and control groups were compared. A *p* value of < 0.05 was considered statistically significant.

3.4. Results

3.4.1. Treatment with amylin or pramlintide increases A β burden measured by ELISA

A β levels from total brain homogenate were analyzed by ELISA and the results demonstrated that only amylin increased the level of soluble A β_{40} by 36% compared to control ($p < 0.01$) and 28% compared to pramlintide ($p < 0.05$); in addition, amylin increased the level of soluble A β_{42} by 101% compared to control group ($p < 0.001$) and by 43% compared to pramlintide ($p < 0.01$). (Figure 3.6.1.A). Moreover, neither amylin nor pramlintide treatment showed significant changes in the level of insoluble A β_{40} compared to control, but both showed significant increase of insoluble A β_{42} compared to control, where amylin increased the insoluble A β_{42} by 76% ($p < 0.01$) whereas pramlintide increased insoluble A β_{42} 109% ($p < 0.001$) (Figure 3.6.1.B). Furthermore, amylin significantly increased oligomeric A β_{40} by 160% compared to control ($p < 0.01$), and 85% compared to pramlintide ($p < 0.01$); however, neither treatment altered the oligomeric A β_{42} (Figure 3.6.1.C).

3.4.2. Treatment with amylin or pramlintide increases A β deposition as measured by IHC analysis

Immunohistochemical analysis of the three groups was performed to show A β burden in the cortex and hippocampus regions of mice brains. The captured images showed a significant increase in total A β (detected by 6E10) in the brains of both amylin (280% increase) and pramlintide (182% increase) compared to control when measured in the cortex (both, $p < 0.001$) (Figure 3.6.2.). Also,

pramlintide significantly increased the level of total A β by 101% in the hippocampus compared to the control group ($p < 0.05$). Compared to pramlintide, amylin significantly increased the total A β ($p < 0.05$). Moreover, the deposition of A β plaques (detected by Thioflavin-S) was significantly higher in hippocampus (212% increase) and cortex (273% increase) of amylin treated mice compared to control group ($p < 0.05$). Also, amylin increased the level of A β plaques in the hippocampus compared to pramlintide treated mice ($p < 0.05$) (Figure 3.6.3.).

3.4.3. Amylin and pramlintide have no clear effect on APP processing when measured in brain homogenate

Findings from Western blotting of mice brain homogenates demonstrated insignificant changes in the level of full-length APP (fAPP) and BACE1 between control and treated mice (Figure 3.6.4.). The cleavage of APP by BACE1 produces sAPP- β and the results demonstrated that only pramlintide significantly increased sAPP- β by 40% compared to control ($p < 0.05$), whereas 68% ($p < 0.01$) and 70% ($p < 0.001$) reduction in the level of sAPP- α were observed after treatment with amylin and pramlintide, respectively (Figure 3.6.5.). To further understand the effect of amylin and pramlintide on APP processing and to explain the increased A β burden in brain homogenates, the γ -secretase complex including PSEN1, PSEN2, nicastrin, and PEN2 were measured by SDS-PAGE. Results from the total brain homogenate showed no significant changes in PSEN1, PSEN2, and nicastrin between the vehicle and peptides treated mice (Figure 3.6.6.). On the other hand, only pramlintide demonstrated a significant increase by 170% and 144% in PEN2 subunit when compared to control and amylin with $p < 0.001$ and $p < 0.05$, respectively. (Figure 3.6.6.). Overall, the results from total brain homogenate did not provide clear explanation for the increased brain A β burden in mice treated with amylin and pramlintide.

3.4.4. Amylin and pramlintide modulate APP processing in lipid rafts

In this study, only pramlintide significantly increased APP in lipid rafts by 50% when compared to control ($p < 0.05$) and 53% compared to amylin ($p < 0.05$) (Figure 3.6.7.). Consistent with total brain homogenate results, BACE1 level in the lipid raft was not altered by amylin or pramlintide (Figure 3.6.7.). However, amylin showed significant increase in the level of PSEN2 by 39%, and PEN2 by 53% compared to the control group in lipid rafts ($p < 0.05$ and $p < 0.001$, respectively) (Figure 3.6.8.). In addition, amylin increased the level of PEN2 compared to pramlintide when measured from lipid rafts ($p < 0.05$) (Figure 3.6.8.). On the other hand, pramlintide increased PSEN1, PSEN2, and Nicastrin in lipid rafts compared to the control group by 143%, 42%, and 112%, respectively, (all, $p < 0.05$) (Figure 3.6.8.). For PSEN1, PSEN2 and nicastrin, these results differ from total brain homogenate.

3.4.5. Amylin or pramlintide modulate GM1, GM2 and B4GALNT1 in total homogenate and/or lipid rafts

Previous reports observed a role of GM1 gangliosides in regulating APP trafficking and processing (311). In addition, GM1 has been shown to increase γ -secretase in membrane rafts (313). Thus, gangliosides synthesis pathway was evaluated. From total brain homogenate, no significant changes in GCS level were observed between the three groups (Figure 3.6.9.). Of relevance to the current work, GM3 ganglioside is converted by B4GALNT1 to GM2, and the addition of galactose to GM2 by B3GALT4 yields GM1 (274). Thus, we analyzed the proximal components of the GM1 synthetic pathway. Both amylin and pramlintide significantly increased the level of B4GALNT1 in total brain homogenate by 180% and 253% with $p < 0.05$ and $p < 0.01$, respectively, but not in lipid rafts (Figure 3.6.9. & 3.6.10.). GM2 was measured in total brain homogenate and lipid rafts using ELISA. Results showed that pramlintide, but not amylin, increased GM2 by 50% in total

homogenate (adjusted $p = 0.07$) (Figure 3.6.11.). In contrast, neither amylin nor pramlintide altered GM2 levels in lipid rafts compared to control (Figure 3.6.11.). Next, we determined GM1 levels in total brain homogenate and lipid rafts; findings from Western blot demonstrated the neither amylin nor pramlintide increased GM1 levels in total brain homogenate compared to the control group (Figure 3.6.9.), while pramlintide increased GM1 levels in lipid rafts by 50% ($p < 0.05$; Figure 3.6.10.). B3GALT4 is the enzyme that synthesizes GM1 from GM2 (274) and was also evaluated. Based on Western blot results, no changes in B3GALT4 levels were produced by amylin or pramlintide (Figure 3.6.9.). Unfortunately, B3GALT3 was not detected in lipid rafts (Figure 3.6.10.). In addition to the synthetic pathway for GM2 and GM1 gangliosides, their degradative pathway also was evaluated by measuring the activity of specific lysosomal enzymes responsible for their hydrolysis. There was no change in the lysosomal enzyme activities as shown in Table 3.4.1.

Table 3.4. 1. Lysosomal enzyme specific activity in mice brain tissues.

Specific activity is expressed as mean \pm SEM for the nmol of 4-methylumbelliferone. Data was analyzed using One-way ANOVA with posthoc analysis using Dunnett's test. [HexA: A isozyme ($\alpha\beta$) of hexosaminidase; Hex Total: total hexosaminidase activity; β -gal: lysosomal β -galactosidase; α -Man: α -mannosidase].

	Specific activity			
	HexA	Hex Total	β -gal	α -Man
Control	173.7 \pm 7.346	1601 \pm 79.42	71.18 \pm 6.301	1.975 \pm 0.3065
Amylin	184.6 \pm 5.602	1747 \pm 44.77	76.83 \pm 3.636	1.867 \pm 0.2404
Pramlintide	183.5 \pm 6.936	1821 \pm 72.72	72.90 \pm 4.212	2.750 \pm 0.05000

3.4.6. Amylin and pramlintide decrease post-synaptic marker PSD-95 and induce the formation of cleaved caspase-3.

Here, we studied the effect of amylin and pramlintide on pre-synaptic markers SNAP-25 and synapsin-1 and post-synaptic marker PSD-95 in mice brain homogenate by Western blotting. Both amylin and pramlintide significantly reduced the level of PSD-95 by 65% and 69%, respectively (both, $p < 0.001$), without altering the level of SNAP-25 or synapsin-1 (Figure 3.6.12.). The level of PSD-95 and SNAP-25 levels did not change in lipid rafts after treatment with amylin or pramlintide compared to control group (Figure 3.6.13). The effect of treatments on the apoptotic marker cleaved caspase-3 was also evaluated in brain homogenate, and the results showed pramlintide significantly increased cleaved caspase-3 levels in mice brains compared to control and amylin groups ($p < 0.01$ and $p < 0.05$, respectively) without altering total caspase 3 (Figure 3.6.14). Moreover, neither peptide altered the matrix metalloproteinase MMP9 level when compared to control group (Figure 3.6.14)

3.4.7. Amylin and pramlintide increase microglial activation without altering astrocytes and IDE.

A β is cleaved by degrading enzymes such as IDE (353), whose level is altered in T2DM and AD (354). In this study, treatment with amylin or pramlintide had no significant effect on IDE level compared to control measured from total brain homogenate (Figure 3.6.15.). Neuroinflammation is another hallmark of AD, and increased brain A β levels is associated with microglia activation and astrogliosis that produce an inflammatory cascade leading to neuronal toxicity and death (355). Treatment effects on glial activation markers were evaluated by immunostaining and Western blotting. Pramlintide significantly increased Iba1, a microglia marker when compared to control and amylin group ($p < 0.05$ and $p < 0.01$, respectively) (Figure 3.6.15.). However, neither peptide

modulated the staining of astrocytes with the astrocytic marker glial fibrillary acidic protein (GFAP) in terms of intensity or morphology (Figure 3.6.15. & Figure 3.6.16.), suggesting that treatment with amylin or pramlintide for 30 days did not induce astrogliosis.

3.4.8. LRP1 localization in lipid rafts is decreased by both peptides

The level of LRP1 in lipid rafts prepared from brain homogenates was also analyzed, and the results showed that both amylin and pramlintide significantly reduced LRP1 levels in lipid rafts by 37% and 38%, respectively (both, $p < 0.05$; Figure 3.6.17.). However, both peptides did not alter the level of P-gp in membrane rafts (Figure 3.6.17.). On the other hand, when LRP1 and P-gp measured from total brain homogenate, amylin showed an increase in the level of LRP1 compared to control ($p < 0.05$) and pramlintide groups ($p < 0.05$); however, the level of P-gp was increased by amylin compared to pramlintide ($p < 0.05$) (Figure 3.6.17)

3.4.9. Amylin receptor level does not change after treatments.

Both amylin and pramlintide bind to amylin receptor, which is a heterodimer of calcitonin receptor and receptor activity modifying protein 3 (CTR-RAMP3) (356). To evaluate the effect of daily treatment of either peptide for 30 days on amylin receptor, RAMP3 was analyzed by Western blot in brain homogenate lysate and lipid rafts. We were not able to detect RAMP3 in lipid rafts, but it was detectable in total brain homogenate. Neither treatment altered the RAMP3 levels detected as monomer, homodimer or heterodimer (Figure 3.6.18.).

3.5. Discussion

Amylin is a gut–brain axis hormone which crosses the BBB (357) and exert its effect in the CNS (358). Pramlintide is amylin analogue that was developed by replacing three amino acids in human amylin by prolines residues as follow: Ala25Pro, Ser28Pro, and Ser29Pro to cease amylin oligomerization or aggregation (359). Amylin shares similar secondary structure with A β (214), thus A β binds amylin receptor as well (220). However, the intracellular signaling is different between the two ligands (amylin and A β). AD models treated with amylin or pramlintide have demonstrated modulation of neuroinflammation and bumping A β to the systemic circulation from the brain (228-231). However, several other studies have elaborated pathological features of amylin in AD by increasing the level of pro-inflammatory cytokines, apoptotic biomarkers, and A β related pathology (164, 203, 214, 317, 360-363). Findings from our study agree with the latter reports, since amylin and pramlintide exacerbated A β -related pathology in the TgSwDI mice brains. The daily intraperitoneal injections of amylin or pramlintide for 30 days with 200 μ g/kg/day increased AD pathology as determined by increased A β burden and neurotoxicity in the brains of TgSwDI mice. In addition, our findings revealed that amylin and pramlintide increased A β deposition in hippocampus and cortical microvessels, which is expected to worsen AD pathology. Our data suggest a previously undisclosed link between APP processing and amylin or pramlintide (203, 229-231). Unlike the effect observed in total brain homogenate, the increased level of amyloidogenic pathway proteins in lipid rafts caused by amylin and pramlintide signifies the importance of evaluating APP processing at the DRMs level. Amylin or pramlintide increased the

expression of γ -secretase subunits PSEN1, PSEN2, nicastrin and PEN2 in lipid rafts, an effect that was absent when measured from total brain homogenate, apart from PEN2 in pramlintide treated mice. The increased level of γ -secretase complex subunits in lipid rafts could be accountable for the increased A β burden as confirmed by ELISA and immunohistochemistry results (192, 364).

To explain the observed effect of amylin and pramlintide on the amyloidogenic pathway for APP processing in DRMs, the effect of both peptides on the synthesis of GM1 and GM2 gangliosides was evaluated. These gangliosides are necessary to maintain the CNS integrity and for neurodevelopment (279, 365, 366). However, several studies have reported that GM1 and GM2 are involved in AD pathology (274, 306, 307, 367), and changes in brain ganglioside composition were observed in patients with AD (293, 311, 368), implicating a direct association of gangliosides with AD. GM1 is the most ample ganglioside in the cerebral environment and it cohere to A β at the cell surface, accelerating its extracellular deposition (306, 307). Furthermore, available studies reported that reduced synthesis of GM1 is associated with decreased transport of APP to cell surface (311), and that treatment of neuronal and non-neuronal cells with GM1 increased A $\beta_{40/42}$ secretion by affecting the activity of γ -secretase (313). In a recent study, Yamaguchi and colleagues reported SK-MEL-28-N1 cells treated with GM2 and GM1 demonstrated higher levels of BACE1 in lipid rafts compared to GM3 treated cells (274). Similarly, our data revealed both amylin and pramlintide increased B4GALNT1, whereas pramlintide increased GM1 in lipid rafts, proposing a role in A β overproduction by modulating APP processing. Further analysis of other gangliosides demonstrated only pramlintide increased GM2 levels ($p = 0.07$) when measured from total brain homogenate without altering its effect in lipid rafts. To explain the increased levels of GM1 caused by pramlintide, B3GALT4, the enzyme responsible for GM1 synthesis from GM2, was analyzed and results showed neither amylin nor pramlintide altered this enzyme. Next, and as

the increased level of GM1 and GM2 could also be explained by alteration in their lysosomal degradation, the activity of β -gal which cleaves GM1 to GM2, and HexA which cleaves GM2 to GM3, were evaluated. However, data showed no significant alteration in lysosomal enzyme activities. Collectively, our findings suggest increased GM1 levels could be explained indirectly by increased B4GALNT1, which increased GM2 ganglioside, the precursor of GM1.

Amylin and pramlintide significantly reduced sAPP- α . One study demonstrated that in SH-SY5Y-APP695 cells treated with GM1, sAPP- α significantly decreased (313). Stiffening of the membrane due to accumulated GM1 may decrease sAPP- α by restricting sideward movement and required contact between α -secretase enzyme and substrate (313). The interaction with GM1 has been reported as an important factor in mediating aggregation and toxicity of A β and amylin (369, 370). In addition, amylin association with plasma membrane is thought to be the driving factor of pancreatic β -cells death in T2D (364), where several in vitro studies reported that seeding and clustering of A β and amylin on synthetic membrane are enhanced by GM1 (371-373).

Increased accumulation of A β due to its increased production by amylin or pramlintide caused synaptic loss and microglial activation as demonstrated by increased Iba-1, increased apoptotic marker cleaved caspase-3 and reduced post-synaptic marker PSD-95. Increased brain A β is expected to activate glial cells and produce inflammatory cascade (355). Furthermore, in a rat model overexpressing hIAPP, the findings showed accumulation of activated microglia in IAPP deposition sites which was accompanied by cognitive impairment (202). This observed effect by our work and others contradicts other studies reported neuroprotective effect of amylin against neuroinflammation where amylin reduced Iba1, CD68, and pro-inflammatory cytokines (229, 230).

Our findings also demonstrated a reduction in total PSD-95 expression following amylin and pramlintide treatments. This effect was associated with reduced LRP1 in lipid rafts fraction, but not in total homogenate. In neuronal cells, LRP1 partitions between both lipid rafts and non-raft membrane fractions (374), and its signaling activation leads to neurite outgrowth and cell growth (375). LRP1 interacts with the active pool of PSD-95 and a reduction in total PSD-95 is expected to reduce total LRP1 in neuronal cells (376). The localization of LRP1 to lipid rafts mirror the activity of PSD-95, which is familiar to cluster dissimilar membrane proteins in rafts through its scaffolding activity (377-379). Therefore, the reduction in total PSD-95 level due to amylin and pramlintide could explain the reduction in LRP1 in lipid rafts. Unlike our findings, pramlintide treatment for 5 weeks increased the level of the synapsin 1 (228). In this study, the authors used SAMP8 mice at the age of 6 months; this mouse model exhibits natural age-related dementia, which is different from the transgenic mouse model TgSwDI model. However, whether similar effect will be observed with pramlintide under a different pathological insult requires further investigation.

The findings of our study demonstrated a new pathological role of amylin and pramlintide in AD. Both peptides increased A β , microglial activation, post-synaptic loss, and apoptosis. The addition of behavioral studies to this project would assist in studying the effect of these observed pathological insults on cognitive function and performance. Furthermore, the addition of a wild-type mice group would be an important addition to study the effect of amylin and pramlintide on lipid rafts, inflammatory markers, synaptic loss, and neuronal cell death in the absence of A β insults. In addition, it worth studying the effect of both peptides in different mouse models of AD and compare the findings.

While studies with pramlintide are limited in the literature, available studies with amylin show contradicting effects against A β -related pathology in AD mouse models. An explanation(s) for this discrepancy is not clear, however, the mouse model used in our study is different from others. In this study we used the CAA/AD model TgSwDI, which is characterized by A β deposition not only in the parenchyma but also on brain microvessels. Though we selected a dose and route of administration shown to be protective (230, 231, 274), the opposite effect was observed. The plasma amylin concentration in fasting condition is in the range 4-25 pmol/ in healthy subjects (380), whereas the maximum concentration of amylin treatment we used for the mice is expected to be \approx 1 nmol/l, with half-life of 20-45 min for exogenous amylin or pramlintide (174, 381). In their review (382), Qiu et al explained the discrepancy observed with amylin could be aggregation dependent. For example, treatment of rat cortical neurons with human amylin at 50 μ M concentration caused neurotoxicity due to amylin aggregation, whereas at the same concentration, rat amylin did not show aggregation or neurotoxicity (383). Also, at lower concentrations (2.5 nM – 2.5 μ M), human amylin was able to antagonize aggregated A β ₄₂-induced neurotoxicity (382). Low vs. high concentrations of amylin could activate different receptors based on the degree of amylin aggregation (229). In this scenario, the neuroprotective effect of non-aggregated amylin is based on binding a different receptor than that bound by aggregated amylin (384). Thus, to better understand and clarify amylin and pramlintide effects against AD, dose dependent studies are necessary.

3.6. Figures and legends

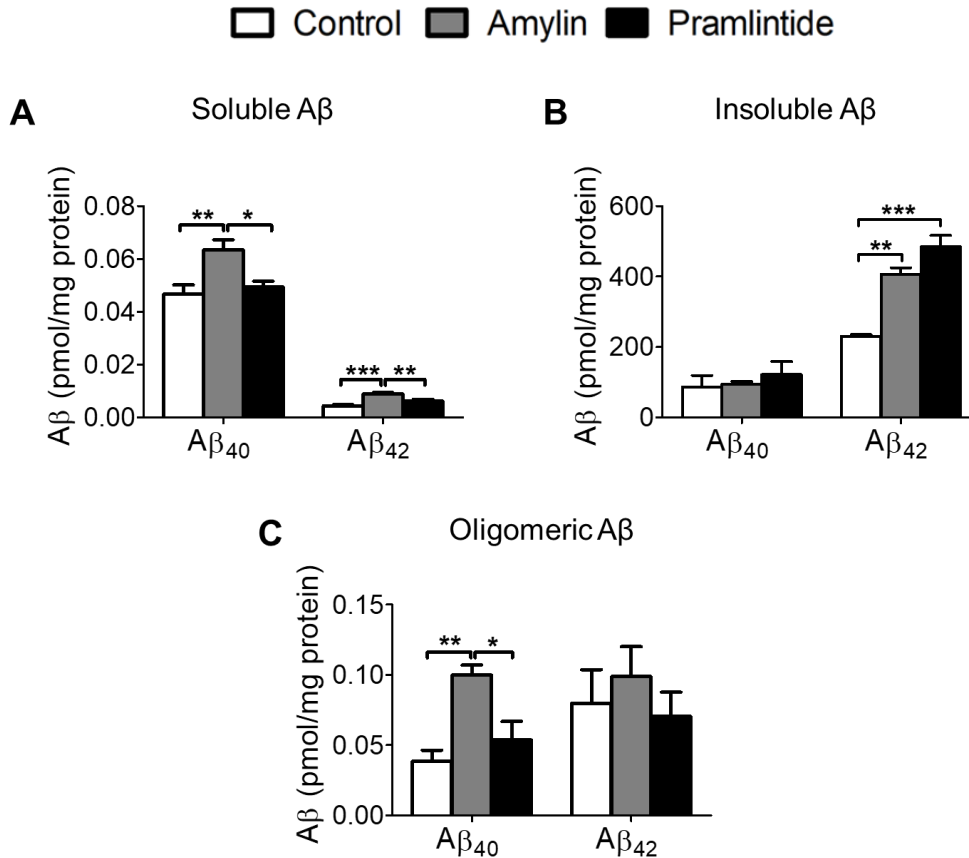


Figure 3.6. 1. Effect of amylin and pramlintide treatments on Aβ burden in TgSwDI mice brains measured by ELISA. (A) Amylin increased the level of soluble Aβ₄₀ by 36% compared to control and 28% compared to pramlintide. Also, amylin increased the level of soluble Aβ₄₂ by 101% compared to control group and by 43% compared to pramlintide. (B) Both peptides showed significant increase of insoluble Aβ₄₂ compared to control, where amylin increased the insoluble Aβ₄₂ by 76%, whereas pramlintide increased insoluble Aβ₄₂ 109%. (C) Amylin significantly increased oligomeric Aβ₄₀ by 160% compared to control, and 85% compared to. Neither treatment

altered the oligomeric A β ₄₂. A β level was normalized to the total protein content in the measured samples. Data is presented as mean \pm SEM for n = 4 mice per group with * p < 0.05, ** p < 0.01, *** p < 0.001.

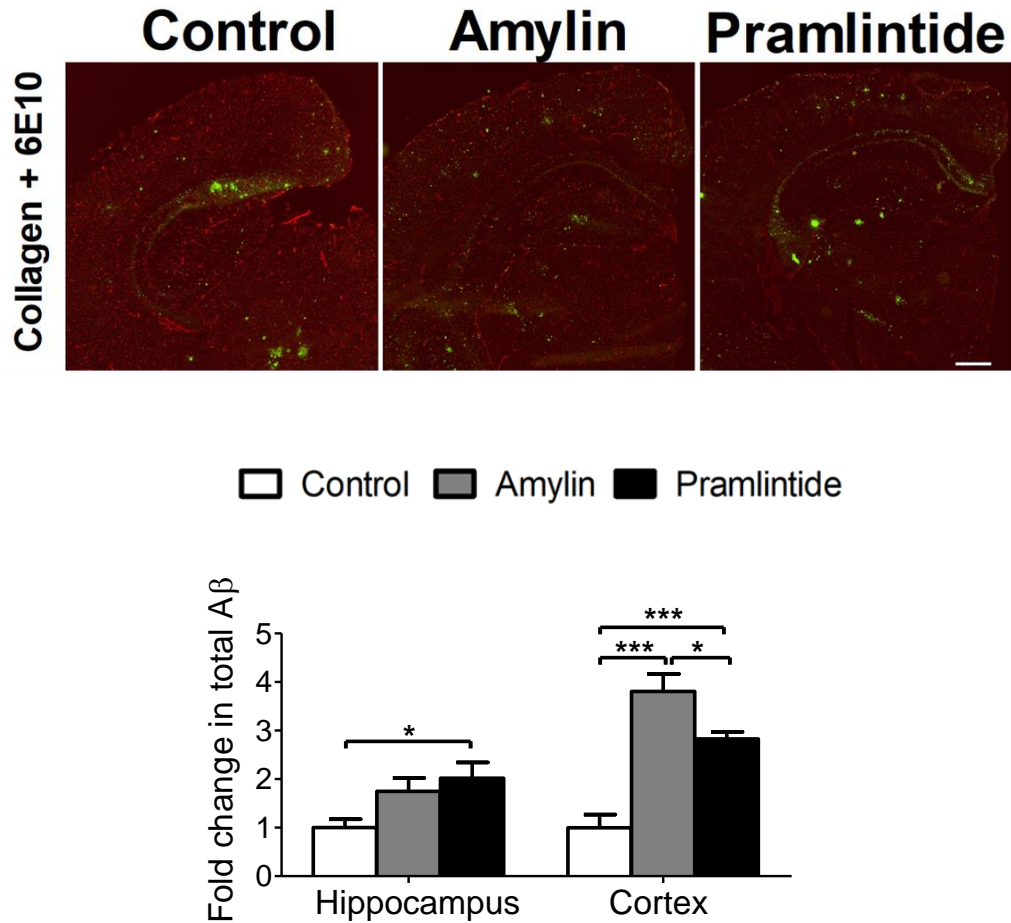


Figure 3.6. 2. Effect of amylin and pramlintide treatments on total A β burden in TgSwDI mice brains measured by IHC. The IHC analysis (lower panel) demonstrated a significant increase in total A β (detected by 6E10, green color) in the brains of both amylin (280% increase) and pramlintide (182% increase) compared to control when measured in the cortex. Moreover, pramlintide significantly increased the level of total A β by 101% in the hippocampus compared to the control group. Brain microvessels are stained by collagen IV antibody (red). Scale bar = 500 μ m. Data is presented as mean \pm SEM for n = 3 mice per group with * $p < 0.05$, *** $p < 0.001$.

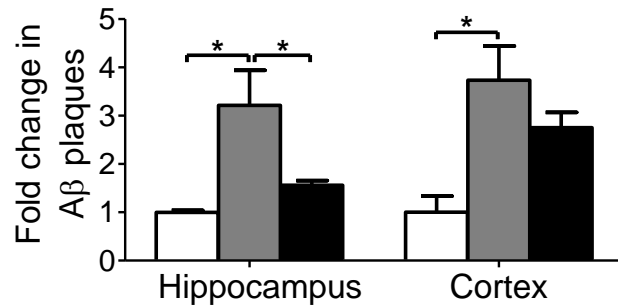
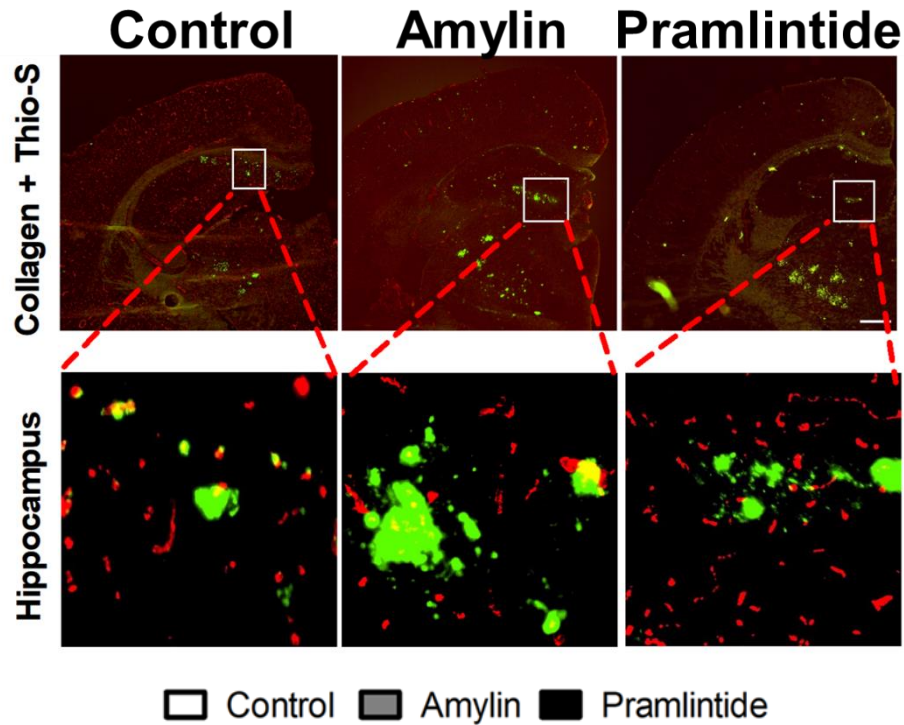


Figure 3.6. 3. Effect of amylin and pramlintide treatments on total A β burden in TgSwDI mice brains measured by IHC. Quantification analysis demonstrated A β plaques (detected by Thioflavin-S, green color) were significantly higher in hippocampus (212% increase) and cortex (273% increase) of amylin treated mice compared to control group. Also, amylin increased the level of A β plaques in the hippocampus compared to pramlintide treated mice. Pramlintide tended to increase A β plaques in both regions when compared to control, however the effect was not

statistically significant. Brain microvessels are stained by collagen IV antibody (red). Scale bar = 500 μm . Data is presented as mean \pm SEM for n = 3 mice per group with * p < 0.05.

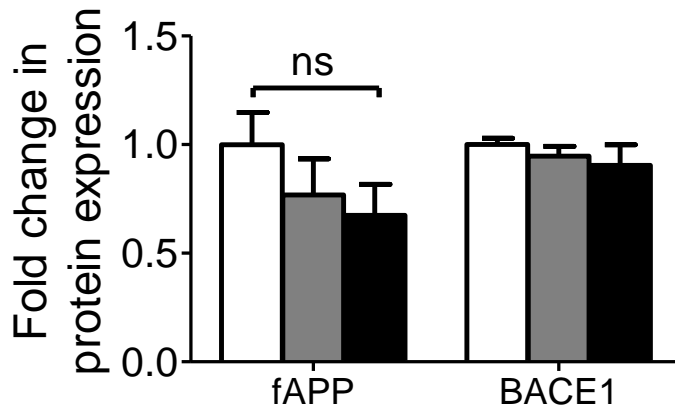
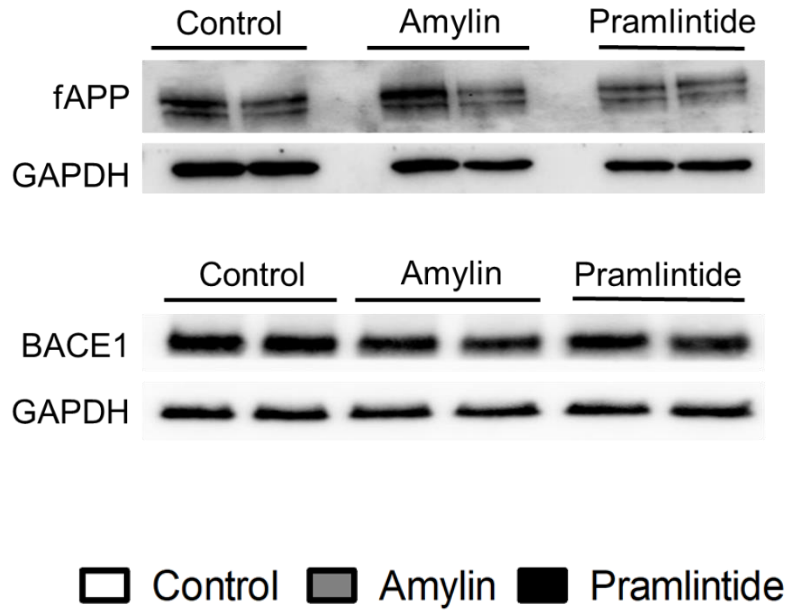
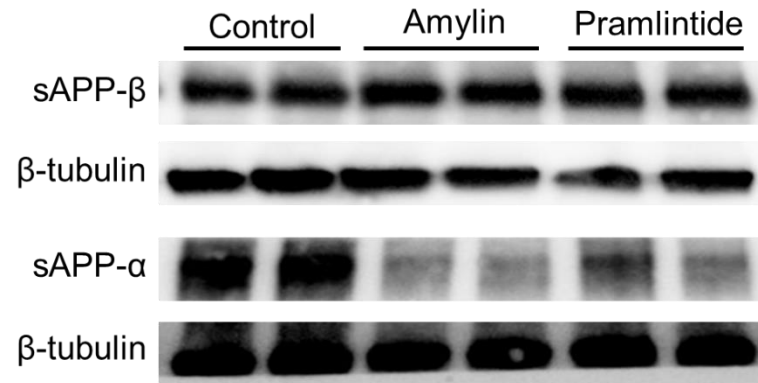


Figure 3.6. 4. Effect of amylin and pramlintide on APP and BACE1 in total brain homogenate. Representative Western blot and densitometry analysis of full-length APP (fAPP) and BACE1 demonstrated Amylin and pramlintide did not alter full-length APP (fAPP) and BACE1 in mice brain homogenates. fAPP and BACE1 levels were normalized to GAPDH level. Data is presented as mean \pm SEM for n = 6 mice per group with ns = not significant.



□ Control ■ Amylin ■ Pramlintide

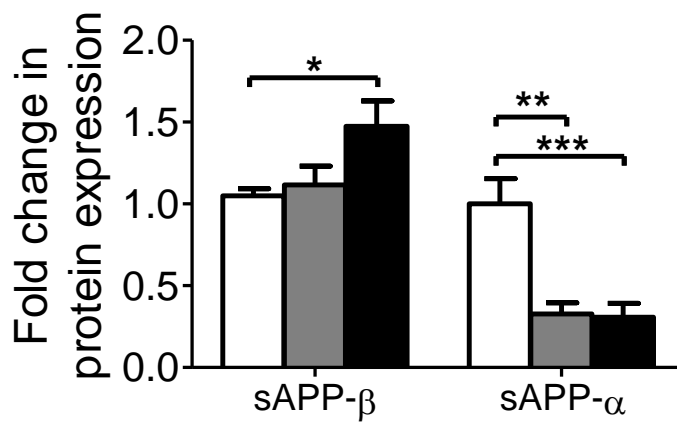


Figure 3.6. 5. Effect of amylin and pramlintide on sAPP production in total brain homogenate. Representative Western blot and densitometry analysis of sAPP-β and sAPP-α in mice brains demonstrated pramlintide significantly increased sAPP-β by 40% compared to control, whereas 68% and 70% reduction in the level of sAPP-α were observed after treatment with amylin and pramlintide, respectively. The levels of sAPP-β and sAPP-α were normalized to the level of β-tubulin. Data is presented as mean ± SEM for n = 6 mice per group with * $p < 0.05$, ** $p < 0.01$, and *** $p < 0.001$ compared to control group.

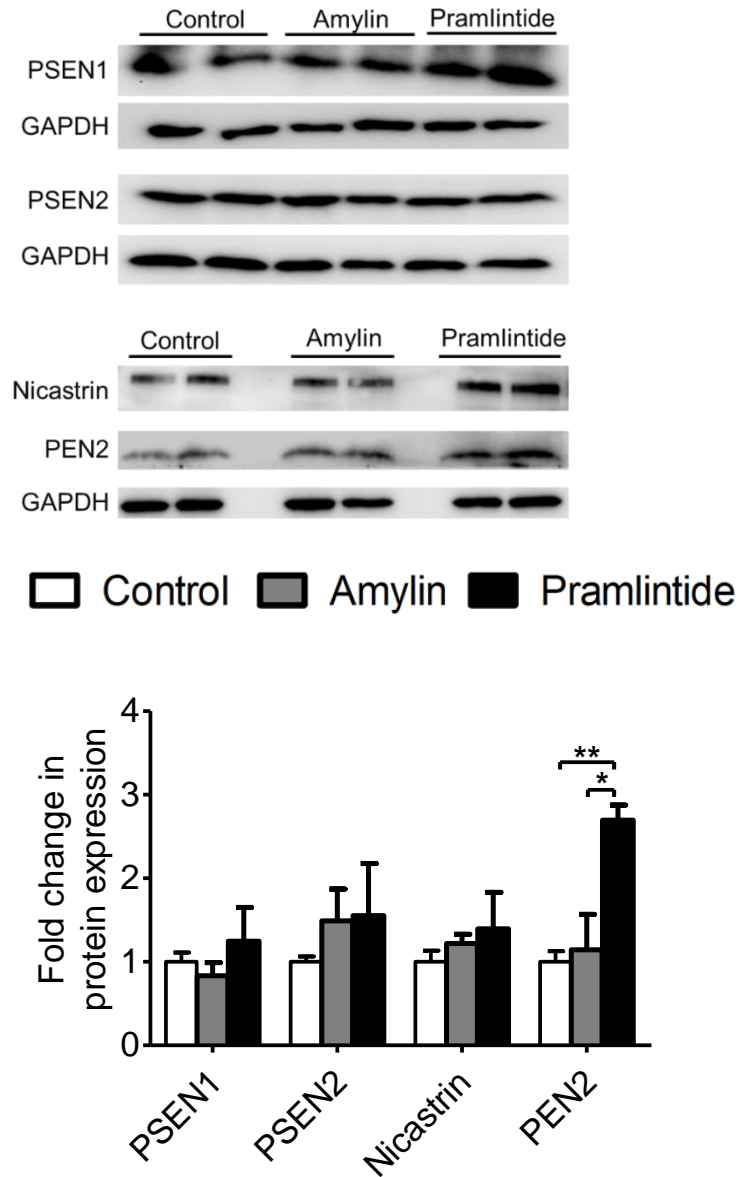
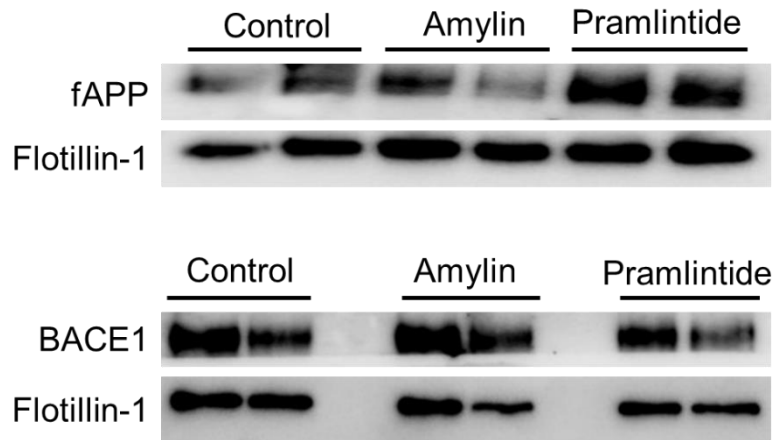


Figure 3.6. 6. Effect of amylin and pramlintide on γ -secretase in total brain homogenate.

Representative Western blot and densitometry analysis of γ -secretase subunits in mice brains demonstrated pramlintide demonstrated a significant increase by 170% and 144% in PEN2 subunit when compared to control and amylin; however, neither peptide had an effect on the other γ -secretase subunits PSEN1, PSEN2 and nicastrin. All proteins were normalized to the level of GAPDH. Data is presented as mean \pm SEM for n = 6 mice per group with * $p < 0.05$, and ** $p < 0.01$.



□ Control ■ Amylin ■ Pramlintide

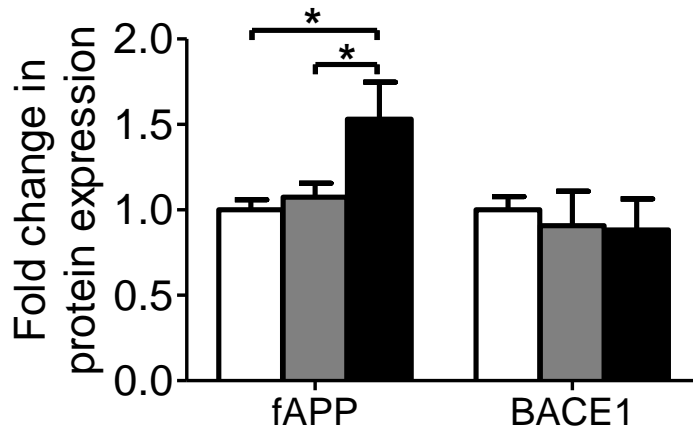


Figure 3.6. 7. Effect of amylin and pramlintide on APP and BACE1 in lipid rafts.

Representative Western blot and densitometry analysis of fAPP and BACE1 in lipid rafts demonstrated pramlintide significantly increased APP in lipid rafts by 50% when compared to control and 53% when compared amylin. The level of BACE1 in lipid rafts did not change between the three groups. All proteins were normalized to the level of flotillin-1. Data is presented as mean \pm SEM for $n = 6$ mice per group with * $p < 0.05$.

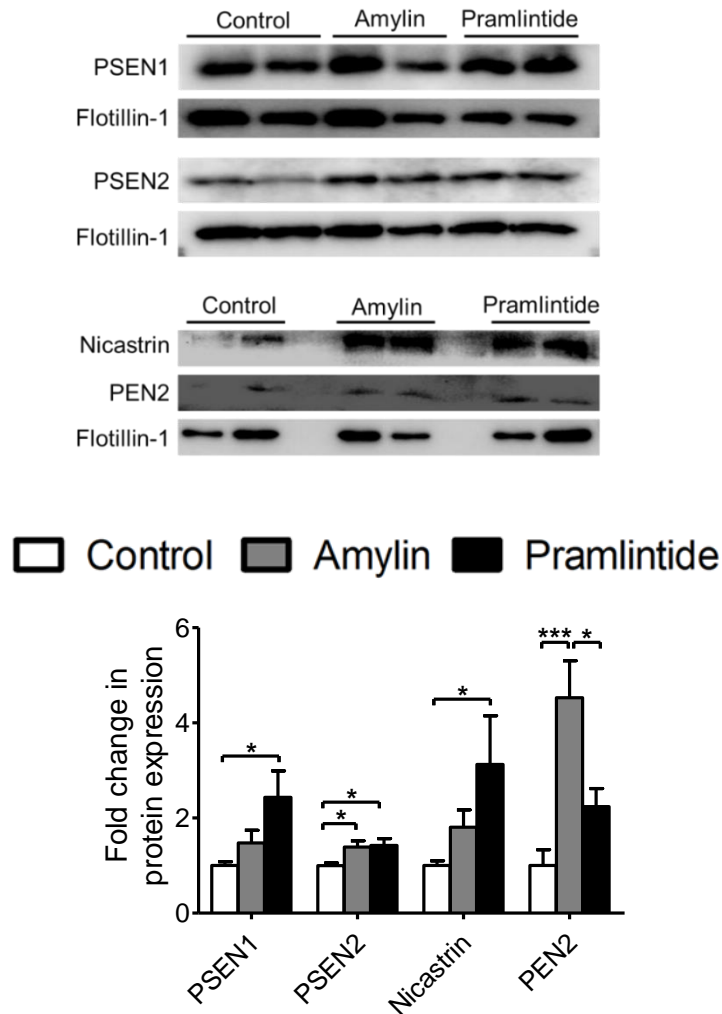


Figure 3.6. 8. Effect of amylin and pramlintide on γ -secretase complex subunits in lipid rafts.

Representative Western blot and densitometry analysis of γ -secretase subunits in lipid rafts demonstrated amylin showed significant increase in the level of PSEN2 by 39%, and PEN2 by 53% compared to the control group in lipid rafts. In addition, amylin increased the level of PEN2 compared to pramlintide when measured from lipid rafts. On the other hand, pramlintide increased PSEN1, PSEN2, and nicastrin in lipid rafts compared to the control group by 143%, 42%, and 112%, respectively. The measured proteins were normalized to the level of flotillin-1. Data is presented as mean \pm SEM for n = 6 mice per group with * $p < 0.05$ and *** $p < 0.001$.

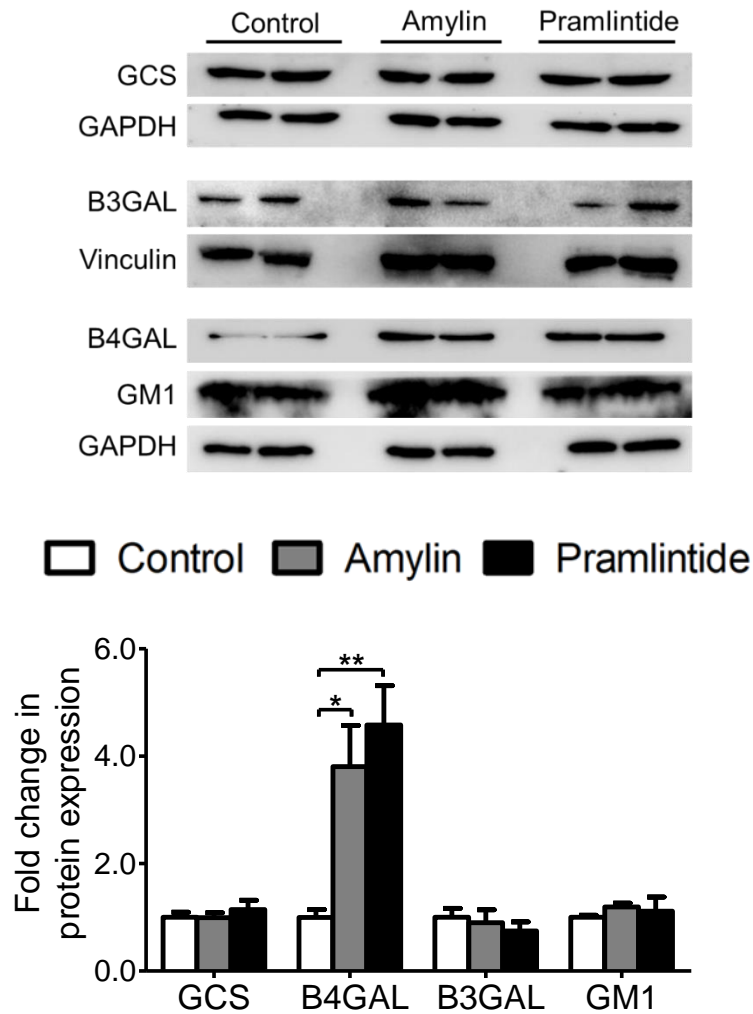


Figure 3.6. 9. Effect of amylin and pramlintide effect on ganglioside production measured from total brain homogenate. Representative Western blot and densitometry analysis of ganglioside demonstrated amylin and pramlintide did not alter the expression of GCS and B3GALT4 (B3GAL); however, both amylin and pramlintide significantly increased the level of B4GALNT1 in total brain homogenate by 180% and 253% with, respectively. The results did not show alteration in the level of GM1 between the three groups when measured from total brain homogenate. The data were normalized to the level of GAPDH or vinculin. Data is presented as mean \pm SEM for $n = 6$ mice per group with * $p < 0.05$ and ** $p < 0.01$.

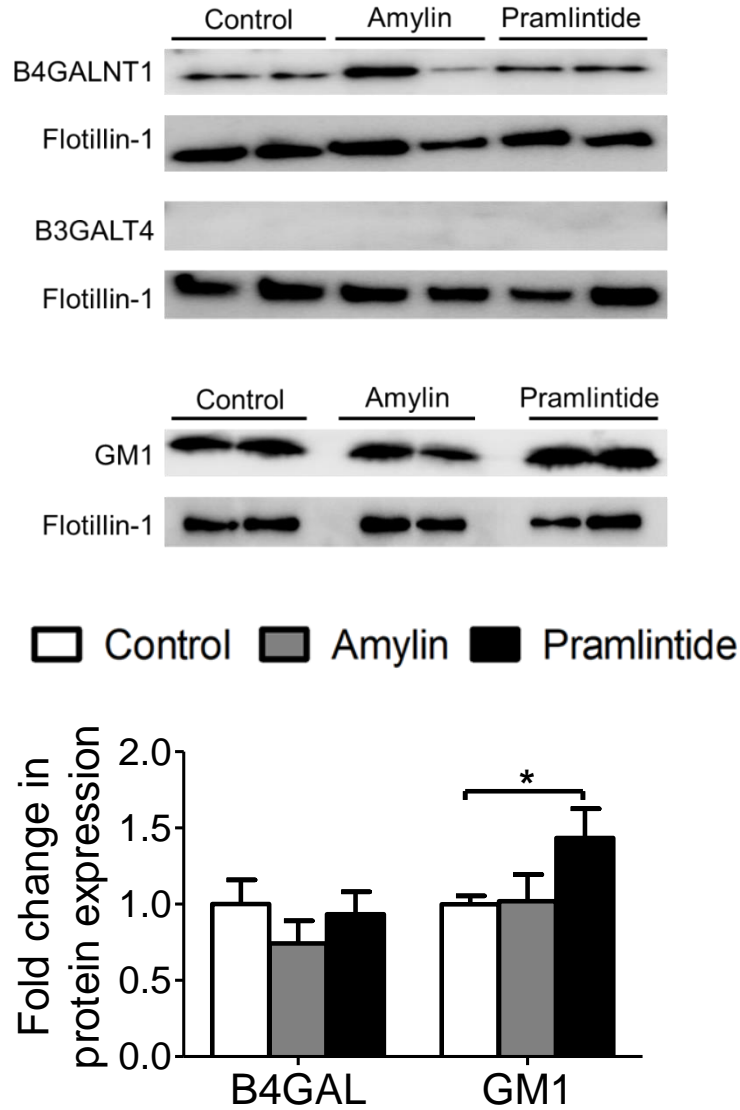


Figure 3.6. 10. Effect of amylin and pramlintide on ganglioside production measured from lipid rafts. Representative Western blot and densitometry analysis of B4GALNT1, B3GALT4 and GM1 in lipid rafts. Only pramlintide increased the level of GM1 in lipids rafts by 50% while neither peptide altered the level of B4GALNT1 in lipid rafts. On the other hand, B3GALT4 was not detected in lipid rafts. B4GALNT1 and GM1 were normalized to the level of flotillin-1. Data is presented as mean \pm SEM for n = 6 mice per group with * $p < 0.05$ compared to control group.

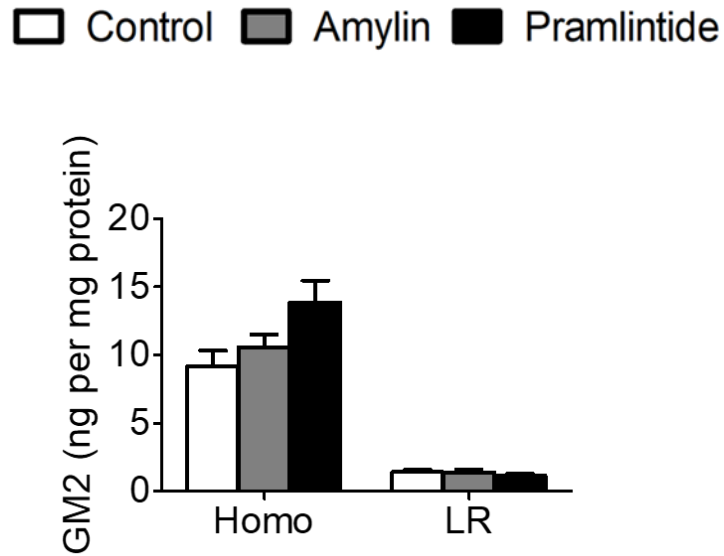
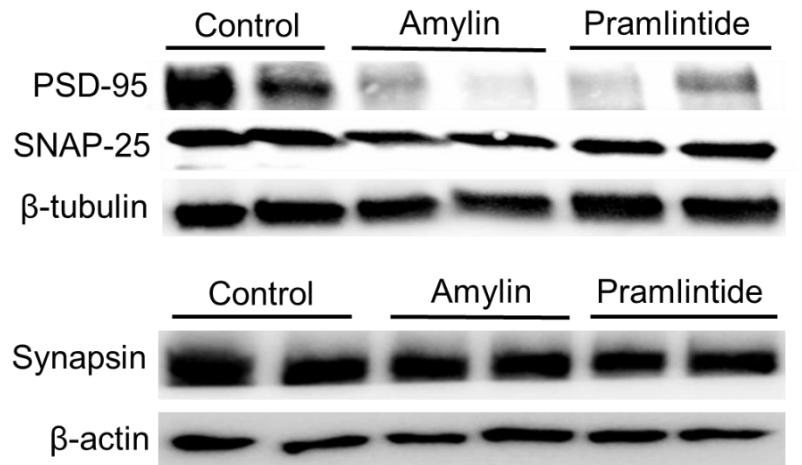


Figure 3.6. 11. The effect of amylin and pramlintide on GM2 gangliosides production in total brain homogenate and lipid rafts. Only pramlintide increased the level of GM2 by 50% when measured from total brain homogenate with 95% CI of diff (-9.365 to 0.03932); however, neither peptide altered GM2 levels in lipid rafts as determined by ELISA. Data were normalized to the total protein content from brain homogenate. Data is presented as mean \pm SEM for n = 4 mice per group.



□ Control ■ Amylin ■ Pramlintide

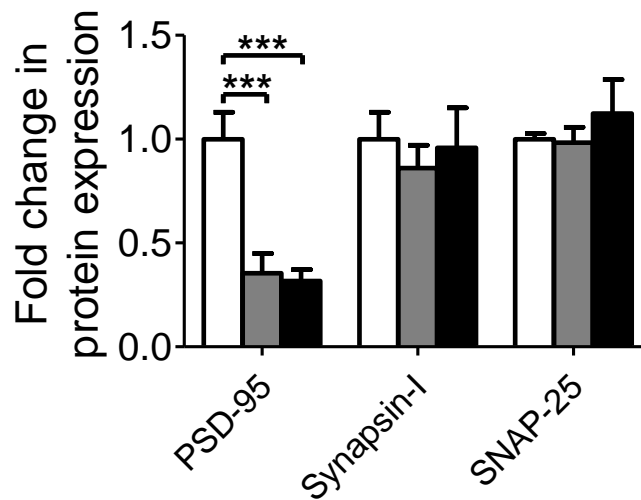


Figure 3.6. 12. Treatments with amylin and pramlintide impair the post-synaptic marker PSD-95. Representative Western blot and densitometry analysis of synaptic markers in mice brain homogenates showed amylin and pramlintide significantly reduced the level of PSD-95 by 65% and 69%, respectively, without affecting SNAP-25 and synapsin-1 in total brain homogenate. Data were normalized to the level of β-tubulin or β-actin. Data is presented as mean ± SEM for n = 6 mice per group with *** $p < 0.001$ compared to control group.

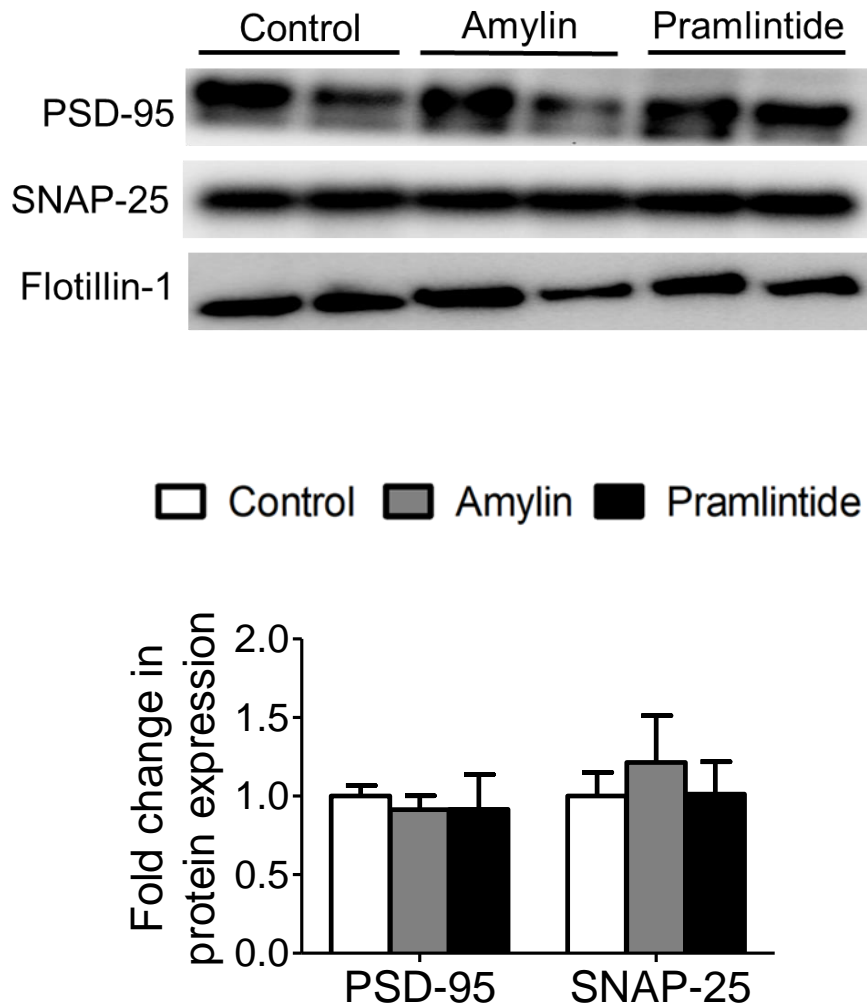
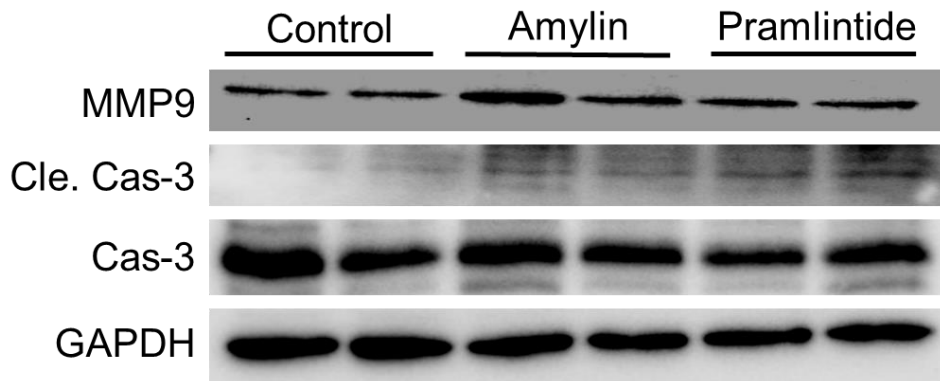


Figure 3.6. 13. Treatment with amylin and pramlintide did not alter synaptic markers in lipid rafts. Representative Western blot and densitometry analysis of synaptic markers in lipid rafts. Amylin and pramlintide had no effect on PSD-95 and SNAP-25 levels in lipid rafts. All proteins were normalized to the level of flotillin-1. Data is presented as mean \pm SEM for n = 4 mice per group.



Control
 Amylin
 Pramlintide

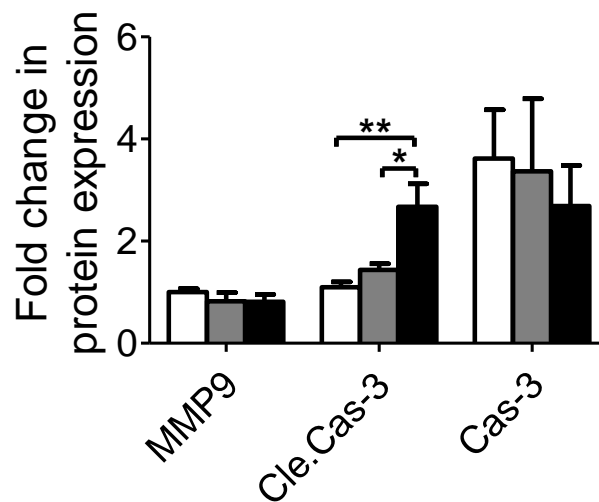


Figure 3.6. 14. The effect of amylin and pramlintide on caspase-3 and MMP9. Pramlintide significantly increased cleaved caspase-3 (Cle.Cas-3) compared to amylin and control group without affecting levels of total caspase-3 (Cas-3) and MMP9. Cleaved caspase 3 was normalized to the total caspase-3. All proteins were normalized to the level of GAPDH. Data is presented as mean \pm SEM for n = 6 mice per group with * $p < 0.05$ and ** $p < 0.01$.

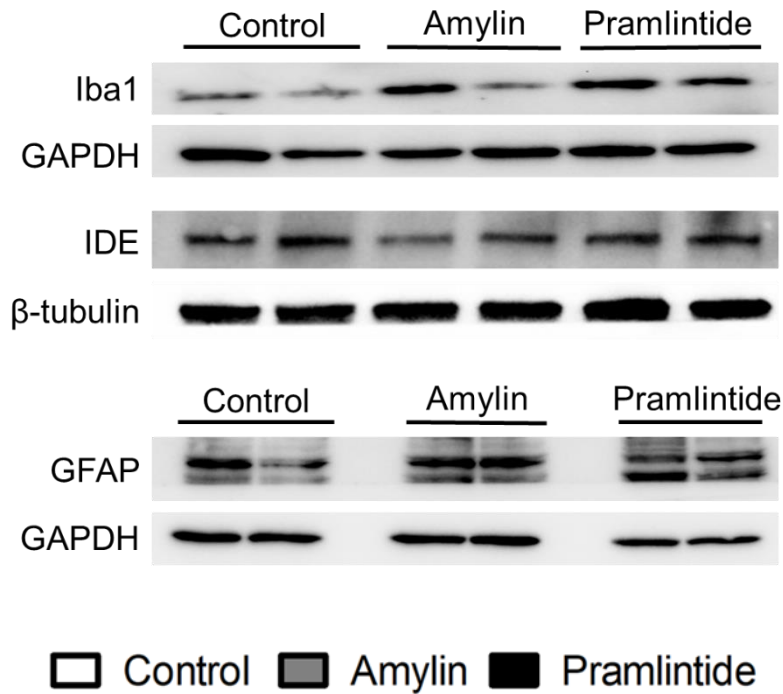


Figure 3.6. 15. The effect of amylin and pramlintide on neuroinflammation and IDE. Pramlintide significantly increased the level of Iba1 compared to control and amylin. Neither treatment altered GFAP or IDE levels in total brain homogenate. All proteins were normalized to the level of GAPDH or β -tubulin. Data is presented as mean \pm SEM for $n = 6$ mice per group with * $p < 0.05$ and ** $p < 0.01$.

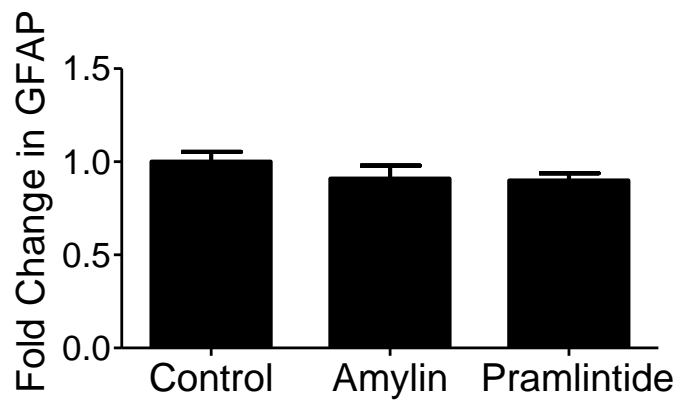
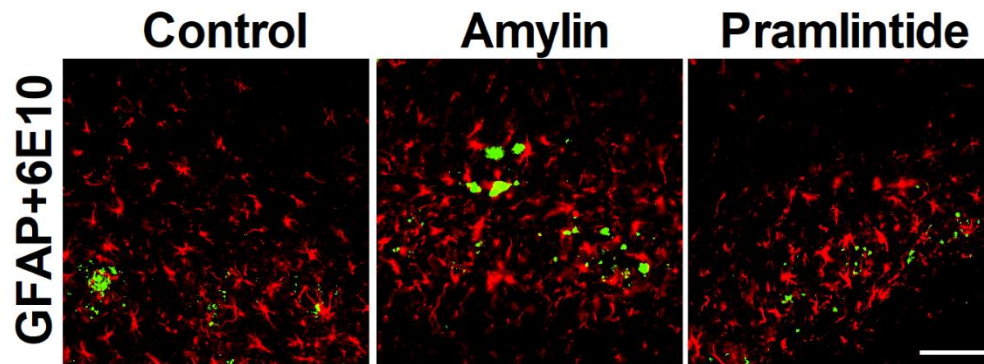


Figure 3.6. 16. The effect of treatment on astrocytes activity determined by IHC. Immunohistochemical analysis of GFAP (red) in brain hippocampus showed the treatments have no effect on GFAP intensity and A β localization (green). Data is presented as mean \pm SEM for n = 3 mice per group.

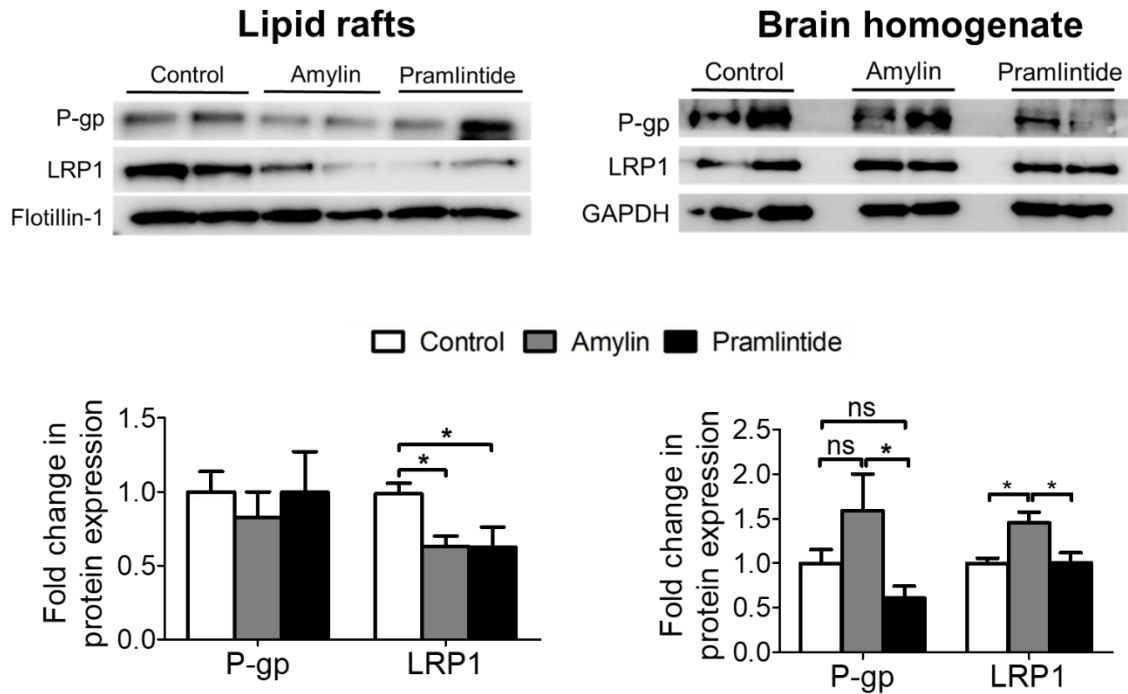


Figure 3.6. 17. The effect of treatments on P-gp and LRP1 in lipid rafts. Amylin and pramlintide significantly reduced LRP1 levels in lipid rafts by 37% and 38%, respectively, without altering P-gp in lipid rafts as determined by Western blot. On the other hand, amylin increased the level of LRP1 compared to the control and pramlintide group measured from total brain homogenate. All proteins from lipid rafts were normalized to the level of flotillin-1, and proteins from brain homogenate were normalized to GAPDH. Data is presented as mean \pm SEM for $n = 6$ mice per group with * $p < 0.05$.

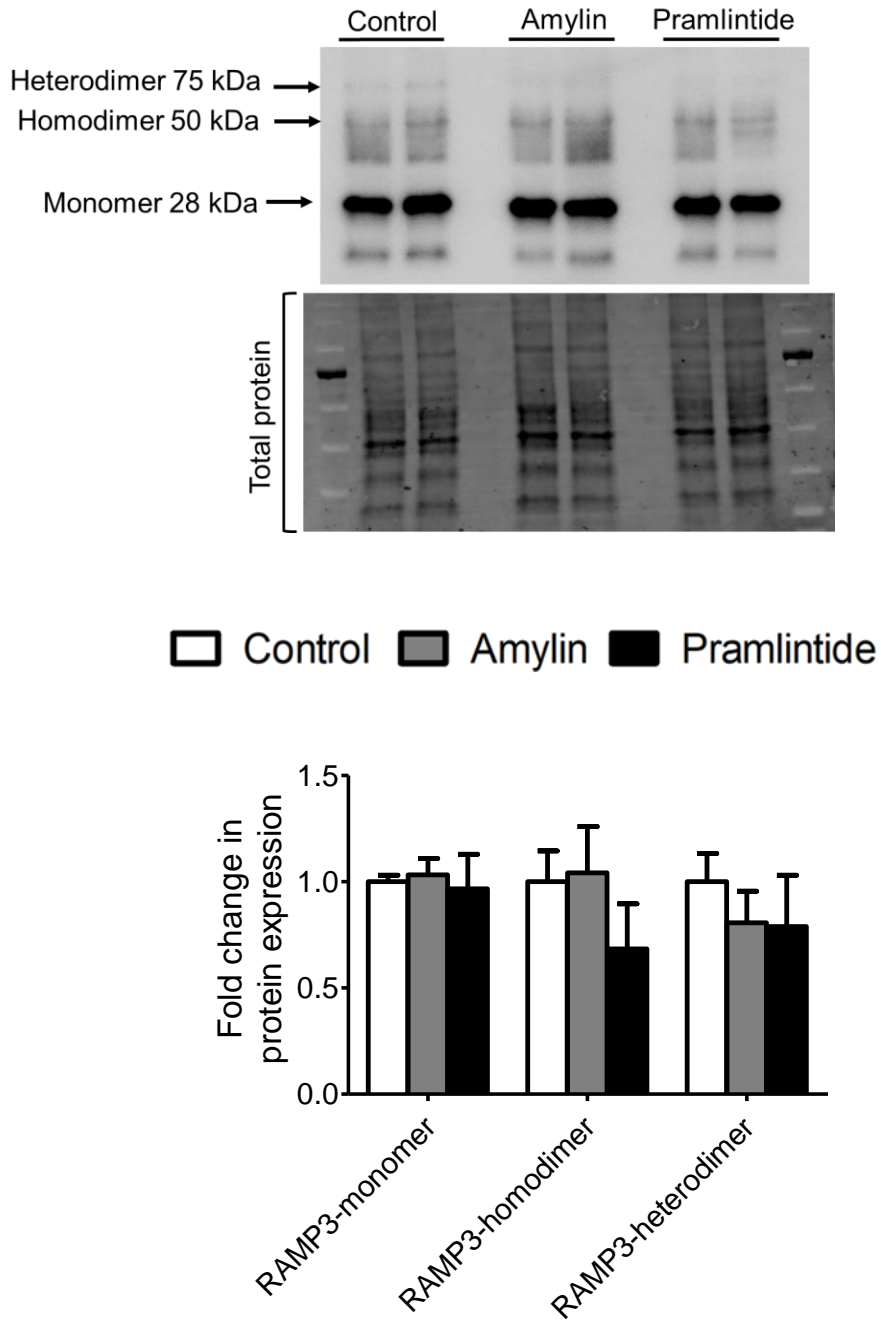


Figure 3.6. 18. The effect of treatment on amylin receptor. Treatment with amylin and pramlintide did not alter the level of amylin receptor measured by the level of RAMP3. Data was normalized to the total protein. Data is presented as mean \pm SEM for n = 4 mice per group.

4. SUMMARY AND CONCLUSION

Membrane rafts are an essential platform to produce A β by hosting the amyloidogenic pathway proteins and enzymes. To detect these proteins and enzymes in lipid rafts, optimized conditions to fractionate membrane rafts are necessary. While certain conditions aid in the isolation of certain protein within the lipid rafts, they might not be suitable for the isolation of other proteins. The purpose of the first project was to isolate lipid rafts from brain tissues, which was successfully accomplished. Next, in the second project, we identified the mechanism by which amylin and pramlintide increased the pathological features of AD. For the first time, amylin and pramlintide have shown to increase the localization of APP and γ -secretase proteins in lipid rafts suggesting an increase in A β production, which was confirmed by ELISA and IHC. This increase in A β burden was associated with increased pathological features in the TgSwDI mouse model.

Gangliosides have been reported in several studies as an integral factor in AD pathology, especially by increasing the production of A β , aggregation of A β , localization of APP, BACE1, and γ -secretase in membrane rafts as well as increasing γ -secretase activity and increased microglial activation. These effects, apart from BACE1, were observed after treatment with amylin and pramlintide for 30 days and were mediated by increased level of GM1 and B4GALNT1 by both peptides.

In conclusion, finding from this work suggest amylin and pramlintide have the potential to increase A β pathology through modulating γ -secretase activity and APP processing in lipid rafts and

increasing B4GALNT1 by both peptides and increasing the level and GM1 and GM2 gangliosides by pramlintide.

4.1. Future directions

Based on my findings from this study, I propose the following studies as future directions:

1. The effect of amylin or pramlintide is variable between different studies. Thus, to better understand and clarify amylin and pramlintide effects against AD, dose dependent studies are necessary.
2. Studying the effect of both peptides on blood-brain barrier (BBB) integrity and the clearance of A β across the BBB.
3. Behavioral studies to evaluate the effect of amylin or pramlintide on memory function and in parallel with wild-type mice.

5. REFERENCES

1. Lage JM. 100 Years of Alzheimer's disease (1906-2006). *J Alzheimers Dis.* 2006;9(3 Suppl):15-26.
2. Strassnig M, Ganguli M. About a peculiar disease of the cerebral cortex: Alzheimer's original case revisited. *Psychiatry (Edgmont).* 2005;2(9):30-3.
3. Selkoe DJ. Alzheimer's disease is a synaptic failure. *Science.* 2002;298(5594):789-91.
4. Alzheimer's Association. 2019 Alzheimer's disease facts and figures 2019, April 15 [Available from: <https://www.alz.org/alzheimers-dementia/facts-figures>].
5. Levy-Lahad E, Wijsman EM, Nemens E, Anderson L, Goddard KA, Weber JL, et al. A familial Alzheimer's disease locus on chromosome 1. *Science.* 1995;269(5226):970-3.
6. St George-Hyslop P, Haines J, Rogaev E, Mortilla M, Vaula G, Pericak-Vance M, et al. Genetic evidence for a novel familial Alzheimer's disease locus on chromosome 14. *Nat Genet.* 1992;2(4):330-4.
7. Wisniewski KE, Wisniewski HM, Wen GY. Occurrence of neuropathological changes and dementia of Alzheimer's disease in Down's syndrome. *Ann Neurol.* 1985;17(3):278-82.
8. van der Flier WM, Pijnenburg YA, Fox NC, Scheltens P. Early-onset versus late-onset Alzheimer's disease: the case of the missing APOE varepsilon4 allele. *Lancet Neurol.* 2011;10(3):280-8.
9. Miyoshi K. What is 'early onset dementia'? *Psychogeriatrics.* 2009;9(2):67-72.

10. Chakrabarti S, Khemka VK, Banerjee A, Chatterjee G, Ganguly A, Biswas A. Metabolic Risk Factors of Sporadic Alzheimer's Disease: Implications in the Pathology, Pathogenesis and Treatment. *Aging Dis.* 2015;6(4):282-99.
11. Shen J, Kelleher RJ, 3rd. The presenilin hypothesis of Alzheimer's disease: evidence for a loss-of-function pathogenic mechanism. *Proc Natl Acad Sci U S A.* 2007;104(2):403-9.
12. Dickson DW, Murray ME. Intraneuronal amyloid-beta accumulation in basal forebrain cholinergic neurons: a marker of vulnerability, yet inversely related to neurodegeneration. *Brain.* 2015;138(Pt 6):1444-5.
13. Kukull WA, Ganguli M. Epidemiology of dementia: concepts and overview. *Neurol Clin.* 2000;18(4):923-50.
14. Iqbal K, Grundke-Iqbal I. Alzheimer's disease, a multifactorial disorder seeking multitherapies. *Alzheimers Dement.* 2010;6(5):420-4.
15. Jellinger KA, Attems J. Neurofibrillary tangle-predominant dementia: comparison with classical Alzheimer disease. *Acta Neuropathol.* 2007;113(2):107-17.
16. Duyckaerts C, Delatour B, Potier MC. Classification and basic pathology of Alzheimer disease. *Acta Neuropathol.* 2009;118(1):5-36.
17. Iqbal K, Flory M, Khatoon S, Soininen H, Pirttila T, Lehtovirta M, et al. Subgroups of Alzheimer's disease based on cerebrospinal fluid molecular markers. *Ann Neurol.* 2005;58(5):748-57.
18. Strittmatter WJ, Roses AD. Apolipoprotein E and Alzheimer disease. *Proc Natl Acad Sci U S A.* 1995;92(11):4725-7.
19. Blacker D, Haines JL, Rodes L, Terwedow H, Go RC, Harrell LE, et al. ApoE-4 and age at onset of Alzheimer's disease: the NIMH genetics initiative. *Neurology.* 1997;48(1):139-47.

20. Kulminski AM, Raghavachari N, Arbeev KG, Culminskaya I, Arbeeva L, Wu D, et al. Protective role of the apolipoprotein E2 allele in age-related disease traits and survival: evidence from the Long Life Family Study. *Biogerontology*. 2016;17(5-6):893-905.
21. Budson AE, Solomon PR. New criteria for Alzheimer disease and mild cognitive impairment: implications for the practicing clinician. *Neurologist*. 2012;18(6):356-63.
22. Weller J, Budson A. Current understanding of Alzheimer's disease diagnosis and treatment. *F1000Res*. 2018;7.
23. Saint-Aubert L, Barbeau EJ, Peran P, Nemmi F, Vervueren C, Mirabel H, et al. Cortical florbetapir-PET amyloid load in prodromal Alzheimer's disease patients. *EJNMMI Res*. 2013;3(1):43.
24. Hampel H, Burger K, Teipel SJ, Bokde AL, Zetterberg H, Blennow K. Core candidate neurochemical and imaging biomarkers of Alzheimer's disease. *Alzheimers Dement*. 2008;4(1):38-48.
25. Shen Y, Wang H, Sun Q, Yao H, Keegan AP, Mullan M, et al. Increased Plasma Beta-Secretase 1 May Predict Conversion to Alzheimer's Disease Dementia in Individuals With Mild Cognitive Impairment. *Biol Psychiatry*. 2018;83(5):447-55.
26. Dong H, Li J, Huang L, Chen X, Li D, Wang T, et al. Serum MicroRNA Profiles Serve as Novel Biomarkers for the Diagnosis of Alzheimer's Disease. *Dis Markers*. 2015;2015:625659.
27. Tang-Wai DF, Graff-Radford NR, Boeve BF, Dickson DW, Parisi JE, Crook R, et al. Clinical, genetic, and neuropathologic characteristics of posterior cortical atrophy. *Neurology*. 2004;63(7):1168-74.

28. McMonagle P, Kertesz A. Exploded drawing in posterior cortical atrophy. *Neurology*. 2006;67(10):1866.
29. Alladi S, Xuereb J, Bak T, Nestor P, Knibb J, Patterson K, et al. Focal cortical presentations of Alzheimer's disease. *Brain*. 2007;130(Pt 10):2636-45.
30. Snowden JS, Stopford CL, Julien CL, Thompson JC, Davidson Y, Gibbons L, et al. Cognitive phenotypes in Alzheimer's disease and genetic risk. *Cortex*. 2007;43(7):835-45.
31. Koedam EL, Lauffer V, van der Vlies AE, van der Flier WM, Scheltens P, Pijnenburg YA. Early-versus late-onset Alzheimer's disease: more than age alone. *J Alzheimers Dis*. 2010;19(4):1401-8.
32. Norfray JF, Provenzale JM. Alzheimer's disease: neuropathologic findings and recent advances in imaging. *AJR Am J Roentgenol*. 2004;182(1):3-13.
33. Jack CR, Jr., Petersen RC, Xu YC, Waring SC, O'Brien PC, Tangalos EG, et al. Medial temporal atrophy on MRI in normal aging and very mild Alzheimer's disease. *Neurology*. 1997;49(3):786-94.
34. Alves L, Correia AS, Miguel R, Alegria P, Bugalho P. Alzheimer's disease: a clinical practice-oriented review. *Front Neurol*. 2012;3:63.
35. Holtzman DM, Morris JC, Goate AM. Alzheimer's disease: the challenge of the second century. *Sci Transl Med*. 2011;3(77):77sr1.
36. Tellechea P, Pujol N, Esteve-Belloch P, Echeveste B, Garcia-Eulate MR, Arbizu J, et al. Early- and late-onset Alzheimer disease: Are they the same entity? *Neurologia*. 2018;33(4):244-53.
37. Braak H, Braak E. Neuropathological staging of Alzheimer-related changes. *Acta Neuropathol*. 1991;82(4):239-59.

38. Murray ME, Graff-Radford NR, Ross OA, Petersen RC, Duara R, Dickson DW. Neuropathologically defined subtypes of Alzheimer's disease with distinct clinical characteristics: a retrospective study. *Lancet Neurol.* 2011;10(9):785-96.
39. Mendez MF. Early-onset Alzheimer's disease: nonamnestic subtypes and type 2 AD. *Arch Med Res.* 2012;43(8):677-85.
40. Lam B, Masellis M, Freedman M, Stuss DT, Black SE. Clinical, imaging, and pathological heterogeneity of the Alzheimer's disease syndrome. *Alzheimers Res Ther.* 2013;5(1):1.
41. Marshall GA, Fairbanks LA, Tekin S, Vinters HV, Cummings JL. Early-onset Alzheimer's disease is associated with greater pathologic burden. *J Geriatr Psychiatry Neurol.* 2007;20(1):29-33.
42. Ho GJ, Hansen LA, Alford MF, Foster K, Salmon DP, Galasko D, et al. Age at onset is associated with disease severity in Lewy body variant and Alzheimer's disease. *Neuroreport.* 2002;13(14):1825-8.
43. Mizuno Y, Ikeda K, Tsuchiya K, Ishihara R, Shibayama H. Two distinct subgroups of senile dementia of Alzheimer type: quantitative study of neurofibrillary tangles. *Neuropathology.* 2003;23(4):282-9.
44. Dorothee G, Bottlaender M, Moukari E, de Souza LC, Maroy R, Corlier F, et al. Distinct patterns of anti-amyloid-beta antibodies in typical and atypical Alzheimer disease. *Arch Neurol.* 2012;69(9):1181-5.
45. Prohovnik I, Perl DP, Davis KL, Libow L, Lesser G, Haroutunian V. Dissociation of neuropathology from severity of dementia in late-onset Alzheimer disease. *Neurology.* 2006;66(1):49-55.

46. Morris GP, Clark IA, Vissel B. Inconsistencies and controversies surrounding the amyloid hypothesis of Alzheimer's disease. *Acta Neuropathol Commun.* 2014;2:135.
47. Herrup K. The case for rejecting the amyloid cascade hypothesis. *Nat Neurosci.* 2015;18(6):794-9.
48. Forner S, Baglietto-Vargas D, Martini AC, Trujillo-Estrada L, LaFerla FM. Synaptic Impairment in Alzheimer's Disease: A Dysregulated Symphony. *Trends Neurosci.* 2017;40(6):347-57.
49. Glabe CG. Structural classification of toxic amyloid oligomers. *J Biol Chem.* 2008;283(44):29639-43.
50. Selkoe DJ. Soluble oligomers of the amyloid beta-protein impair synaptic plasticity and behavior. *Behav Brain Res.* 2008;192(1):106-13.
51. Mucke L, Selkoe DJ. Neurotoxicity of amyloid beta-protein: synaptic and network dysfunction. *Cold Spring Harb Perspect Med.* 2012;2(7):a006338.
52. Tsigelny IF, Sharikov Y, Kouznetsova VL, Greenberg JP, Wrasidlo W, Gonzalez T, et al. Structural diversity of Alzheimer's disease amyloid-beta dimers and their role in oligomerization and fibril formation. *J Alzheimers Dis.* 2014;39(3):583-600.
53. Lambert MP, Barlow AK, Chromy BA, Edwards C, Freed R, Liosatos M, et al. Diffusible, nonfibrillar ligands derived from A β 1-42 are potent central nervous system neurotoxins. *Proc Natl Acad Sci U S A.* 1998;95(11):6448-53.
54. Walsh DM, Klyubin I, Fadeeva JV, Cullen WK, Anwyl R, Wolfe MS, et al. Naturally secreted oligomers of amyloid beta protein potently inhibit hippocampal long-term potentiation in vivo. *Nature.* 2002;416(6880):535-9.

55. Shankar GM, Bloodgood BL, Townsend M, Walsh DM, Selkoe DJ, Sabatini BL. Natural oligomers of the Alzheimer amyloid-beta protein induce reversible synapse loss by modulating an NMDA-type glutamate receptor-dependent signaling pathway. *J Neurosci.* 2007;27(11):2866-75.
56. Hsia AY, Masliah E, McConlogue L, Yu GQ, Tatsuno G, Hu K, et al. Plaque-independent disruption of neural circuits in Alzheimer's disease mouse models. *Proc Natl Acad Sci U S A.* 1999;96(6):3228-33.
57. Wang HW, Pasternak JF, Kuo H, Ristic H, Lambert MP, Chromy B, et al. Soluble oligomers of beta amyloid (1-42) inhibit long-term potentiation but not long-term depression in rat dentate gyrus. *Brain Res.* 2002;924(2):133-40.
58. Marsh J, Alifragis P. Synaptic dysfunction in Alzheimer's disease: the effects of amyloid beta on synaptic vesicle dynamics as a novel target for therapeutic intervention. *Neural Regen Res.* 2018;13(4):616-23.
59. Lacor PN, Buniel MC, Chang L, Fernandez SJ, Gong Y, Viola KL, et al. Synaptic targeting by Alzheimer's-related amyloid beta oligomers. *J Neurosci.* 2004;24(45):10191-200.
60. Molnar Z, Soos K, Lengyel I, Penke B, Szegedi V, Budai D. Enhancement of NMDA responses by beta-amyloid peptides in the hippocampus in vivo. *Neuroreport.* 2004;15(10):1649-52.
61. Koffie RM, Meyer-Luehmann M, Hashimoto T, Adams KW, Mielke ML, Garcia-Alloza M, et al. Oligomeric amyloid beta associates with postsynaptic densities and correlates with excitatory synapse loss near senile plaques. *Proc Natl Acad Sci U S A.* 2009;106(10):4012-7.

62. Grundke-Iqbal I, Iqbal K, George L, Tung YC, Kim KS, Wisniewski HM. Amyloid protein and neurofibrillary tangles coexist in the same neuron in Alzheimer disease. *Proc Natl Acad Sci U S A*. 1989;86(8):2853-7.
63. Wilson CA, Doms RW, Lee VM. Intracellular APP processing and A beta production in Alzheimer disease. *J Neuropathol Exp Neurol*. 1999;58(8):787-94.
64. Gouras GK, Tsai J, Naslund J, Vincent B, Edgar M, Checler F, et al. Intraneuronal Abeta42 accumulation in human brain. *Am J Pathol*. 2000;156(1):15-20.
65. Kokubo H, Kaye R, Glabe CG, Yamaguchi H. Soluble Abeta oligomers ultrastructurally localize to cell processes and might be related to synaptic dysfunction in Alzheimer's disease brain. *Brain Res*. 2005;1031(2):222-8.
66. Sokolow S, Luu SH, Nandy K, Miller CA, Vinters HV, Poon WW, et al. Preferential accumulation of amyloid-beta in presynaptic glutamatergic terminals (VGluT1 and VGluT2) in Alzheimer's disease cortex. *Neurobiol Dis*. 2012;45(1):381-7.
67. Puzzo D, Privitera L, Leznik E, Fa M, Staniszewski A, Palmeri A, et al. Picomolar amyloid-beta positively modulates synaptic plasticity and memory in hippocampus. *J Neurosci*. 2008;28(53):14537-45.
68. Li S, Jin M, Koeglsperger T, Shepardson NE, Shankar GM, Selkoe DJ. Soluble Abeta oligomers inhibit long-term potentiation through a mechanism involving excessive activation of extrasynaptic NR2B-containing NMDA receptors. *J Neurosci*. 2011;31(18):6627-38.
69. Parodi J, Sepulveda FJ, Roa J, Opazo C, Inestrosa NC, Aguayo LG. Beta-amyloid causes depletion of synaptic vesicles leading to neurotransmission failure. *J Biol Chem*. 2010;285(4):2506-14.

70. Russell CL, Semerdjieva S, Empson RM, Austen BM, Beesley PW, Alifragis P. Amyloid-beta acts as a regulator of neurotransmitter release disrupting the interaction between synaptophysin and VAMP2. *PLoS One*. 2012;7(8):e43201.
71. Gibson PH. EM study of the numbers of cortical synapses in the brains of ageing people and people with Alzheimer-type dementia. *Acta Neuropathol*. 1983;62(1-2):127-33.
72. Perdahl E, Adolfsson R, Alafuzoff I, Albert KA, Nestler EJ, Greengard P, et al. Synapsin I (protein I) in different brain regions in senile dementia of Alzheimer type and in multi-infarct dementia. *J Neural Transm*. 1984;60(2):133-41.
73. Tannenberg RK, Scott HL, Tannenberg AE, Dodd PR. Selective loss of synaptic proteins in Alzheimer's disease: evidence for an increased severity with APOE varepsilon4. *Neurochem Int*. 2006;49(7):631-9.
74. Marksteiner J, Kaufmann WA, Gurka P, Humpel C. Synaptic proteins in Alzheimer's disease. *J Mol Neurosci*. 2002;18(1-2):53-63.
75. Shim KS, Lubec G. Drebrin, a dendritic spine protein, is manifold decreased in brains of patients with Alzheimer's disease and Down syndrome. *Neurosci Lett*. 2002;324(3):209-12.
76. Leuba G, Savioz A, Vernay A, Carnal B, Kraftsik R, Tardif E, et al. Differential changes in synaptic proteins in the Alzheimer frontal cortex with marked increase in PSD-95 postsynaptic protein. *J Alzheimers Dis*. 2008;15(1):139-51.
77. Gylys KH, Fein JA, Yang F, Wiley DJ, Miller CA, Cole GM. Synaptic changes in Alzheimer's disease: increased amyloid-beta and gliosis in surviving terminals is accompanied by decreased PSD-95 fluorescence. *Am J Pathol*. 2004;165(5):1809-17.
78. Pham E, Crews L, Ubhi K, Hansen L, Adame A, Cartier A, et al. Progressive accumulation of amyloid-beta oligomers in Alzheimer's disease and in amyloid precursor protein

- transgenic mice is accompanied by selective alterations in synaptic scaffold proteins. *FEBS J.* 2010;277(14):3051-67.
79. Freir DB, Fedriani R, Scully D, Smith IM, Selkoe DJ, Walsh DM, et al. Abeta oligomers inhibit synapse remodelling necessary for memory consolidation. *Neurobiol Aging.* 2011;32(12):2211-8.
 80. Alonso-Nanclares L, Merino-Serrais P, Gonzalez S, DeFelipe J. Synaptic changes in the dentate gyrus of APP/PS1 transgenic mice revealed by electron microscopy. *J Neuropathol Exp Neurol.* 2013;72(5):386-95.
 81. Terry RD, Masliah E, Salmon DP, Butters N, DeTeresa R, Hill R, et al. Physical basis of cognitive alterations in Alzheimer's disease: synapse loss is the major correlate of cognitive impairment. *Ann Neurol.* 1991;30(4):572-80.
 82. Scheff SW, Price DA. Synapse loss in the temporal lobe in Alzheimer's disease. *Ann Neurol.* 1993;33(2):190-9.
 83. Karch CM, Goate AM. Alzheimer's disease risk genes and mechanisms of disease pathogenesis. *Biol Psychiatry.* 2015;77(1):43-51.
 84. Bu G. Apolipoprotein E and its receptors in Alzheimer's disease: pathways, pathogenesis and therapy. *Nat Rev Neurosci.* 2009;10(5):333-44.
 85. Qiu C, Kivipelto M, von Strauss E. Epidemiology of Alzheimer's disease: occurrence, determinants, and strategies toward intervention. *Dialogues Clin Neurosci.* 2009;11(2):111-28.
 86. Raber J, Huang Y, Ashford JW. ApoE genotype accounts for the vast majority of AD risk and AD pathology. *Neurobiol Aging.* 2004;25(5):641-50.
 87. Spinney L. Alzheimer's disease: The forgetting gene. *Nature.* 2014;510(7503):26-8.

88. Holtzman DM, Herz J, Bu G. Apolipoprotein E and apolipoprotein E receptors: normal biology and roles in Alzheimer disease. *Cold Spring Harb Perspect Med.* 2012;2(3):a006312.
89. Hickman RA, Faustin A, Wisniewski T. Alzheimer Disease and Its Growing Epidemic: Risk Factors, Biomarkers, and the Urgent Need for Therapeutics. *Neurol Clin.* 2016;34(4):941-53.
90. Farrer LA, Cupples LA, Haines JL, Hyman B, Kukull WA, Mayeux R, et al. Effects of age, sex, and ethnicity on the association between apolipoprotein E genotype and Alzheimer disease. A meta-analysis. APOE and Alzheimer Disease Meta Analysis Consortium. *JAMA.* 1997;278(16):1349-56.
91. Deary IJ, Whiteman MC, Pattie A, Starr JM, Hayward C, Wright AF, et al. Apolipoprotein e gene variability and cognitive functions at age 79: a follow-up of the Scottish mental survey of 1932. *Psychol Aging.* 2004;19(2):367-71.
92. Guo Z, Cupples LA, Kurz A, Auerbach SH, Volicer L, Chui H, et al. Head injury and the risk of AD in the MIRAGE study. *Neurology.* 2000;54(6):1316-23.
93. Mayeux R, Ottman R, Maestre G, Ngai C, Tang MX, Ginsberg H, et al. Synergistic effects of traumatic head injury and apolipoprotein-epsilon 4 in patients with Alzheimer's disease. *Neurology.* 1995;45(3 Pt 1):555-7.
94. Esiri MM. Ageing and the brain. *J Pathol.* 2007;211(2):181-7.
95. Bayer TA, Cappai R, Masters CL, Beyreuther K, Multhaup G. It all sticks together--the APP-related family of proteins and Alzheimer's disease. *Mol Psychiatry.* 1999;4(6):524-8.

96. Jonsson T, Atwal JK, Steinberg S, Snaedal J, Jonsson PV, Bjornsson S, et al. A mutation in APP protects against Alzheimer's disease and age-related cognitive decline. *Nature*. 2012;488(7409):96-9.
97. Blennow K, de Leon MJ, Zetterberg H. Alzheimer's disease. *Lancet*. 2006;368(9533):387-403.
98. Hartley D, Blumenthal T, Carrillo M, DiPaolo G, Esralew L, Gardiner K, et al. Down syndrome and Alzheimer's disease: Common pathways, common goals. *Alzheimers Dement*. 2015;11(6):700-9.
99. Breteler MM, Claus JJ, Grobbee DE, Hofman A. Cardiovascular disease and distribution of cognitive function in elderly people: the Rotterdam Study. *BMJ*. 1994;308(6944):1604-8.
100. Stampfer MJ. Cardiovascular disease and Alzheimer's disease: common links. *J Intern Med*. 2006;260(3):211-23.
101. Cheng CK, Tsao YC, Su YC, Sung FC, Tai HC, Kung WM. Metabolic Risk Factors of Alzheimer's Disease, Dementia with Lewy Bodies, and Normal Elderly: A Population-Based Study. *Behav Neurol*. 2018;2018:8312346.
102. Reitz C, Brayne C, Mayeux R. Epidemiology of Alzheimer disease. *Nat Rev Neurol*. 2011;7(3):137-52.
103. Launer LJ, Masaki K, Petrovitch H, Foley D, Havlik RJ. The association between midlife blood pressure levels and late-life cognitive function. The Honolulu-Asia Aging Study. *JAMA*. 1995;274(23):1846-51.
104. Swan GE, Carmelli D, Larue A. Systolic blood pressure tracking over 25 to 30 years and cognitive performance in older adults. *Stroke*. 1998;29(11):2334-40.

105. Kivipelto M, Helkala EL, Hanninen T, Laakso MP, Hallikainen M, Alhainen K, et al. Midlife vascular risk factors and late-life mild cognitive impairment: A population-based study. *Neurology*. 2001;56(12):1683-9.
106. Kalaria RN. Vascular basis for brain degeneration: faltering controls and risk factors for dementia. *Nutr Rev*. 2010;68 Suppl 2:S74-87.
107. Deane R, Wu Z, Zlokovic BV. RAGE (yin) versus LRP (yang) balance regulates alzheimer amyloid beta-peptide clearance through transport across the blood-brain barrier. *Stroke*. 2004;35(11 Suppl 1):2628-31.
108. Reitz C, Mayeux R. Alzheimer disease: epidemiology, diagnostic criteria, risk factors and biomarkers. *Biochem Pharmacol*. 2014;88(4):640-51.
109. Luchsinger JA, Tang MX, Stern Y, Shea S, Mayeux R. Diabetes mellitus and risk of Alzheimer's disease and dementia with stroke in a multiethnic cohort. *Am J Epidemiol*. 2001;154(7):635-41.
110. Ott A, Stolk RP, van Harskamp F, Pols HA, Hofman A, Breteler MM. Diabetes mellitus and the risk of dementia: The Rotterdam Study. *Neurology*. 1999;53(9):1937-42.
111. Arvanitakis Z, Schneider JA, Wilson RS, Li Y, Arnold SE, Wang Z, et al. Diabetes is related to cerebral infarction but not to AD pathology in older persons. *Neurology*. 2006;67(11):1960-5.
112. Arvanitakis Z, Wilson RS, Bienias JL, Evans DA, Bennett DA. Diabetes mellitus and risk of Alzheimer disease and decline in cognitive function. *Arch Neurol*. 2004;61(5):661-6.
113. Watson GS, Peskind ER, Asthana S, Purganan K, Wait C, Chapman D, et al. Insulin increases CSF A β 42 levels in normal older adults. *Neurology*. 2003;60(12):1899-903.

114. Park CR. Cognitive effects of insulin in the central nervous system. *Neurosci Biobehav Rev.* 2001;25(4):311-23.
115. Morris JK, Burns JM. Insulin: an emerging treatment for Alzheimer's disease dementia? *Curr Neurol Neurosci Rep.* 2012;12(5):520-7.
116. Roozenbeek B, Maas AI, Menon DK. Changing patterns in the epidemiology of traumatic brain injury. *Nat Rev Neurol.* 2013;9(4):231-6.
117. Coronado VG, McGuire LC, Sarmiento K, Bell J, Lionbarger MR, Jones CD, et al. Trends in Traumatic Brain Injury in the U.S. and the public health response: 1995-2009. *J Safety Res.* 2012;43(4):299-307.
118. Fazel S, Wolf A, Pillas D, Lichtenstein P, Langstrom N. Suicide, fatal injuries, and other causes of premature mortality in patients with traumatic brain injury: a 41-year Swedish population study. *JAMA Psychiatry.* 2014;71(3):326-33.
119. McKee AC, Stern RA, Nowinski CJ, Stein TD, Alvarez VE, Daneshvar DH, et al. The spectrum of disease in chronic traumatic encephalopathy. *Brain.* 2013;136(Pt 1):43-64.
120. Goldstein LE, Fisher AM, Tagge CA, Zhang XL, Velisek L, Sullivan JA, et al. Chronic traumatic encephalopathy in blast-exposed military veterans and a blast neurotrauma mouse model. *Sci Transl Med.* 2012;4(134):134ra60.
121. Shively S, Scher AI, Perl DP, Diaz-Arrastia R. Dementia resulting from traumatic brain injury: what is the pathology? *Arch Neurol.* 2012;69(10):1245-51.
122. Johnson VE, Stewart JE, Begbie FD, Trojanowski JQ, Smith DH, Stewart W. Inflammation and white matter degeneration persist for years after a single traumatic brain injury. *Brain.* 2013;136(Pt 1):28-42.

123. Van den Heuvel C, Blumbergs PC, Finnie JW, Manavis J, Jones NR, Reilly PL, et al. Upregulation of amyloid precursor protein messenger RNA in response to traumatic brain injury: an ovine head impact model. *Exp Neurol*. 1999;159(2):441-50.
124. Nadler Y, Alexandrovich A, Grigoriadis N, Hartmann T, Rao KS, Shohami E, et al. Increased expression of the gamma-secretase components presenilin-1 and nicastrin in activated astrocytes and microglia following traumatic brain injury. *Glia*. 2008;56(5):552-67.
125. Blasko I, Beer R, Bigl M, Apelt J, Franz G, Rudzki D, et al. Experimental traumatic brain injury in rats stimulates the expression, production and activity of Alzheimer's disease beta-secretase (BACE-1). *J Neural Transm (Vienna)*. 2004;111(4):523-36.
126. Clinton J, Roberts GW, Gentleman SM, Royston MC. Differential pattern of beta-amyloid protein deposition within cortical sulci and gyri in Alzheimer's disease. *Neuropathol Appl Neurobiol*. 1993;19(3):277-81.
127. Johnson VE, Stewart W, Graham DI, Stewart JE, Praestgaard AH, Smith DH. A neprilysin polymorphism and amyloid-beta plaques after traumatic brain injury. *J Neurotrauma*. 2009;26(8):1197-202.
128. Chen XH, Johnson VE, Uryu K, Trojanowski JQ, Smith DH. A lack of amyloid beta plaques despite persistent accumulation of amyloid beta in axons of long-term survivors of traumatic brain injury. *Brain Pathol*. 2009;19(2):214-23.
129. Michikawa M. Cholesterol paradox: is high total or low HDL cholesterol level a risk for Alzheimer's disease? *J Neurosci Res*. 2003;72(2):141-6.

130. Kuo YM, Emmerling MR, Bisgaier CL, Essenburg AD, Lampert HC, Drumm D, et al. Elevated low-density lipoprotein in Alzheimer's disease correlates with brain abeta 1-42 levels. *Biochem Biophys Res Commun.* 1998;252(3):711-5.
131. Cataldo JK, Prochaska JJ, Glantz SA. Cigarette smoking is a risk factor for Alzheimer's Disease: an analysis controlling for tobacco industry affiliation. *J Alzheimers Dis.* 2010;19(2):465-80.
132. Aggarwal NT, Bienias JL, Bennett DA, Wilson RS, Morris MC, Schneider JA, et al. The relation of cigarette smoking to incident Alzheimer's disease in a biracial urban community population. *Neuroepidemiology.* 2006;26(3):140-6.
133. Barnes DE, Yaffe K. The projected effect of risk factor reduction on Alzheimer's disease prevalence. *Lancet Neurol.* 2011;10(9):819-28.
134. Traber MG, van der Vliet A, Reznick AZ, Cross CE. Tobacco-related diseases. Is there a role for antioxidant micronutrient supplementation? *Clin Chest Med.* 2000;21(1):173-87, x.
135. Sprecher CA, Grant FJ, Grimm G, O'Hara PJ, Norris F, Norris K, et al. Molecular cloning of the cDNA for a human amyloid precursor protein homolog: evidence for a multigene family. *Biochemistry.* 1993;32(17):4481-6.
136. Wasco W, Bupp K, Magendantz M, Gusella JF, Tanzi RE, Solomon F. Identification of a mouse brain cDNA that encodes a protein related to the Alzheimer disease-associated amyloid beta protein precursor. *Proc Natl Acad Sci U S A.* 1992;89(22):10758-62.
137. Wasco W, Gurubhagavatula S, Paradis MD, Romano DM, Sisodia SS, Hyman BT, et al. Isolation and characterization of APLP2 encoding a homologue of the Alzheimer's associated amyloid beta protein precursor. *Nat Genet.* 1993;5(1):95-100.

138. Wilkins HM, Swerdlow RH. Amyloid precursor protein processing and bioenergetics. *Brain Res Bull.* 2017;133:71-9.
139. Haass C, Selkoe DJ. Soluble protein oligomers in neurodegeneration: lessons from the Alzheimer's amyloid beta-peptide. *Nat Rev Mol Cell Biol.* 2007;8(2):101-12.
140. Selkoe DJ. Alzheimer's disease: genes, proteins, and therapy. *Physiol Rev.* 2001;81(2):741-66.
141. Findeis MA. The role of amyloid beta peptide 42 in Alzheimer's disease. *Pharmacol Ther.* 2007;116(2):266-86.
142. De Strooper B, Annaert W. Proteolytic processing and cell biological functions of the amyloid precursor protein. *J Cell Sci.* 2000;113 (Pt 11):1857-70.
143. Vingtdeux V, Sergeant N, Buee L. Potential contribution of exosomes to the prion-like propagation of lesions in Alzheimer's disease. *Front Physiol.* 2012;3:229.
144. Werb Z, Yan Y. A cellular striptease act. *Science.* 1998;282(5392):1279-80.
145. Lammich S, Kojro E, Postina R, Gilbert S, Pfeiffer R, Jasionowski M, et al. Constitutive and regulated alpha-secretase cleavage of Alzheimer's amyloid precursor protein by a disintegrin metalloprotease. *Proc Natl Acad Sci U S A.* 1999;96(7):3922-7.
146. Koike H, Tomioka S, Sorimachi H, Saido TC, Maruyama K, Okuyama A, et al. Membrane-anchored metalloprotease MDC9 has an alpha-secretase activity responsible for processing the amyloid precursor protein. *Biochem J.* 1999;343 Pt 2:371-5.
147. De Strooper B, Umans L, Van Leuven F, Van Den Berghe H. Study of the synthesis and secretion of normal and artificial mutants of murine amyloid precursor protein (APP): cleavage of APP occurs in a late compartment of the default secretion pathway. *J Cell Biol.* 1993;121(2):295-304.

148. Kuentzel SL, Ali SM, Altman RA, Greenberg BD, Raub TJ. The Alzheimer beta-amyloid protein precursor/protease nexin-II is cleaved by secretase in a trans-Golgi secretory compartment in human neuroglioma cells. *Biochem J.* 1993;295 (Pt 2):367-78.
149. Venugopal C, Demos CM, Rao KS, Pappolla MA, Sambamurti K. Beta-secretase: structure, function, and evolution. *CNS Neurol Disord Drug Targets.* 2008;7(3):278-94.
150. Citron M, Vigo-Pelfrey C, Teplow DB, Miller C, Schenk D, Johnston J, et al. Excessive production of amyloid beta-protein by peripheral cells of symptomatic and presymptomatic patients carrying the Swedish familial Alzheimer disease mutation. *Proc Natl Acad Sci U S A.* 1994;91(25):11993-7.
151. Vassar R, Bennett BD, Babu-Khan S, Kahn S, Mendiaz EA, Denis P, et al. Beta-secretase cleavage of Alzheimer's amyloid precursor protein by the transmembrane aspartic protease BACE. *Science.* 1999;286(5440):735-41.
152. Perez RG, Squazzo SL, Koo EH. Enhanced release of amyloid beta-protein from codon 670/671 "Swedish" mutant beta-amyloid precursor protein occurs in both secretory and endocytic pathways. *J Biol Chem.* 1996;271(15):9100-7.
153. Martin BL, Schrader-Fischer G, Busciglio J, Duke M, Paganetti P, Yankner BA. Intracellular accumulation of beta-amyloid in cells expressing the Swedish mutant amyloid precursor protein. *J Biol Chem.* 1995;270(45):26727-30.
154. Thinakaran G, Teplow DB, Siman R, Greenberg B, Sisodia SS. Metabolism of the "Swedish" amyloid precursor protein variant in neuro2a (N2a) cells. Evidence that cleavage at the "beta-secretase" site occurs in the golgi apparatus. *J Biol Chem.* 1996;271(16):9390-7.
155. Haass C, De Strooper B. The presenilins in Alzheimer's disease--proteolysis holds the key. *Science.* 1999;286(5441):916-9.

156. Annaert W, De Strooper B. Presenilins: molecular switches between proteolysis and signal transduction. *Trends Neurosci.* 1999;22(10):439-43.
157. Annaert WG, Levesque L, Craessaerts K, Dierinck I, Snellings G, Westaway D, et al. Presenilin 1 controls gamma-secretase processing of amyloid precursor protein in pre-golgi compartments of hippocampal neurons. *J Cell Biol.* 1999;147(2):277-94.
158. Georgakopoulos A, Marambaud P, Efthimiopoulos S, Shioi J, Cui W, Li HC, et al. Presenilin-1 forms complexes with the cadherin/catenin cell-cell adhesion system and is recruited to intercellular and synaptic contacts. *Mol Cell.* 1999;4(6):893-902.
159. Ray WJ, Yao M, Mumm J, Schroeter EH, Saftig P, Wolfe M, et al. Cell surface presenilin-1 participates in the gamma-secretase-like proteolysis of Notch. *J Biol Chem.* 1999;274(51):36801-7.
160. Chang CL, Roh J, Hsu SY. Intermedin, a novel calcitonin family peptide that exists in teleosts as well as in mammals: a comparison with other calcitonin/intermedin family peptides in vertebrates. *Peptides.* 2004;25(10):1633-42.
161. Nishi M, Sanke T, Seino S, Eddy RL, Fan YS, Byers MG, et al. Human islet amyloid polypeptide gene: complete nucleotide sequence, chromosomal localization, and evolutionary history. *Mol Endocrinol.* 1989;3(11):1775-81.
162. Mosselman S, Hoppener JW, Lips CJ, Jansz HS. The complete islet amyloid polypeptide precursor is encoded by two exons. *FEBS Lett.* 1989;247(1):154-8.
163. Sanke T, Bell GI, Sample C, Rubenstein AH, Steiner DF. An islet amyloid peptide is derived from an 89-amino acid precursor by proteolytic processing. *J Biol Chem.* 1988;263(33):17243-6.

164. Zhang Y, Song W. Islet amyloid polypeptide: Another key molecule in Alzheimer's pathogenesis? *Prog Neurobiol.* 2017;153:100-20.
165. Marzban L, Trigo-Gonzalez G, Zhu X, Rhodes CJ, Halban PA, Steiner DF, et al. Role of beta-cell prohormone convertase (PC)1/3 in processing of pro-islet amyloid polypeptide. *Diabetes.* 2004;53(1):141-8.
166. Marzban L, Soukhatcheva G, Verchere CB. Role of carboxypeptidase E in processing of pro-islet amyloid polypeptide in {beta}-cells. *Endocrinology.* 2005;146(4):1808-17.
167. Percy AJ, Trainor DA, Rittenhouse J, Phelps J, Koda JE. Development of sensitive immunoassays to detect amylin and amylin-like peptides in unextracted plasma. *Clin Chem.* 1996;42(4):576-85.
168. Zerze GH, Mittal J. Effect of O-Linked Glycosylation on the Equilibrium Structural Ensemble of Intrinsically Disordered Polypeptides. *J Phys Chem B.* 2015;119(51):15583-92.
169. Martin C. The physiology of amylin and insulin: maintaining the balance between glucose secretion and glucose uptake. *Diabetes Educ.* 2006;32 Suppl 3:101S-4S.
170. Sanke T, Hanabusa T, Nakano Y, Oki C, Okai K, Nishimura S, et al. Plasma islet amyloid polypeptide (Amylin) levels and their responses to oral glucose in type 2 (non-insulin-dependent) diabetic patients. *Diabetologia.* 1991;34(2):129-32.
171. Leckstrom A, Bjorklund K, Permert J, Larsson R, Westermark P. Renal elimination of islet amyloid polypeptide. *Biochem Biophys Res Commun.* 1997;239(1):265-8.
172. Bennett RG, Duckworth WC, Hamel FG. Degradation of amylin by insulin-degrading enzyme. *J Biol Chem.* 2000;275(47):36621-5.

173. Muff R, Buhlmann N, Fischer JA, Born W. An amylin receptor is revealed following co-transfection of a calcitonin receptor with receptor activity modifying proteins-1 or -3. *Endocrinology*. 1999;140(6):2924-7.
174. Young A. Receptor pharmacology. *Adv Pharmacol*. 2005;52:47-65.
175. Poyner DR, Sexton PM, Marshall I, Smith DM, Quirion R, Born W, et al. International Union of Pharmacology. XXXII. The mammalian calcitonin gene-related peptides, adrenomedullin, amylin, and calcitonin receptors. *Pharmacol Rev*. 2002;54(2):233-46.
176. Tilakaratne N, Christopoulos G, Zumpe ET, Foord SM, Sexton PM. Amylin receptor phenotypes derived from human calcitonin receptor/RAMP coexpression exhibit pharmacological differences dependent on receptor isoform and host cell environment. *J Pharmacol Exp Ther*. 2000;294(1):61-72.
177. Qiu WQ, Zhu H. Amylin and its analogs: a friend or foe for the treatment of Alzheimer's disease? *Front Aging Neurosci*. 2014;6:186.
178. Karlsson E. IAPP as a regulator of glucose homeostasis and pancreatic hormone secretion (review). *Int J Mol Med*. 1999;3(6):577-84.
179. Silvestre RA, Rodriguez-Gallardo J, Jodka C, Parkes DG, Pittner RA, Young AA, et al. Selective amylin inhibition of the glucagon response to arginine is extrinsic to the pancreas. *Am J Physiol Endocrinol Metab*. 2001;280(3):E443-9.
180. Gedulin BR, Jodka CM, Herrmann K, Young AA. Role of endogenous amylin in glucagon secretion and gastric emptying in rats demonstrated with the selective antagonist, AC187. *Regul Pept*. 2006;137(3):121-7.

181. Samsom M, Szarka LA, Camilleri M, Vella A, Zinsmeister AR, Rizza RA. Pramlintide, an amylin analog, selectively delays gastric emptying: potential role of vagal inhibition. *Am J Physiol Gastrointest Liver Physiol.* 2000;278(6):G946-51.
182. Lutz TA, Meyer U. Amylin at the interface between metabolic and neurodegenerative disorders. *Front Neurosci.* 2015;9:216.
183. Lutz TA. Pancreatic amylin as a centrally acting satiating hormone. *Curr Drug Targets.* 2005;6(2):181-9.
184. Geary N. A new way of looking at eating. *Am J Physiol Regul Integr Comp Physiol.* 2005;288(6):R1444-6.
185. Reidelberger R, Haver A, Chelikani PK. Role of peptide YY(3-36) in the satiety produced by gastric delivery of macronutrients in rats. *Am J Physiol Endocrinol Metab.* 2013;304(9):E944-50.
186. Wielinga PY, Lowenstein C, Muff S, Munz M, Woods SC, Lutz TA. Central amylin acts as an adiposity signal to control body weight and energy expenditure. *Physiol Behav.* 2010;101(1):45-52.
187. Fernandes-Santos C, Zhang Z, Morgan DA, Guo DF, Russo AF, Rahmouni K. Amylin acts in the central nervous system to increase sympathetic nerve activity. *Endocrinology.* 2013;154(7):2481-8.
188. Fox A, Snollaerts T, Errecart Casanova C, Calciano A, Nogaj LA, Moffet DA. Selection for nonamyloidogenic mutants of islet amyloid polypeptide (IAPP) identifies an extended region for amyloidogenicity. *Biochemistry.* 2010;49(36):7783-9.

189. Nonoyama A, Laurence JS, Garriques L, Qi H, Le T, Middaugh CR. A biophysical characterization of the peptide drug pramlintide (AC137) using empirical phase diagrams. *J Pharm Sci.* 2008;97(7):2552-67.
190. Trevaskis JL, Coffey T, Cole R, Lei C, Wittmer C, Walsh B, et al. Amylin-mediated restoration of leptin responsiveness in diet-induced obesity: magnitude and mechanisms. *Endocrinology.* 2008;149(11):5679-87.
191. Hollander PA, Levy P, Fineman MS, Maggs DG, Shen LZ, Strobel SA, et al. Pramlintide as an adjunct to insulin therapy improves long-term glycemic and weight control in patients with type 2 diabetes: a 1-year randomized controlled trial. *Diabetes Care.* 2003;26(3):784-90.
192. Eisenberg D, Jucker M. The amyloid state of proteins in human diseases. *Cell.* 2012;148(6):1188-203.
193. Betsholtz C, Christmansson L, Engstrom U, Rorsman F, Svensson V, Johnson KH, et al. Sequence divergence in a specific region of islet amyloid polypeptide (IAPP) explains differences in islet amyloid formation between species. *FEBS Lett.* 1989;251(1-2):261-4.
194. Westermark P, Andersson A, Westermark GT. Islet amyloid polypeptide, islet amyloid, and diabetes mellitus. *Physiol Rev.* 2011;91(3):795-826.
195. Clark A, Nilsson MR. Islet amyloid: a complication of islet dysfunction or an aetiological factor in Type 2 diabetes? *Diabetologia.* 2004;47(2):157-69.
196. Abedini A, Meng F, Raleigh DP. A single-point mutation converts the highly amyloidogenic human islet amyloid polypeptide into a potent fibrillization inhibitor. *J Am Chem Soc.* 2007;129(37):11300-1.

197. Meng F, Raleigh DP, Abedini A. Combination of kinetically selected inhibitors in trans leads to highly effective inhibition of amyloid formation. *J Am Chem Soc.* 2010;132(41):14340-2.
198. Bailey J, Potter KJ, Verchere CB, Edelstein-Keshet L, Coombs D. Reverse engineering an amyloid aggregation pathway with dimensional analysis and scaling. *Phys Biol.* 2011;8(6):066009.
199. Marzban L, Tomas A, Becker TC, Rosenberg L, Oberholzer J, Fraser PE, et al. Small interfering RNA-mediated suppression of proislet amyloid polypeptide expression inhibits islet amyloid formation and enhances survival of human islets in culture. *Diabetes.* 2008;57(11):3045-55.
200. Rhoades E, Gafni A. Micelle formation by a fragment of human islet amyloid polypeptide. *Biophys J.* 2003;84(5):3480-7.
201. Jackson K, Barisone GA, Diaz E, Jin LW, DeCarli C, Despa F. Amylin deposition in the brain: A second amyloid in Alzheimer disease? *Ann Neurol.* 2013;74(4):517-26.
202. Srodulski S, Sharma S, Bachstetter AB, Brelsfoard JM, Pascual C, Xie XS, et al. Neuroinflammation and neurologic deficits in diabetes linked to brain accumulation of amylin. *Mol Neurodegener.* 2014;9:30.
203. Oskarsson ME, Paulsson JF, Schultz SW, Ingelsson M, Westermark P, Westermark GT. In vivo seeding and cross-seeding of localized amyloidosis: a molecular link between type 2 diabetes and Alzheimer disease. *Am J Pathol.* 2015;185(3):834-46.
204. Banks WA, Kastin AJ, Maness LM, Huang W, Jaspan JB. Permeability of the blood-brain barrier to amylin. *Life Sci.* 1995;57(22):1993-2001.

205. Chaitanya GV, Cromer WE, Wells SR, Jennings MH, Couraud PO, Romero IA, et al. Gliovascular and cytokine interactions modulate brain endothelial barrier in vitro. *J Neuroinflammation*. 2011;8:162.
206. Andreetto E, Yan LM, Tatarek-Nossol M, Velkova A, Frank R, Kapurniotu A. Identification of hot regions of the Abeta-IAPP interaction interface as high-affinity binding sites in both cross- and self-association. *Angew Chem Int Ed Engl*. 2010;49(17):3081-5.
207. Berhanu WM, Yasar F, Hansmann UH. In silico cross seeding of Abeta and amylin fibril-like oligomers. *ACS Chem Neurosci*. 2013;4(11):1488-500.
208. Hu R, Zhang M, Chen H, Jiang B, Zheng J. Cross-Seeding Interaction between beta-Amyloid and Human Islet Amyloid Polypeptide. *ACS Chem Neurosci*. 2015;6(10):1759-68.
209. Baglioni S, Casamenti F, Bucciantini M, Luheshi LM, Taddei N, Chiti F, et al. Prefibrillar amyloid aggregates could be generic toxins in higher organisms. *J Neurosci*. 2006;26(31):8160-7.
210. Bucciantini M, Calloni G, Chiti F, Formigli L, Nosi D, Dobson CM, et al. Prefibrillar amyloid protein aggregates share common features of cytotoxicity. *J Biol Chem*. 2004;279(30):31374-82.
211. Vieira MN, Forny-Germano L, Saraiva LM, Sebollela A, Martinez AM, Houzel JC, et al. Soluble oligomers from a non-disease related protein mimic Abeta-induced tau hyperphosphorylation and neurodegeneration. *J Neurochem*. 2007;103(2):736-48.
212. Anguiano M, Nowak RJ, Lansbury PT, Jr. Protofibrillar islet amyloid polypeptide permeabilizes synthetic vesicles by a pore-like mechanism that may be relevant to type II diabetes. *Biochemistry*. 2002;41(38):11338-43.

213. Kawahara M, Kuroda Y, Arispe N, Rojas E. Alzheimer's beta-amyloid, human islet amylin, and prion protein fragment evoke intracellular free calcium elevations by a common mechanism in a hypothalamic GnRH neuronal cell line. *J Biol Chem.* 2000;275(19):14077-83.
214. Lim YA, Ittner LM, Lim YL, Gotz J. Human but not rat amylin shares neurotoxic properties with A β 42 in long-term hippocampal and cortical cultures. *FEBS Lett.* 2008;582(15):2188-94.
215. Brender JR, Salamekh S, Ramamoorthy A. Membrane disruption and early events in the aggregation of the diabetes related peptide IAPP from a molecular perspective. *Acc Chem Res.* 2012;45(3):454-62.
216. Engel MF, Khemtemourian L, Kleijer CC, Meeldijk HJ, Jacobs J, Verkleij AJ, et al. Membrane damage by human islet amyloid polypeptide through fibril growth at the membrane. *Proc Natl Acad Sci U S A.* 2008;105(16):6033-8.
217. Last NB, Rhoades E, Miranker AD. Islet amyloid polypeptide demonstrates a persistent capacity to disrupt membrane integrity. *Proc Natl Acad Sci U S A.* 2011;108(23):9460-5.
218. Brender JR, Lee EL, Hartman K, Wong PT, Ramamoorthy A, Steel DG, et al. Biphasic effects of insulin on islet amyloid polypeptide membrane disruption. *Biophys J.* 2011;100(3):685-92.
219. Quist A, Doudevski I, Lin H, Azimova R, Ng D, Frangione B, et al. Amyloid ion channels: a common structural link for protein-misfolding disease. *Proc Natl Acad Sci U S A.* 2005;102(30):10427-32.

220. Fu W, Ruangkittisakul A, MacTavish D, Shi JY, Ballanyi K, Jhamandas JH. Amyloid beta (Abeta) peptide directly activates amylin-3 receptor subtype by triggering multiple intracellular signaling pathways. *J Biol Chem.* 2012;287(22):18820-30.
221. Masters SL, Dunne A, Subramanian SL, Hull RL, Tannahill GM, Sharp FA, et al. Activation of the NLRP3 inflammasome by islet amyloid polypeptide provides a mechanism for enhanced IL-1beta in type 2 diabetes. *Nat Immunol.* 2010;11(10):897-904.
222. Westwell-Roper C, Dai DL, Soukhatcheva G, Potter KJ, van Rooijen N, Ehses JA, et al. IL-1 blockade attenuates islet amyloid polypeptide-induced proinflammatory cytokine release and pancreatic islet graft dysfunction. *J Immunol.* 2011;187(5):2755-65.
223. Park YJ, Lee S, Kieffer TJ, Warnock GL, Safikhan N, Speck M, et al. Deletion of Fas protects islet beta cells from cytotoxic effects of human islet amyloid polypeptide. *Diabetologia.* 2012.
224. Heneka MT, Sastre M, Dumitrescu-Ozimek L, Dewachter I, Walter J, Klockgether T, et al. Focal glial activation coincides with increased BACE1 activation and precedes amyloid plaque deposition in APP[V717I] transgenic mice. *J Neuroinflammation.* 2005;2:22.
225. Cacabelos R, Barquero M, Garcia P, Alvarez XA, Varela de Seijas E. Cerebrospinal fluid interleukin-1 beta (IL-1 beta) in Alzheimer's disease and neurological disorders. *Methods Find Exp Clin Pharmacol.* 1991;13(7):455-8.
226. Ly H, Despa F. Hyperamylinemia as a risk factor for accelerated cognitive decline in diabetes. *Expert Rev Proteomics.* 2015;12(6):575-7.
227. Fawver JN, Ghiwot Y, Koola C, Carrera W, Rodriguez-Rivera J, Hernandez C, et al. Islet amyloid polypeptide (IAPP): a second amyloid in Alzheimer's disease. *Curr Alzheimer Res.* 2014;11(10):928-40.

228. Adler BL, Yarchoan M, Hwang HM, Louneva N, Blair JA, Palm R, et al. Neuroprotective effects of the amylin analogue pramlintide on Alzheimer's disease pathogenesis and cognition. *Neurobiol Aging*. 2014;35(4):793-801.
229. Zhu H, Xue X, Wang E, Wallack M, Na H, Hooker JM, et al. Amylin receptor ligands reduce the pathological cascade of Alzheimer's disease. *Neuropharmacology*. 2017;119:170-81.
230. Wang E, Zhu H, Wang X, Gower AC, Wallack M, Blusztajn JK, et al. Amylin Treatment Reduces Neuroinflammation and Ameliorates Abnormal Patterns of Gene Expression in the Cerebral Cortex of an Alzheimer's Disease Mouse Model. *J Alzheimers Dis*. 2017;56(1):47-61.
231. Zhu H, Wang X, Wallack M, Li H, Carreras I, Dedeoglu A, et al. Intraperitoneal injection of the pancreatic peptide amylin potently reduces behavioral impairment and brain amyloid pathology in murine models of Alzheimer's disease. *Mol Psychiatry*. 2015;20(2):252-62.
232. Schubert D, Behl C, Lesley R, Brack A, Dargusch R, Sagara Y, et al. Amyloid peptides are toxic via a common oxidative mechanism. *Proc Natl Acad Sci U S A*. 1995;92(6):1989-93.
233. Kimura R, MacTavish D, Yang J, Westaway D, Jhamandas JH. Pramlintide Antagonizes Beta Amyloid (A β)- and Human Amylin-Induced Depression of Hippocampal Long-Term Potentiation. *Mol Neurobiol*. 2017;54(1):748-54.
234. Simons K, van Meer G. Lipid sorting in epithelial cells. *Biochemistry*. 1988;27(17):6197-202.
235. Simons K, Ikonen E. Functional rafts in cell membranes. *Nature*. 1997;387(6633):569-72.
236. Pike LJ. Rafts defined: a report on the Keystone Symposium on Lipid Rafts and Cell Function. *J Lipid Res*. 2006;47(7):1597-8.
237. Pike LJ. Lipid rafts: bringing order to chaos. *J Lipid Res*. 2003;44(4):655-67.

238. Brown DA, London E. Structure and function of sphingolipid- and cholesterol-rich membrane rafts. *J Biol Chem.* 2000;275(23):17221-4.
239. Brown DA, Rose JK. Sorting of GPI-anchored proteins to glycolipid-enriched membrane subdomains during transport to the apical cell surface. *Cell.* 1992;68(3):533-44.
240. Fridriksson EK, Shipkova PA, Sheets ED, Holowka D, Baird B, McLafferty FW. Quantitative analysis of phospholipids in functionally important membrane domains from RBL-2H3 mast cells using tandem high-resolution mass spectrometry. *Biochemistry.* 1999;38(25):8056-63.
241. Pike LJ, Han X, Chung KN, Gross RW. Lipid rafts are enriched in arachidonic acid and plasmalogen phospholipids and their composition is independent of caveolin-1 expression: a quantitative electrospray ionization/mass spectrometric analysis. *Biochemistry.* 2002;41(6):2075-88.
242. le Maire M, Champeil P, Moller JV. Interaction of membrane proteins and lipids with solubilizing detergents. *Biochim Biophys Acta.* 2000;1508(1-2):86-111.
243. Munro S. Lipid rafts: elusive or illusive? *Cell.* 2003;115(4):377-88.
244. Drevot P, Langlet C, Guo XJ, Bernard AM, Colard O, Chauvin JP, et al. TCR signal initiation machinery is pre-assembled and activated in a subset of membrane rafts. *EMBO J.* 2002;21(8):1899-908.
245. Roper K, Corbeil D, Huttner WB. Retention of prominin in microvilli reveals distinct cholesterol-based lipid micro-domains in the apical plasma membrane. *Nat Cell Biol.* 2000;2(9):582-92.
246. Song KS, Li S, Okamoto T, Quilliam LA, Sargiacomo M, Lisanti MP. Co-purification and direct interaction of Ras with caveolin, an integral membrane protein of caveolae

- microdomains. Detergent-free purification of caveolae microdomains. *J Biol Chem.* 1996;271(16):9690-7.
247. Bickel PE, Scherer PE, Schnitzer JE, Oh P, Lisanti MP, Lodish HF. Flotillin and epidermal surface antigen define a new family of caveolae-associated integral membrane proteins. *J Biol Chem.* 1997;272(21):13793-802.
248. Gorodinsky A, Harris DA. Glycolipid-anchored proteins in neuroblastoma cells form detergent-resistant complexes without caveolin. *J Cell Biol.* 1995;129(3):619-27.
249. Chun M, Liyanage UK, Lisanti MP, Lodish HF. Signal transduction of a G protein-coupled receptor in caveolae: colocalization of endothelin and its receptor with caveolin. *Proc Natl Acad Sci U S A.* 1994;91(24):11728-32.
250. Sargiacomo M, Sudol M, Tang Z, Lisanti MP. Signal transducing molecules and glycosylphosphatidylinositol-linked proteins form a caveolin-rich insoluble complex in MDCK cells. *J Cell Biol.* 1993;122(4):789-807.
251. Mineo C, James GL, Smart EJ, Anderson RG. Localization of epidermal growth factor-stimulated Ras/Raf-1 interaction to caveolae membrane. *J Biol Chem.* 1996;271(20):11930-5.
252. Liu P, Ying Y, Ko YG, Anderson RG. Localization of platelet-derived growth factor-stimulated phosphorylation cascade to caveolae. *J Biol Chem.* 1996;271(17):10299-303.
253. Smart EJ, Graf GA, McNiven MA, Sessa WC, Engelman JA, Scherer PE, et al. Caveolins, liquid-ordered domains, and signal transduction. *Mol Cell Biol.* 1999;19(11):7289-304.
254. Scheiffele P, Roth MG, Simons K. Interaction of influenza virus haemagglutinin with sphingolipid-cholesterol membrane domains via its transmembrane domain. *EMBO J.* 1997;16(18):5501-8.

255. Shaul PW, Smart EJ, Robinson LJ, German Z, Yuhanna IS, Ying Y, et al. Acylation targets endothelial nitric-oxide synthase to plasmalemmal caveolae. *J Biol Chem.* 1996;271(11):6518-22.
256. Shenoy-Scaria AM, Dietzen DJ, Kwong J, Link DC, Lublin DM. Cysteine³ of Src family protein tyrosine kinase determines palmitoylation and localization in caveolae. *J Cell Biol.* 1994;126(2):353-63.
257. Benjannet S, Elagöz A, Wickham L, Mamarbachi M, Munzer JS, Basak A, et al. Post-translational processing of beta-secretase (beta-amyloid-converting enzyme) and its ectodomain shedding. The pro- and transmembrane/cytosolic domains affect its cellular activity and amyloid-beta production. *J Biol Chem.* 2001;276(14):10879-87.
258. Hattori C, Asai M, Onishi H, Sasagawa N, Hashimoto Y, Saido TC, et al. BACE1 interacts with lipid raft proteins. *J Neurosci Res.* 2006;84(4):912-7.
259. Cordy JM, Hussain I, Dingwall C, Hooper NM, Turner AJ. Exclusively targeting beta-secretase to lipid rafts by GPI-anchor addition up-regulates beta-site processing of the amyloid precursor protein. *Proc Natl Acad Sci U S A.* 2003;100(20):11735-40.
260. Riddell DR, Christie G, Hussain I, Dingwall C. Compartmentalization of beta-secretase (Asp²) into low-buoyant density, noncaveolar lipid rafts. *Curr Biol.* 2001;11(16):1288-93.
261. Ehehalt R, Keller P, Haass C, Thiele C, Simons K. Amyloidogenic processing of the Alzheimer beta-amyloid precursor protein depends on lipid rafts. *J Cell Biol.* 2003;160(1):113-23.
262. Abad-Rodriguez J, Ledesma MD, Craessaerts K, Perga S, Medina M, Delacourte A, et al. Neuronal membrane cholesterol loss enhances amyloid peptide generation. *J Cell Biol.* 2004;167(5):953-60.

263. Vetrivel KS, Cheng H, Lin W, Sakurai T, Li T, Nukina N, et al. Association of gamma-secretase with lipid rafts in post-Golgi and endosome membranes. *J Biol Chem.* 2004;279(43):44945-54.
264. Vetrivel KS, Thinakaran G. Membrane rafts in Alzheimer's disease beta-amyloid production. *Biochim Biophys Acta.* 2010;1801(8):860-7.
265. Cheng H, Vetrivel KS, Gong P, Meckler X, Parent A, Thinakaran G. Mechanisms of disease: new therapeutic strategies for Alzheimer's disease--targeting APP processing in lipid rafts. *Nat Clin Pract Neurol.* 2007;3(7):374-82.
266. Hur JY, Welander H, Behbahani H, Aoki M, Franberg J, Winblad B, et al. Active gamma-secretase is localized to detergent-resistant membranes in human brain. *FEBS J.* 2008;275(6):1174-87.
267. Vetrivel KS, Cheng H, Kim SH, Chen Y, Barnes NY, Parent AT, et al. Spatial segregation of gamma-secretase and substrates in distinct membrane domains. *J Biol Chem.* 2005;280(27):25892-900.
268. Urano Y, Hayashi I, Isoo N, Reid PC, Shibasaki Y, Noguchi N, et al. Association of active gamma-secretase complex with lipid rafts. *J Lipid Res.* 2005;46(5):904-12.
269. Matsumura N, Takami M, Okochi M, Wada-Kakuda S, Fujiwara H, Tagami S, et al. gamma-Secretase associated with lipid rafts: multiple interactive pathways in the stepwise processing of beta-carboxyl-terminal fragment. *J Biol Chem.* 2014;289(8):5109-21.
270. Kokubo H, Saido TC, Iwata N, Helms JB, Shinohara R, Yamaguchi H. Part of membrane-bound Abeta exists in rafts within senile plaques in Tg2576 mouse brain. *Neurobiol Aging.* 2005;26(4):409-18.

271. Yu RK, Tsai YT, Ariga T, Yanagisawa M. Structures, biosynthesis, and functions of gangliosides--an overview. *J Oleo Sci.* 2011;60(10):537-44.
272. Grimm MO, Mett J, Grimm HS, Hartmann T. APP Function and Lipids: A Bidirectional Link. *Front Mol Neurosci.* 2017;10:63.
273. Maccioni HJ. Glycosylation of glycolipids in the Golgi complex. *J Neurochem.* 2007;103 Suppl 1:81-90.
274. Yamaguchi T, Yamauchi Y, Furukawa K, Ohmi Y, Ohkawa Y, Zhang Q, et al. Expression of B4GALNT1, an essential glycosyltransferase for the synthesis of complex gangliosides, suppresses BACE1 degradation and modulates APP processing. *Sci Rep.* 2016;6:34505.
275. Arbor SC, LaFontaine M, Cumbay M. Amyloid-beta Alzheimer targets - protein processing, lipid rafts, and amyloid-beta pores. *Yale J Biol Med.* 2016;89(1):5-21.
276. Yu RK, Macala LJ, Taki T, Weinfield HM, Yu FS. Developmental changes in ganglioside composition and synthesis in embryonic rat brain. *J Neurochem.* 1988;50(6):1825-9.
277. Ngamukote S, Yanagisawa M, Ariga T, Ando S, Yu RK. Developmental changes of glycosphingolipids and expression of glycogenes in mouse brains. *J Neurochem.* 2007;103(6):2327-41.
278. Suzuki Y, Yanagisawa M, Ariga T, Yu RK. Histone acetylation-mediated glycosyltransferase gene regulation in mouse brain during development. *J Neurochem.* 2011;116(5):874-80.
279. Yu RK, Nakatani Y, Yanagisawa M. The role of glycosphingolipid metabolism in the developing brain. *J Lipid Res.* 2009;50 Suppl:S440-5.
280. Simons K, Toomre D. Lipid rafts and signal transduction. *Nat Rev Mol Cell Biol.* 2000;1(1):31-9.

281. Anderson RG. The caveolae membrane system. *Annu Rev Biochem.* 1998;67:199-225.
282. Ledeen RW, Wu G. Nuclear sphingolipids: metabolism and signaling. *J Lipid Res.* 2008;49(6):1176-86.
283. Yoshikawa M, Go S, Takasaki K, Kakazu Y, Ohashi M, Nagafuku M, et al. Mice lacking ganglioside GM3 synthase exhibit complete hearing loss due to selective degeneration of the organ of Corti. *Proc Natl Acad Sci U S A.* 2009;106(23):9483-8.
284. Chiavegatto S, Sun J, Nelson RJ, Schnaar RL. A functional role for complex gangliosides: motor deficits in GM2/GD2 synthase knockout mice. *Exp Neurol.* 2000;166(2):227-34.
285. Takamiya K, Yamamoto A, Furukawa K, Yamashiro S, Shin M, Okada M, et al. Mice with disrupted GM2/GD2 synthase gene lack complex gangliosides but exhibit only subtle defects in their nervous system. *Proc Natl Acad Sci U S A.* 1996;93(20):10662-7.
286. Tajima O, Egashira N, Ohmi Y, Fukue Y, Mishima K, Iwasaki K, et al. Reduced motor and sensory functions and emotional response in GM3-only mice: emergence from early stage of life and exacerbation with aging. *Behav Brain Res.* 2009;198(1):74-82.
287. Tajima O, Egashira N, Ohmi Y, Fukue Y, Mishima K, Iwasaki K, et al. Dysfunction of muscarinic acetylcholine receptors as a substantial basis for progressive neurological deterioration in GM3-only mice. *Behav Brain Res.* 2010;206(1):101-8.
288. Ohmi Y, Tajima O, Ohkawa Y, Yamauchi Y, Sugiura Y, Furukawa K, et al. Gangliosides are essential in the protection of inflammation and neurodegeneration via maintenance of lipid rafts: elucidation by a series of ganglioside-deficient mutant mice. *J Neurochem.* 2011;116(5):926-35.

289. Yamashita T, Wu YP, Sandhoff R, Werth N, Mizukami H, Ellis JM, et al. Interruption of ganglioside synthesis produces central nervous system degeneration and altered axon-glia interactions. *Proc Natl Acad Sci U S A.* 2005;102(8):2725-30.
290. Kesner RP. Behavioral functions of the CA3 subregion of the hippocampus. *Learn Mem.* 2007;14(11):771-81.
291. Schnaar RL. Gangliosides of the Vertebrate Nervous System. *J Mol Biol.* 2016;428(16):3325-36.
292. Gottfries CG, Karlsson I, Svennerholm L. Membrane components separate early-onset Alzheimer's disease from senile dementia of the Alzheimer type. *Int Psychogeriatr.* 1996;8(3):365-72.
293. Svennerholm L, Gottfries CG. Membrane lipids, selectively diminished in Alzheimer brains, suggest synapse loss as a primary event in early-onset form (type I) and demyelination in late-onset form (type II). *J Neurochem.* 1994;62(3):1039-47.
294. Kracun I, Rosner H, Drnovsek V, Heffer-Lauc M, Cosovic C, Lauc G. Human brain gangliosides in development, aging and disease. *Int J Dev Biol.* 1991;35(3):289-95.
295. Molander-Melin M, Blennow K, Bogdanovic N, Dellheden B, Mansson JE, Fredman P. Structural membrane alterations in Alzheimer brains found to be associated with regional disease development; increased density of gangliosides GM1 and GM2 and loss of cholesterol in detergent-resistant membrane domains. *J Neurochem.* 2005;92(1):171-82.
296. Nishinaka T, Iwata D, Shimada S, Kosaka K, Suzuki Y. Anti-ganglioside GD1a monoclonal antibody recognizes senile plaques in the brains of patients with Alzheimer-type dementia. *Neurosci Res.* 1993;17(2):171-6.

297. Cebebauer M, Hof M, Amaro M. Impact of GM1 on Membrane-Mediated Aggregation/Oligomerization of beta-Amyloid: Unifying View. *Biophys J*. 2017;113(6):1194-9.
298. Fezoui Y, Teplow DB. Kinetic studies of amyloid beta-protein fibril assembly. Differential effects of alpha-helix stabilization. *J Biol Chem*. 2002;277(40):36948-54.
299. Yagi-Utsumi M, Kameda T, Yamaguchi Y, Kato K. NMR characterization of the interactions between lyso-GM1 aqueous micelles and amyloid beta. *FEBS Lett*. 2010;584(4):831-6.
300. Utsumi M, Yamaguchi Y, Sasakawa H, Yamamoto N, Yanagisawa K, Kato K. Up-and-down topological mode of amyloid beta-peptide lying on hydrophilic/hydrophobic interface of ganglioside clusters. *Glycoconj J*. 2009;26(8):999-1006.
301. Yanagisawa K. GM1 ganglioside and Alzheimer's disease. *Glycoconj J*. 2015;32(3-4):87-91.
302. Yagi-Utsumi M, Matsuo K, Yanagisawa K, Gekko K, Kato K. Spectroscopic Characterization of Intermolecular Interaction of Amyloid beta Promoted on GM1 Micelles. *Int J Alzheimers Dis*. 2010;2011:925073.
303. Hoshino T, Mahmood MI, Mori K, Matsuzaki K. Binding and aggregation mechanism of amyloid beta-peptides onto the GM1 ganglioside-containing lipid membrane. *J Phys Chem B*. 2013;117(27):8085-94.
304. Matsuzaki K. How do membranes initiate Alzheimer's Disease? Formation of toxic amyloid fibrils by the amyloid beta-protein on ganglioside clusters. *Acc Chem Res*. 2014;47(8):2397-404.

305. Manna M, Mukhopadhyay C. Binding, conformational transition and dimerization of amyloid-beta peptide on GM1-containing ternary membrane: insights from molecular dynamics simulation. *PLoS One*. 2013;8(8):e71308.
306. Hong S, Ostaszewski BL, Yang T, O'Malley TT, Jin M, Yanagisawa K, et al. Soluble Abeta oligomers are rapidly sequestered from brain ISF in vivo and bind GM1 ganglioside on cellular membranes. *Neuron*. 2014;82(2):308-19.
307. Yanagisawa K, Odaka A, Suzuki N, Ihara Y. GM1 ganglioside-bound amyloid beta-protein (A beta): a possible form of preamyloid in Alzheimer's disease. *Nat Med*. 1995;1(10):1062-6.
308. Ariga T. The Pathogenic Role of Ganglioside Metabolism in Alzheimer's Disease-Cholinergic Neuron-Specific Gangliosides and Neurogenesis. *Mol Neurobiol*. 2017;54(1):623-38.
309. Ueno H, Yamaguchi T, Fukunaga S, Okada Y, Yano Y, Hoshino M, et al. Comparison between the aggregation of human and rodent amyloid beta-proteins in GM1 ganglioside clusters. *Biochemistry*. 2014;53(48):7523-30.
310. Holmes O, Paturi S, Ye W, Wolfe MS, Selkoe DJ. Effects of membrane lipids on the activity and processivity of purified gamma-secretase. *Biochemistry*. 2012;51(17):3565-75.
311. Tamboli IY, Prager K, Barth E, Heneka M, Sandhoff K, Walter J. Inhibition of glycosphingolipid biosynthesis reduces secretion of the beta-amyloid precursor protein and amyloid beta-peptide. *J Biol Chem*. 2005;280(30):28110-7.
312. Grimm MO, Hundsdorfer B, Grosgen S, Mett J, Zimmer VC, Stahlmann CP, et al. PS dependent APP cleavage regulates glucosylceramide synthase and is affected in Alzheimer's disease. *Cell Physiol Biochem*. 2014;34(1):92-110.

313. Zha Q, Ruan Y, Hartmann T, Beyreuther K, Zhang D. GM1 ganglioside regulates the proteolysis of amyloid precursor protein. *Mol Psychiatry*. 2004;9(10):946-52.
314. Matsuoka Y, Saito M, LaFrancois J, Saito M, Gaynor K, Olm V, et al. Novel therapeutic approach for the treatment of Alzheimer's disease by peripheral administration of agents with an affinity to beta-amyloid. *J Neurosci*. 2003;23(1):29-33.
315. Bernardo A, Harrison FE, McCord M, Zhao J, Bruchey A, Davies SS, et al. Elimination of GD3 synthase improves memory and reduces amyloid-beta plaque load in transgenic mice. *Neurobiol Aging*. 2009;30(11):1777-91.
316. Grimm MO, Zinser EG, Grosgen S, Hundsdorfer B, Rothhaar TL, Burg VK, et al. Amyloid precursor protein (APP) mediated regulation of ganglioside homeostasis linking Alzheimer's disease pathology with ganglioside metabolism. *PLoS One*. 2012;7(3):e34095.
317. Soudy R, Patel A, Fu W, Kaur K, MacTavish D, Westaway D, et al. Cyclic AC253, a novel amylin receptor antagonist, improves cognitive deficits in a mouse model of Alzheimer's disease. *Alzheimers Dement (N Y)*. 2017;3(1):44-56.
318. Jhamandas JH, Li Z, Westaway D, Yang J, Jassar S, MacTavish D. Actions of beta-amyloid protein on human neurons are expressed through the amylin receptor. *Am J Pathol*. 2011;178(1):140-9.
319. Calamai M, Pavone FS. Partitioning and confinement of GM1 ganglioside induced by amyloid aggregates. *FEBS Lett*. 2013;587(9):1385-91.
320. Okabayashi S, Shimosawa N, Yasutomi Y, Yanagisawa K, Kimura N. Diabetes mellitus accelerates Abeta pathology in brain accompanied by enhanced GAbeta generation in nonhuman primates. *PLoS One*. 2015;10(2):e0117362.

321. Jeyakumar M, Thomas R, Elliot-Smith E, Smith DA, van der Spoel AC, d'Azzo A, et al. Central nervous system inflammation is a hallmark of pathogenesis in mouse models of GM1 and GM2 gangliosidosis. *Brain*. 2003;126(Pt 4):974-87.
322. Kakio A, Nishimoto SI, Yanagisawa K, Kozutsumi Y, Matsuzaki K. Cholesterol-dependent formation of GM1 ganglioside-bound amyloid beta-protein, an endogenous seed for Alzheimer amyloid. *J Biol Chem*. 2001;276(27):24985-90.
323. Yuyama K, Yanagisawa K. Sphingomyelin accumulation provides a favorable milieu for GM1 ganglioside-induced assembly of amyloid beta-protein. *Neurosci Lett*. 2010;481(3):168-72.
324. Michaelis ML, Jiang L, Michaelis EK. Isolation of Synaptosomes, Synaptic Plasma Membranes, and Synaptic Junctional Complexes. *Methods Mol Biol*. 2017;1538:107-19.
325. Oikawa N, Hatsuta H, Murayama S, Suzuki A, Yanagisawa K. Influence of APOE genotype and the presence of Alzheimer's pathology on synaptic membrane lipids of human brains. *J Neurosci Res*. 2014;92(5):641-50.
326. Yamamoto N, Igbabvoa U, Shimada Y, Ohno-Iwashita Y, Kobayashi M, Wood WG, et al. Accelerated A β aggregation in the presence of GM1-ganglioside-accumulated synaptosomes of aged apoE4-knock-in mouse brain. *FEBS Lett*. 2004;569(1-3):135-9.
327. Cataldo AM, Peterhoff CM, Troncoso JC, Gomez-Isla T, Hyman BT, Nixon RA. Endocytic pathway abnormalities precede amyloid beta deposition in sporadic Alzheimer's disease and Down syndrome: differential effects of APOE genotype and presenilin mutations. *Am J Pathol*. 2000;157(1):277-86.
328. Yuyama K, Yanagisawa K. Late endocytic dysfunction as a putative cause of amyloid fibril formation in Alzheimer's disease. *J Neurochem*. 2009;109(5):1250-60.

329. Yuyama K, Yamamoto N, Yanagisawa K. Chloroquine-induced endocytic pathway abnormalities: Cellular model of GM1 ganglioside-induced Abeta fibrillogenesis in Alzheimer's disease. *FEBS Lett.* 2006;580(30):6972-6.
330. Keilani S, Lun Y, Stevens AC, Williams HN, Sjoberg ER, Khanna R, et al. Lysosomal dysfunction in a mouse model of Sandhoff disease leads to accumulation of ganglioside-bound amyloid-beta peptide. *J Neurosci.* 2012;32(15):5223-36.
331. Oikawa N, Matsubara T, Fukuda R, Yasumori H, Hatsuta H, Murayama S, et al. Imbalance in fatty-acid-chain length of gangliosides triggers Alzheimer amyloid deposition in the precuneus. *PLoS One.* 2015;10(3):e0121356.
332. Simons K, Sampaio JL. Membrane organization and lipid rafts. *Cold Spring Harb Perspect Biol.* 2011;3(10):a004697.
333. Heffer-Lauc M, Lauc G, Nimrichter L, Fromholt SE, Schnaar RL. Membrane redistribution of gangliosides and glycosylphosphatidylinositol-anchored proteins in brain tissue sections under conditions of lipid raft isolation. *Biochim Biophys Acta.* 2005;1686(3):200-8.
334. Heffer-Lauc M, Viljetic B, Vajn K, Schnaar RL, Lauc G. Effects of detergents on the redistribution of gangliosides and GPI-anchored proteins in brain tissue sections. *J Histochem Cytochem.* 2007;55(8):805-12.
335. Selkoe DJ. Deciphering the genesis and fate of amyloid beta-protein yields novel therapies for Alzheimer disease. *J Clin Invest.* 2002;110(10):1375-81.
336. Citron M, Oltersdorf T, Haass C, McConlogue L, Hung AY, Seubert P, et al. Mutation of the beta-amyloid precursor protein in familial Alzheimer's disease increases beta-protein production. *Nature.* 1992;360(6405):672-4.

337. Levy E, Carman MD, Fernandez-Madrid IJ, Power MD, Lieberburg I, van Duinen SG, et al. Mutation of the Alzheimer's disease amyloid gene in hereditary cerebral hemorrhage, Dutch type. *Science*. 1990;248(4959):1124-6.
338. Wattendorff AR, Frangione B, Luyendijk W, Bots GT. Hereditary cerebral haemorrhage with amyloidosis, Dutch type (HCHWA-D): clinicopathological studies. *J Neurol Neurosurg Psychiatry*. 1995;58(6):699-705.
339. Davis J, Van Nostrand WE. Enhanced pathologic properties of Dutch-type mutant amyloid beta-protein. *Proc Natl Acad Sci U S A*. 1996;93(7):2996-3000.
340. Miravalle L, Tokuda T, Chiarle R, Giaccone G, Bugiani O, Tagliavini F, et al. Substitutions at codon 22 of Alzheimer's abeta peptide induce diverse conformational changes and apoptotic effects in human cerebral endothelial cells. *J Biol Chem*. 2000;275(35):27110-6.
341. Van Nostrand WE, Melchor JP, Cho HS, Greenberg SM, Rebeck GW. Pathogenic effects of D23N Iowa mutant amyloid beta -protein. *J Biol Chem*. 2001;276(35):32860-6.
342. Davis J, Xu F, Deane R, Romanov G, Previti ML, Zeigler K, et al. Early-onset and robust cerebral microvascular accumulation of amyloid beta-protein in transgenic mice expressing low levels of a vasculotropic Dutch/Iowa mutant form of amyloid beta-protein precursor. *J Biol Chem*. 2004;279(19):20296-306.
343. Miao J, Xu F, Davis J, Otte-Holler I, Verbeek MM, Van Nostrand WE. Cerebral microvascular amyloid beta protein deposition induces vascular degeneration and neuroinflammation in transgenic mice expressing human vasculotropic mutant amyloid beta precursor protein. *Am J Pathol*. 2005;167(2):505-15.

344. Maruvada P, Dmitrieva NI, East-Palmer J, Yen PM. Cell cycle-dependent expression of thyroid hormone receptor-beta is a mechanism for variable hormone sensitivity. *Mol Biol Cell*. 2004;15(4):1895-903.
345. Kawarabayashi T, Shoji M, Younkin LH, Wen-Lang L, Dickson DW, Murakami T, et al. Dimeric amyloid beta protein rapidly accumulates in lipid rafts followed by apolipoprotein E and phosphorylated tau accumulation in the Tg2576 mouse model of Alzheimer's disease. *J Neurosci*. 2004;24(15):3801-9.
346. Radeva G, Sharom FJ. Isolation and characterization of lipid rafts with different properties from RBL-2H3 (rat basophilic leukaemia) cells. *Biochem J*. 2004;380(Pt 1):219-30.
347. Kang MS, Baek SH, Chun YS, Moore AZ, Landman N, Berman D, et al. Modulation of lipid kinase PI4KIIalpha activity and lipid raft association of presenilin 1 underlies gamma-secretase inhibition by ginsenoside (20S)-Rg3. *J Biol Chem*. 2013;288(29):20868-82.
348. Vial C, Evans RJ. Disruption of lipid rafts inhibits P2X1 receptor-mediated currents and arterial vasoconstriction. *J Biol Chem*. 2005;280(35):30705-11.
349. Murphy MP, Beckett TL, Ding Q, Patel E, Markesbery WR, St Clair DK, et al. Abeta solubility and deposition during AD progression and in APPxPS-1 knock-in mice. *Neurobiol Dis*. 2007;27(3):301-11.
350. Qosa H, Batarseh YS, Mohyeldin MM, El Sayed KA, Keller JN, Kaddoumi A. Oleocanthal enhances amyloid-beta clearance from the brains of TgSwDI mice and in vitro across a human blood-brain barrier model. *ACS Chem Neurosci*. 2015;6(11):1849-59.
351. Martin DR, Cox NR, Morrison NE, Kennamer DM, Peck SL, Dodson AN, et al. Mutation of the GM2 activator protein in a feline model of GM2 gangliosidosis. *Acta Neuropathol*. 2005;110(5):443-50.

352. Vassar R. The beta-secretase, BACE: a prime drug target for Alzheimer's disease. *J Mol Neurosci.* 2001;17(2):157-70.
353. Baranello RJ, Bharani KL, Padmaraju V, Chopra N, Lahiri DK, Greig NH, et al. Amyloid-beta protein clearance and degradation (ABCD) pathways and their role in Alzheimer's disease. *Curr Alzheimer Res.* 2015;12(1):32-46.
354. Qiu WQ, Folstein MF. Insulin, insulin-degrading enzyme and amyloid-beta peptide in Alzheimer's disease: review and hypothesis. *Neurobiol Aging.* 2006;27(2):190-8.
355. Grossi C, Rigacci S, Ambrosini S, Ed Dami T, Luccarini I, Traini C, et al. The polyphenol oleuropein aglycone protects TgCRND8 mice against Ass plaque pathology. *PLoS One.* 2013;8(8):e71702.
356. Gotz J, Lim YA, Eckert A. Lessons from two prevalent amyloidoses-what amylin and Abeta have in common. *Front Aging Neurosci.* 2013;5:38.
357. Banks WA, Kastin AJ. Differential permeability of the blood-brain barrier to two pancreatic peptides: insulin and amylin. *Peptides.* 1998;19(5):883-9.
358. Hay DL, Chen S, Lutz TA, Parkes DG, Roth JD. Amylin: Pharmacology, Physiology, and Clinical Potential. *Pharmacol Rev.* 2015;67(3):564-600.
359. Roth JD, Erickson MR, Chen S, Parkes DG. GLP-1R and amylin agonism in metabolic disease: complementary mechanisms and future opportunities. *Br J Pharmacol.* 2012;166(1):121-36.
360. Kimura R, MacTavish D, Yang J, Westaway D, Jhamandas JH. Beta amyloid-induced depression of hippocampal long-term potentiation is mediated through the amylin receptor. *J Neurosci.* 2012;32(48):17401-6.

361. Verma N, Ly H, Liu M, Chen J, Zhu H, Chow M, et al. Intraneuronal Amylin Deposition, Peroxidative Membrane Injury and Increased IL-1beta Synthesis in Brains of Alzheimer's Disease Patients with Type-2 Diabetes and in Diabetic HIP Rats. *J Alzheimers Dis.* 2016;53(1):259-72.
362. Jhamandas JH, MacTavish D. Antagonist of the amylin receptor blocks beta-amyloid toxicity in rat cholinergic basal forebrain neurons. *J Neurosci.* 2004;24(24):5579-84.
363. Fu W, Patel A, Jhamandas JH. Amylin receptor: a common pathophysiological target in Alzheimer's disease and diabetes mellitus. *Front Aging Neurosci.* 2013;5:42.
364. Engel MF. Membrane permeabilization by Islet Amyloid Polypeptide. *Chem Phys Lipids.* 2009;160(1):1-10.
365. Ohmi Y, Ohkawa Y, Yamauchi Y, Tajima O, Furukawa K, Furukawa K. Essential roles of gangliosides in the formation and maintenance of membrane microdomains in brain tissues. *Neurochem Res.* 2012;37(6):1185-91.
366. Ohmi Y, Tajima O, Ohkawa Y, Mori A, Sugiura Y, Furukawa K, et al. Gangliosides play pivotal roles in the regulation of complement systems and in the maintenance of integrity in nerve tissues. *Proc Natl Acad Sci U S A.* 2009;106(52):22405-10.
367. Ariga T, McDonald MP, Yu RK. Role of ganglioside metabolism in the pathogenesis of Alzheimer's disease--a review. *J Lipid Res.* 2008;49(6):1157-75.
368. Yanagisawa K. Role of gangliosides in Alzheimer's disease. *Biochim Biophys Acta.* 2007;1768(8):1943-51.
369. Lammers KM, Herrera MG, Dodero VI. Translational Chemistry Meets Gluten-Related Disorders. *ChemistryOpen.* 2018;7(3):217-32.

370. Gellermann GP, Appel TR, Tannert A, Radestock A, Hortschansky P, Schroeckh V, et al. Raft lipids as common components of human extracellular amyloid fibrils. *Proc Natl Acad Sci U S A*. 2005;102(18):6297-302.
371. Matsuzaki K. Formation of Toxic Amyloid Fibrils by Amyloid beta-Protein on Ganglioside Clusters. *Int J Alzheimers Dis*. 2011;2011:956104.
372. Kurganov B, Doh M, Arispe N. Aggregation of liposomes induced by the toxic peptides Alzheimer's Abetas, human amylin and prion (106-126): facilitation by membrane-bound GM1 ganglioside. *Peptides*. 2004;25(2):217-32.
373. Ikeda K, Yamaguchi T, Fukunaga S, Hoshino M, Matsuzaki K. Mechanism of amyloid beta-protein aggregation mediated by GM1 ganglioside clusters. *Biochemistry*. 2011;50(29):6433-40.
374. Wu L, Gonias SL. The low-density lipoprotein receptor-related protein-1 associates transiently with lipid rafts. *J Cell Biochem*. 2005;96(5):1021-33.
375. Laudati E, Gilder AS, Lam MS, Misasi R, Sorice M, Gonias SL, et al. The activities of LDL Receptor-related Protein-1 (LRP1) compartmentalize into distinct plasma membrane microdomains. *Mol Cell Neurosci*. 2016;76:42-51.
376. May P, Rohlmann A, Bock HH, Zurhove K, Marth JD, Schomburg ED, et al. Neuronal LRP1 functionally associates with postsynaptic proteins and is required for normal motor function in mice. *Mol Cell Biol*. 2004;24(20):8872-83.
377. Yoshii A, Constantine-Paton M. BDNF induces transport of PSD-95 to dendrites through PI3K-AKT signaling after NMDA receptor activation. *Nat Neurosci*. 2007;10(6):702-11.
378. Wong W, Schlichter LC. Differential recruitment of Kv1.4 and Kv4.2 to lipid rafts by PSD-95. *J Biol Chem*. 2004;279(1):444-52.

379. Hering H, Lin CC, Sheng M. Lipid rafts in the maintenance of synapses, dendritic spines, and surface AMPA receptor stability. *J Neurosci.* 2003;23(8):3262-71.
380. Nyholm B, Fineman MS, Koda JE, Schmitz O. Plasma amylin immunoreactivity and insulin resistance in insulin resistant relatives of patients with non-insulin-dependent diabetes mellitus. *Horm Metab Res.* 1998;30(4):206-12.
381. Colburn WA, Gottlieb AB, Koda J, Kolterman OG. Pharmacokinetics and pharmacodynamics of AC137 (25,28,29 tripro-amylin, human) after intravenous bolus and infusion doses in patients with insulin-dependent diabetes. *J Clin Pharmacol.* 1996;36(1):13-24.
382. Qiu WQ. Amylin and its G-protein-coupled receptor: A probable pathological process and drug target for Alzheimer's disease. *Neuroscience.* 2017;356:44-51.
383. May PC, Boggs LN, Fuson KS. Neurotoxicity of human amylin in rat primary hippocampal cultures: similarity to Alzheimer's disease amyloid-beta neurotoxicity. *J Neurochem.* 1993;61(6):2330-3.
384. Zlokovic BV. The blood-brain barrier in health and chronic neurodegenerative disorders. *Neuron.* 2008;57(2):178-201.